NTNU – Trondheim
Norwegian University of
Science and Technology

Thermo-physical properties of anisotropic materials - A comparison between experiments and numerical calculations

Ane Ringseth

Master of Energy and Environmental Engineering
Submission date: June 2014
Supervisor: Erling Næss, EPT
Co-supervisor: Christian Schlemminger, EPT

Norwegian University of Science and Technology
Department of Energy and Process Engineering

NTNU
Norwegian University
of Science and Technology

Department of Energy
and Process Engineering

EPT-M-2014-97

MASTER THESIS

for

Student Ane Ringseth

Spring 2014

Thermo-physical properties of anisotropic materials - A comparison between experiments and numerical calculations

Termofysikalske egenskaper for anisotrope materialer – en sammenlikning mellom eksperimenter og numeriske beregninger

Background and objective

Hydrogen can be an energy carrier for the future. The main challenges of the investigation in hydrogen technology are the potential disadvantages in handling. The present project work efforts are focused on hydrogen material properties for hydrogen storage technologies.

The most promising hydrogen storage methods are: gas compression, liquefaction, chemical storage via metal hydrides and gas adsorption via physisorption. Adsorption type storage systems are inexpensive alternatives that also have the potential to reach the goals for handling hydrogen in on-board storage systems. Sorption type materials, like e.g. metal organic frameworks (MOF) have been identified as a viable option. These are characterized by high porosity and specific surface area.

However, the transient processes during charging and discharging of a storage system play an important role in the utilization of the hydrogen adsorption storage systems. Thermo-physical material properties like thermal conductivity are crucial for determining storage internal heat and mass transfer. Earlier emphasizes of material characterizations were showing large measurement uncertainties.

Therefore, the main objective of this work is to install and verify a new characterization setup for thermal conductivity and specific heat capacity measurements. Furthermore, experimental investigation of porous materials provided by NTNU with an additional comparison with available literature data.

The following tasks are to be considered:

1. Perform a literature survey concerning thermo-physical material properties of anisotropic materials (e.g. vacuum insulation panels)
2. Conduct measurements to determine thermo physical properties of selected anisotropic materials including a details uncertainty analysis of the measured properties.
3. Develop a numerical model based on e.g. Comsol Multyphysics, to determine the influences of anisotropy and measurements technique related uncertainty parameters.

4. Present and compare experimental and numerical results with respect anisotropy measurements technique.
5. Suggestions for further work shall be presented.

-- " --

Within 14 days of receiving the written text on the master thesis, the candidate shall submit a research plan for his project to the department.

When the thesis is evaluated, emphasis is put on processing of the results, and that they are presented in tabular and/or graphic form in a clear manner, and that they are analyzed carefully.

The thesis should be formulated as a research report with summary both in English and Norwegian, conclusion, literature references, table of contents etc. During the preparation of the text, the candidate should make an effort to produce a well-structured and easily readable report. In order to ease the evaluation of the thesis, it is important that the cross-references are correct. In the making of the report, strong emphasis should be placed on both a thorough discussion of the results and an orderly presentation.

The candidate is requested to initiate and keep close contact with his/her academic supervisor(s) throughout the working period. The candidate must follow the rules and regulations of NTNU as well as passive directions given by the Department of Energy and Process Engineering.

Risk assessment of the candidate's work shall be carried out according to the department's procedures. The risk assessment must be documented and included as part of the final report. Events related to the candidate's work adversely affecting the health, safety or security, must be documented and included as part of the final report. If the documentation on risk assessment represents a large number of pages, the full version is to be submitted electronically to the supervisor and an excerpt is included in the report.

Pursuant to "Regulations concerning the supplementary provisions to the technology study program/Master of Science" at NTNU §20, the Department reserves the permission to utilize all the results and data for teaching and research purposes as well as in future publications.

The final report is to be submitted digitally in DAIM. An executive summary of the thesis including title, student's name, supervisor's name, year, department name, and NTNU's logo and name, shall be submitted to the department as a separate pdf file. Based on an agreement with the supervisor, the final report and other material and documents may be given to the supervisor in digital format.

☒ Work to be done in lab (Water power lab, Fluids engineering lab, Thermal engineering lab)
☐ Field work

Department of Energy and Process Engineering, 14. January 2014

Olav Bolland
Department Head

Erling Næss
Academic Supervisor

Research Advisor: PhD-student Christian Schlemminger

Abstract

Hydrogen has the potential to become a replacement for fossil energy carriers in the future. Thermophysical properties like thermal conductivity and specific heat will be very important when determining the internal heat and mass transfer of the storage.

The transient plane source method is used to analyse the thermophysical properties of different anisotropic materials. The aim is to see if the method can measure an accurate effective thermal conductivity, and to see whether the method can be used for long-term investigation of hydrogen storage materials.

Interleaving plates of different isotropic materials interleaved make the anisotropic materials investigated in this thesis. The results from the laboratory are surprising. When the material with the lowest thermal conductivity is stacked closest to the sensor, the effective thermal conductivity got higher than when the material with the highest thermal conductivity was stacked closest to the sensor. This is because of the probing depth of the measurement.

It can be hard to interpret the temperature increase in the sensor of anisotropic measurements. The higher the anisotropy, the harder the temperature increase is to interpret. This is the reason why the simulation tool, Comsol Multiphysics, is used to simulate a temperature increase from a sensor. This increase is compared to the increase from the anisotropic measurements in the laboratory.

It is calculated that the temperature increase is very dependent of the thermal contact resistance between both the two materials and the materials and the sensor. The thermal contact resistance is dependent of the pressure upon the surface of the material and the surface roughness of the material. Steel, which is cut in the laboratory at NTNU, has some irregularities at the edges, and this will affect the measurements.

Sammendrag

Hydrogen har potensialet til å bli en erstatning for fossile energibærere i fremtiden. Termofysiske egenskaper som termisk ledningsevne og spesifikk varme vil være veldig viktig når man skal bestemme den indre varme- og masseoverføring for lagring av hydrogen.

Den transiente plane source (TPS) metoden kan brukes til å analysere de termofysiske egenskapene til forskjellige anisotropiske materialer. Det tas sikte på å se om fremgangsmåten kan måle en nøyaktig effektiv varmeledningsevne, og for å se om metoden kan benyttes for langtids undersøkelse av hydrogenlagringsmaterialer.

Ved å stable plater med forskjellige isotropiske materialer annenhver kan man lage anisotropiske materialer som vil bli undersøkt i denne oppgaven. Resultatet fra laboratoriet er overraskende. Når materialet med lavest termiske ledningsevne er stablet nærmest sensoren ble den effektive termiske ledningsevnen høyere enn når materialet med høyest ledningsevne var stablet nærmest sensoren. Dette har mye med sondringsdybden til målingene.

Det kan være vanskelig å tolke temperaturøkningen i sensoren av de anisotropiske målingene. Jo høyere anisotropi, jo vanskeligere er det å tolke temperaturøkningen. Dette er grunnen til at simuleringsverktøyet, Comsol Multiphysics, er brukt for å simulere temperaturøkningen i sensoren. Denne økningen er sammenlignet med økningen fra de anisotropiske målingene i laboratoriet.

Det er kalkulert at temperaturøkningen er veldig avhengig av den termiske kontaktmotstanden mellom både de to materialene og materialene og sensoren. Den termiske kontaktmotstanden er avhengig av trykket på overflaten til materialet og ruheten til materialet. Stål, som er kuttet i laboratoriet på NTNU, har noen uregelmessigheter ved kanten, og dette vil påvirke målingene.

Preface

This work is a result of my master thesis at The Norwegian University of Science and Technology (NTNU), department of Energy and Process Engineering, located in Trondheim, Norway.

The thesis was conducted between January 16th and June 12th under the supervision of professor Erling Næss and PhD student Christian Schlemminger.

This work gave me the opportunity to learn more about research and laboratory experiments. It also taught me to look at my work with more critical eyes, and always reach for better setup solutions in the laboratory.

I would like to give a big thanks to my supervisor, Erling Næss, for helping me to progress my work and giving me much insightful theory to back up my results. I would also like to thank my co- supervisor, Christian Schlemminger, who has always been there when I needed help. He has given a lot of good advise and has also been a good discussion partner.

Trondheim, June 12th, 2014

Ane Ringseth

Table of content

List of figures

List of tables

Nomenclature

Symbols	Property	Si- unit
Bi	Biot number	
C_p	specific heat capacity	kJ/ (kg K)
Fo	Fourier number	
k_B	Boltzmann constant	$m^2kg/(s^2K)$
l	length of plate	mm
h	height of plate	mm
w	width of plate	mm
k	thermal conductivity	W/(m K)
$\dot{q}$	heat flux	W/ m^2
q	net heat	W
V	volume	m^3
W	weight	g
ρ	density	kg/m^3
α	thermal diffusivity	m^2/s
dT/ dx	temperature gradient through conducting medium	

1. Introduction

Since our primary energy carrier, fossil fuels, someday in the future will run out, we have to look at new sustainable renewable energy sources. Hydrogen can than become a possible energy carrier for the future. It can be produced from electrolysis of water by using renewable electricity coming from solar or wind power.

The transient process during the discharge and charging will be important when exploiting the hydrogen adsorption storage systems. When determining the storage internal heat and mass transfer, thermophysical properties like thermal conductivity and specific heat are important.

This master thesis is organized into two main tasks. The first one is to investigate the thermophysical properties of anisotropic materials. This is done by investigating the thermal conductivity by using the transient plane source method in the laboratory. The second is to develop a numerical model based on the analysis and simulation tool Comsol Multiphysics.

The investigation of thermophysical properties of different anisotropic materials will be explained with heat transfer theory. This is mainly at the macroscale level, but a short description of microscale and nanoscale heat transfer will also be given. Heat transfer include conduction, convection and radiation, but since heat conduction is most important in the experiment, this is the main focus area.

The scope of this thesis is limited to the investigation of three materials, Teflon, Lexan and stainless steel 316 L. These materials are isotropic, but an anisotropic material is made by stacking two of the materials interleaved.

Comsol Multiphysics will be used to compare the temperature increase in the sensor in a simulated model to the increase measured by the transient plane source method. The aim of this is to see how the thermal contact resistance between the material and the sensor or between two materials influence the results. The temperature increase will influence the thermal conductivity.

An uncertainty analysis is conducted to see how large the uncertainty is for the volume, density and the thermal conductivity measured. The volumetric specific heat is used in the anisotropic measurements, and the density's uncertainty will therefore be very important. The uncertainty of the volume and density will influence the uncertainty measured of the thermal conductivity.

At the end of the thesis there is a suggestion for further work. In this section there is an explanation of how the laboratory experiments could be improved to achieve more accurate results.

Part 1: Theory

1. Heat transfer

Heat transfer is the process of moving heat from one location, to another. In physics, this is accomplished by conduction, convection or radiation. Conduction heat transfer is due to molecular activity. Energy is transferred from more energetic to less energetic particles due to the energy gradient. Convection heat transfer is due to energy transfer in fluid or gas due to bulk or macroscopic motion. Radiation heat transfer is due to energy emitted by matter caused by change in electron configurations that results in changes in energy via EM waves or photons.

1.1 Heat conduction

1.1.1 Conduction electrons and lattice vibrations

Conduction is spontaneous energy transfer from energetic particles of a medium to the adjacent less energetic ones. Molecules, atoms, electrons or phonons can be the particles. In solids, the heat conduction is caused by a combination of lattice vibration of molecules and the energy transport by free electrons.

Heat can be transferred by the conduction electrons or by lattice vibrations. In solids, the electrons are bound to the atom in local orbits. However, a small fraction of the electrons can move easily through the entire material. This small fraction is called conduction electrons, and they carry the electrical current. Metals have many conduction electrons. In an insulator, most of the electrons are bound, and there will be few conduction electrons (Fitzpatrick, 2006).

When the lattice is at equilibrium, each atom is placed exactly at its normal lattice position, see Figure 1. When the solid is heated, the atoms vibrate around their sites like a set of harmonic oscillators. If an atom is displaced from this site by a small amount, they will tend to return to their position. Lattice vibrations occur due to force acting on an atom when it returns to its equilibrium position.

There will be thermal energy associated with vibrations of atoms. The atoms cannot vibrate independently, because they are tied together with bonds. The vibration takes the form of collective modes that propagate through the material (Schroeder, 2000). These propagating lattice vibrations can be considered as sound waves.

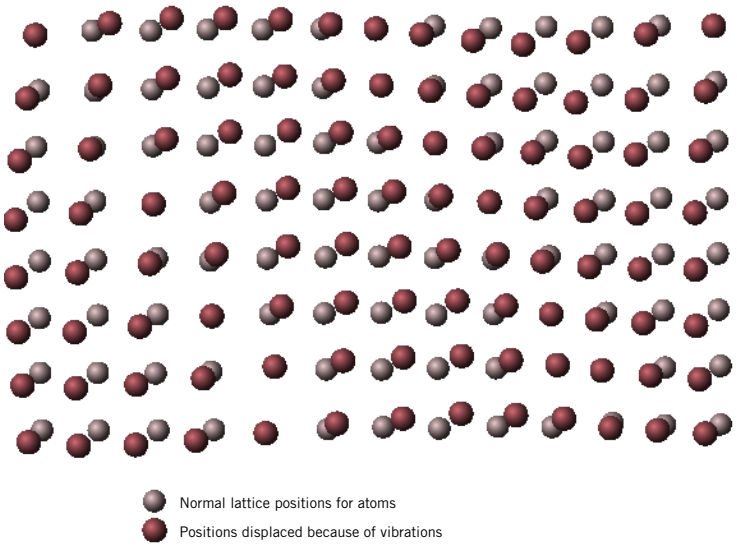

Figure 1: Lattice vibrations (Ziman, 1967).

The energy of the vibration molecules is calculated by: $\Delta E = h\omega$. This means that it can lose or accept energy only in discrete units of energy $h\omega$. This discrete amount of energy is called phonons. Phonons can be explained as quanta of lattice vibrations.

According to the Bose-Einstein equation, the number of phonons can be calculated from:

$$n = \frac{1}{\exp\left(\frac{h\omega}{k_B T}\right) - 1} \approx \frac{k_B T}{h\omega} \qquad \text{[Eq. 1]}$$

where h is the Planck's constant, ω is the frequency of phonons (rad/s), k_B is the Boltzmann constant and T is the absolute temperature.

1.1.2 Thermal conductivity, thermal diffusivity and specific heat capacity

To describe the heat transfer trough a material, three properties are used. These are thermal conductivity, thermal diffusivity and specific heat.

The thermal conductivity, k or λ, is the measure of a materials ability to conduct heat. There are thermal conductivity associated with both lattice vibration and the number of free electrons in solid materials, and the total thermal conductivity is describes as:

$$k_{total} = k_e + k_{ph} \qquad \text{[Eq. 2]}$$

The total thermal conductivity, k, is calculated as:

$$k = \alpha \cdot Cp \cdot \rho \qquad \text{[Eq. 3]}$$

Where α is the thermal diffusivity, C_p is the specific heat and ρ is the density. The thermal conductivity of a material depends on its chemical composition and structure. It also depends on temperature and pressure. However, in most cases, the thermal conductivity is more dependent on temperature than pressure. Pressure dependence can than be neglected. The thermal diffusivity, α, says something about how fast heat diffuses through a material. The property is calculated as:

$$\alpha = \frac{heat\ conducted}{heat\ stored} = \frac{k}{\rho C_p} \qquad \text{[Eq. 4]}$$

The heat capacity, ρC_p, describes the heat storage capability of a material. This values is denoted as per unit volume, while specific heat capacity, C_p, is denoted as per unit mass.

$$C_p = \frac{Q}{m \cdot \Delta T} \left[\frac{kJ}{kg \cdot K}\right] \qquad \text{[Eq. 5]}$$

where Q is the heat added, m is the mass and ΔT is the change in temperature. This relation does not apply if there is a phase change involved. This is because the heat added or removed during phase change does not change in temperature.

1.1.3 Fourier's law and the energy equation

Heat transfer problems can either be one- dimensional, two- dimensional or three-dimensional, depending on level of accuracy or relative magnitude of heat transfer rates in different directions. Heat transfer is generally categorized as three- dimensional. This means that the temperature distribution through the material can be described in the Cartesian coordinates by x, y and z (Cengel, Turner, & Cimbala, 2008).

However, if the variation of temperature in the third direction is negligible, the system is two-dimensional. If the heat is transferred only in one direction, and the temperature varies only in this direction, the system is one- dimensional. One example is heat transfer through the glass of a window. Here, the heat transfer occurs predominantly in one direction, which is the direction normal to the surface of the glass, and heat transfer in other directions is negligible.

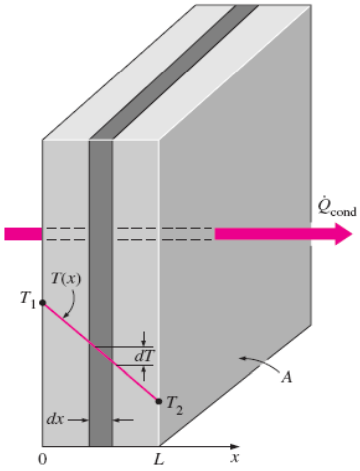

Figure 2: Heat conduction (Cengel, Turner, & Cimbala, 2008).

In Figure 2, one- dimensional heat conduction is shown. The initial temperature is larger than the outlet temperature, and due to this temperature gradient, the heat transfer through conduction takes place in positive x- direction. Fourier's law of heat conduction describes the 1- dimensional heat conduction as (Incropera, DeWitt, Bergmann, & Lavine, 2006):

$$\dot{q}\,(x) = -k \cdot A \cdot \frac{dT}{dx}\ [W] \qquad \text{[Eq.6]}$$

where k is the thermal conductivity and dT/dx is the temperature gradient.

Most engineering materials are isotropic, which means that they have the same properties in all directions. In these materials you do not have to be concerned about the variation of properties with direction. However, in anisotropic materials, such as fibrous or composite materials, the properties change with direction. The thermal conductivity should be expressed as tensor quantity to account for the variation with direction.

For one- dimensional heat conduction, the conservation of energy is as follows:

$$C_p \cdot \rho \frac{dT}{dt} = \frac{d}{dx}\left(k\frac{dT}{dx}\right) + \dot{q} \quad \text{[Eq. 7]}$$

where the second term defines the longitudinal conduction and $\dot{q}$ defines the internal heat source or sink. If there were no change in time, called steady state, the first term would be zero. If the thermal conductivity, k, is constant:

$$\frac{d^2T}{dx^2} + \frac{q}{k} = \frac{1}{\alpha}\frac{dT}{dt} \quad \text{[Eq. 8]}$$

However, if the heat transfer is 3-dimensional, the heat equation is as follows:

$$\frac{d}{dx}\left(k\frac{dT}{dx}\right) + \frac{d}{dy}\left(k\frac{dT}{dy}\right) + \frac{d}{dz}\left(k\frac{dT}{dz}\right) + \dot{q} = C_p \cdot \rho \frac{dT}{dt} \quad \text{[Eq. 9]}$$

This equation is in Cartesian coordinates, and this is the tool for heat conduction analysis. The equation describes the conservation of energy, and states that the rate of energy transfer by conduction into a unit volume plus the volumetric rate of thermal energy generation must be equal to the rate of change in thermal energy stored within the volume in any point of the medium. If the thermal conductivity is constant you get what is called Fourier- Biot equation (Peles):

$$\frac{d^2T}{dx^2} + \frac{d^2T}{dy^2} + \frac{d^2T}{dz^2} + \frac{\dot{q}}{k} = \frac{1}{\alpha}\frac{dT}{dt} \quad \text{[Eq. 10]}$$

1.2 Microscale and nanoscale heat transfer

Size effects are important when studying and calculating the thermal transport phenomena as thermophysical properties such as the bulk thermal conductivity. These are a result from macroscopic flux laws (Sobhan & Peterson, 2008). To analyse the results of transport from small domains, the size effects are important to investigate.

It is not clear "how small is small" when deciding whether conventional theory can be applied to the microscale. It is, however, clear that at some level of physical dimension the size effect will be important when there is deviation from the conventional approach. This will be relevant in microchannels, conduction and radiation in thin films and in microscale structures.

1.2.1 Conduction at the microscale.

The study of microscale conduction has recently been important because size effect in electron transport have been observed in small dimensions. This is for example in thin films and wires. Thin films are widely used in semiconductor technologies, as microelectronics utilizing silicon-on-insulator (SOI) devices is more commonly utilized. The manufacturers point to the thermal management as the main challenge. In these types of systems, an analysis of conduction heat transfer in microstructures is required for the design of the thermal effects (Sobhan & Peterson, 2008).

In structures where the characteristic length is the same as the scattering mean free path of the electrons, the size effect will be important when investigating conduction heat transfer. In this region, there is expected that the thermal conductivity is reduced due to the presence of the boundary.

Although Fouriers law is used to describe the heat transfer by conduction in the macroscopic domain, it is not adequate when investigating the size effect dominated problems. This is because the law is based on a continuum assumption. However, Fouriers law can be used, but this may result in inaccurate results. This means that other approaches should be used when dealing with microscale and nanoscale heat transfer.

When analysing the microscale heat transfer, the effect of space and timescales must be considered in relation to the physical dimensions, the speed of the process and the temperature range where the heat transfer occurs.

Tien and Chen have presented useful approaches to analyse the space problem at the microscale for thin filmes. They categorized two regimes: the classical size- effect domain and the quantum size- effect domain. The classical regime can be useful when analysing microscale heat transfer in micron- sized environments and the quantum regime are more relevant in nanoscale conduction. The classical size- effect domain is noted as:

$$\frac{h}{\Lambda} < O(1) \; or \; \frac{d_r}{\Lambda} \qquad \text{[Eq. 11]}$$

The quantum size- effect domain is characterized as:

$$\frac{h}{\lambda_c} > O(1) \qquad \text{[Eq. 12]}$$

where h is the device dimension, d_r is the penetration depth of the temperature into the domain, Λ is the mean free path of the heat carriers and λ_c is the characteristic wavelength of the electrons or phonons. Boltzmann transport equation or molecular dynamics modelling can be used at the classical domain, while phonon transport theory can be used for the quantum size- effect domain.

According to Cercignani, Boltzmann transport equation is described as (Sobhan & Peterson, 2008):

$$\frac{\partial f}{\partial t} + v \cdot \nabla_r f + F \cdot \nabla_p f = \left(\frac{\partial f}{\partial t}\right)_{sc} \qquad \text{[Eq. 13]}$$

where f is the distribution function of particles expressed as f = f (r,p,t). This indicates the probability of occupation of particles with momentum p at location r and time t.

Molecular dynamics can be used to predict the thermal conductivity. The Green- Kubo (GK) method is most widely used once the velocities of the molecules are obtained through molecular dynamics simulations. The method is based on the fluctuation- dissipation theorem of statistical mechanics. The GK formula is given as:

$$k = \frac{1}{k_B V T^2} \int_0^\infty \frac{S(t) \cdot S(0)}{3} dt \qquad \text{[Eq. 14]}$$

where S is the heat current vector, described as:

$$S = \frac{d}{dt} \sum_i r_i E_i \qquad \text{[Eq. 15]}$$

where E_i is the total energy of the particle and r_i is the position vector of the particle. The total energy is the sum of the potential energy and the kinetic energy. At equilibrium, S fluctuates around zero. $S(t) \cdot S(0)$ is called the heat current autocorrelation function (HCACF). The value of the thermal conductivity of a material is influenced by the decay rate of HCACF. A low decay rate means a small fluctuation in heat current vector due to small mean phonon relaxation time. This will lead to a small thermal conductivity, which can be seen in equation 14.

The phonon transport theory builds on the fact that the transport of thermal energy in an ideal solid consists of lattice vibrations and free electrons. These are quantized phenomena. The resistive heat transfer is then expressed as energy dissipation due to collision of quanta (Sobhan & Peterson, 2008).

Majumdar (1993) researched microscale heat conduction in dielectric thin films, and indicated that heat transport by lattice vibration or phonons can be seen as a radiative transfer problem in the microscale region. With the Boltzmann transport theorem in mind, an equation for phonon radiative transfer (EPRT) was made.

1.2.2 Nanoscale heat transfer

In microscale heat transfer, the first to be done is to identify if the analysis should include size effects. This means to decide if a macroscopic continuum approach is sufficient, or the analysis should include discrete, particle- based phenomena to describe the thermal energy transport. However, in nanoscale heat transfer, the sizes are so small that they affect the thermophysical properties based on macroscopic considerations. This means that it is not possible to use a continuum analysis, and the investigation could be microscopic.

In many of the nanoscale systems, the heat transfer can be analysed more or less as microscopic, but the investigations often applies to much smaller dimensions. The size of the domain in nanoscale processes places the calculations in the free molecular flow regime, which means that continuum modelling is not adequate (Sobhan & Peterson, 2008).

The nanoscale phenomena often include energy carriers to have both particle and wave characteristics. The characteristic length dimension should be compared with characteristic length scales to understand when to consider the wave nature. Figure 3 shows a nanoscale size effect regime map. This is used to decide how to analyse nanoscale heat transport phenomena (Chen, Borca-Tasciuc, & Yang).

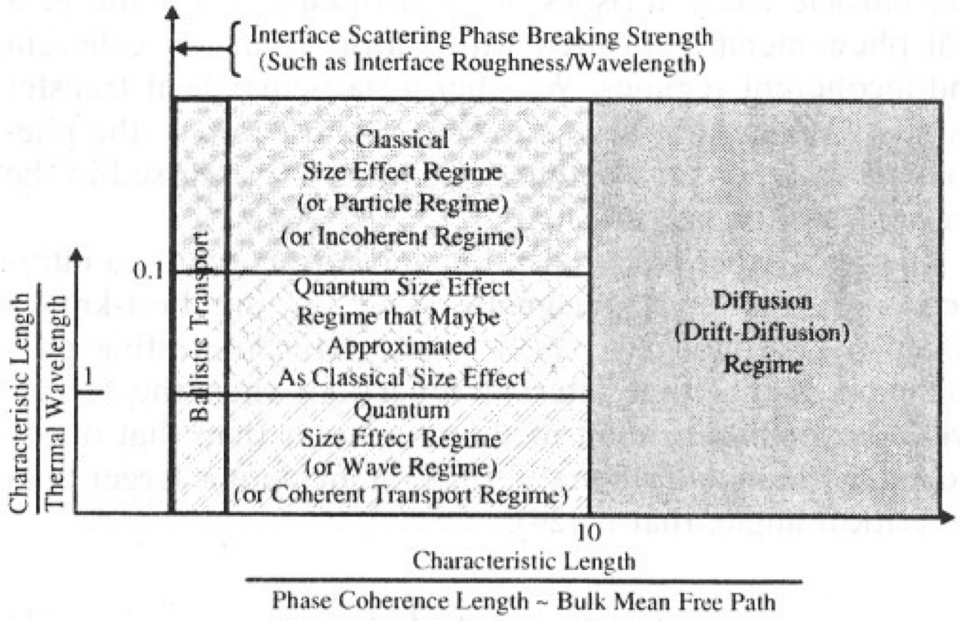

Figure 3: Different nanoscale heat transfer regimes (Sobhan & Peterson, 2008).

When the thermal conductivity is known, the mean free path can be calculated from:

$$k = \frac{1}{3} C v^2 \tau = \frac{1}{3} C v \Lambda \quad \text{(for gases)} \qquad \text{[Eq. 16]}$$

$$k = \frac{\pi^2 n k_B^2 T}{m v_F} \Lambda \quad \text{(for electrons in metals)} \qquad \text{[Eq. 17]}$$

$$k = \frac{1}{3} \int_0^{\omega_{max}} C_\omega v_\omega^2 \tau_\omega d\omega = \frac{\Lambda}{3} \int_0^{\omega_{max}} C_\omega v_\omega d\omega \quad \text{(for phonons)} \qquad \text{[Eq. 18]}$$

where k is the thermal conductivity, Λ is the mean free path, C is the volumetric specific heat, τ is the relaxation time, v is the velocity of the carriers, m is the electron mass, n is the electron number density at the Fermi surface, C_ω is the volumetric specific heat at each frequency, v_ω is the velocity at each frequency, τ_ω is the relaxation time at each frequency and k_B is Boltzmann constant. These equations build on kinetic theory, and the relaxation time is a characteristic timescale. The Fermi surface is an abstract boundary that defines the allowable energies of electrons in a solid. It is used to determine the electrical, magnetic, thermal and optical properties of metals, semimetals, and doped semiconductors (Perkowitz, 2013).

To include the wave effects, the mean free path should be compared to the characteristic length. This means that the wavelength should be analysed:

$$\lambda_t = \frac{h}{\sqrt{3 m k_B T}} \quad \text{(for electrons or molecules)} \qquad \text{[Eq. 19]}$$

$$\lambda_t = \frac{2hv}{k_B T} \quad \text{(for photons)} \qquad \text{[Eq. 20]}$$

where h is Planck's constant, λ_t is wavelength of the energy carriers, v is the velocity of the energy carriers, m is the mass of energy carriers and k_B is Boltzmann constant.

The last characteristic length to be considered is the one that considers the spread in energy and wavelength of the carriers. This length is called the coherence length in optics and are given by:

$$l_c \approx \frac{c}{\Delta v} \qquad \text{[Eq. 21]}$$

where c is the speed of light and Δv is the bandwidth of radiation (Sobhan & Peterson, 2008).

It is difficult to measure heat transport at the nanoscale due to the small sizes of the system and structure. The effective thermal conductivity of nanoparticles, however, can be measured by a couple of methods: the transient approach, which uses a hot- wire method; the steady-state method, which uses a guarded hot plate, a temperature oscillation technique or a cut-bar apparatus. The transient hot- wire method is most commonly used when measuring fluids and nanoparticles. In this method, the thermal conductivity is calculated by using the relationship between the electrical and thermal conductivity. This is because the hot- wire is utilized as a heating element through electrical resistance heating and as a thermometer by measuring the electrical resistivity of the fluid (Sobhan & Peterson, 2008).

2 Anisotropic materials

An anisotropic material is a material that is directionally dependent. Isotropic materials are the opposite, which means identical in all directions.

The direction dependent physical properties of anisotropic materials are important because it says something about how the materials behave. Which orientation the structure of the material is directed will affect the strength, stiffness and the thermal properties of the material. Heat conduction of the anisotropic material is dependent on the geometry and material type.

As will be discussed later on, the TPS method offers fast measurements of thermal properties of different materials. However, high degree of anisotropy makes it difficult to interpret the temperature increase in the sensor.

There are many different types of anisotropic materials, for example wood and composites. It can be seen that wood is an anisotropic material because it is easier to split along its grain than against it. Composite materials are obtained by combining two or more materials at the macroscale to get a useful structural material. At macroscale level these materials can be considered homogenous, while at the microscale level they are considered as inhomogeneous. Vacuum insulated panels are anisotropic, and are commonly used in building retrofitting.

The materials used to transfer and reject heat from the heat source in electronics are often anisotropic. In the next subchapters, different anisotropic materials are discussed and explained.

2.1 Vacuum insulation panels

To reach the targets and regulations in the European Union, the energy consumption in buildings has to be reduced. The target according to the European Parliament is a reduction in energy consumption of 20% by 2020 and 50% by 2050. To reach these targets, an energy retrofitting is necessary of the existing building stocks. To reduce the energy demand for heating in buildings, vacuum insulated panels could be used.

A vacuum insulated panel (VIP) is a form of thermal insulation consisting of a nearly gas-tight enclosure surrounding a rigid core, from which the air has been evacuated. The core material is porous, with a surrounding of a multi- layered polymer film (Canada, 2010). The VIPs ensures five to ten times better insulation performance than conventional insulation materials (Johansson, Adl-Zarrabi, & Hagentoft, 2012).

Heat transfer through a volume occurs by convection, conduction and radiation. But if a vacuum is created, the heat transfer during convection is eliminated. This is because convection is dependent on the presence of gas molecules that transfer heat by bulk motion through the insulator. A creation of vacuum would also lead to a reduction of conduction because there will be fewer collisions between adjacent gas molecules.

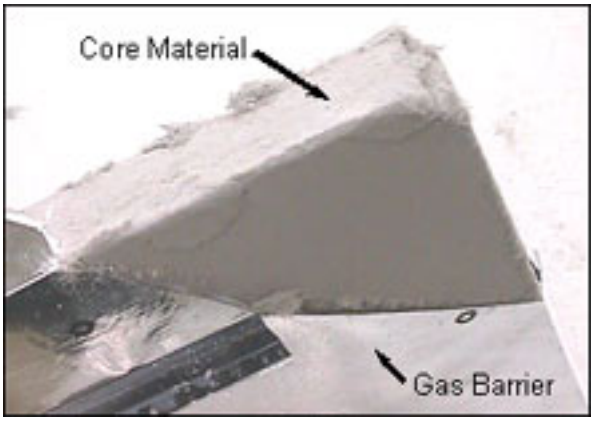

Figure 4: Schematic construction of VIPs (Canada, 2010).

2.1 Comparison analytical and numerical results for VIPs.

Caps (2004) has described a measurement method to calculate the thermal conductivity of the finished panel. The method is integrated in the production line. The thermal conductivity of a known fibrous material at different pressures together with an integrated heat sink in the core material makes it possible to measure the thermal conductivity of the panel. A warm sensor is placed near the heat sink, at the surface of the panel. This sensor detects the temperature decrease, and this along with the known thermal conductivity of the fibrous material can be used to determine the internal pressure of the VIPs.

However, Johansson (2011), compared the temperature increase from the transient plane source (TPS) sensor with numerical three dimensional simulation. It was shown that the TPS method, which is explained further in part 2, could be used in VIP measurements.

In P. Johanssons studies, the numerical and the analytical results for a VIP is analysed. First, the numerical model was compared to TPS measurements of polystyrene. Later, the numerical model was compared to TPS measurement of polystyrene with aluminium film. Matlab was used to calculate the numerical results.

The temperature increase in the analytical solution and numerical results for isotropic polystyrene were in good agreement, with only a small deviation. The temperature increase was also compared in the numerical simulation with the TPS measurement. This showed a large difference after 40 seconds, which was the measurement time. However, the difference in temperature increase in polystyrene covered with aluminium was not that large. This shows the importance of the heat transfer through the film.

The cause for the deviation between the simulated and the measured temperature increase is probably because of losses in the wire and surface contact resistances. The thermal properties also has a impact. These properties may deviate some from the literature (Johansson, Adl-Zarrabi, & Hagentoft, 2012).

2.2 Composites

As mentioned, composite materials are materials obtained by combining two or more materials to get a useful structural material. The composite material consists of two separate components, the matrix and the filler. The filler is held together by the matrix to form the bulk of the material. Usually, the matrix consists of various epoxy type polymers. Different

materials could be used, as for example metal matrix composites and thermoplastic matrix composites. The filler, which is impregnated in the matrix, have the purpose of giving its advantage to the composite. This advantage is usually strength. The materials of the filler can be many different materials, as carbon fiber, glass bead, sand and ceramic.

According to which filler type is being used, the composites are categorized in three or four types. These are particulate, short fiber, long fiber and laminate.

In the particulate composites, the filler material is nearly round. Unreinforced concrete is an example of this with the cement as the matrix and the sand as the filler. Another example is the lead particles in a copper matrix. In this, the filler and the matrix is metal.

The filler materials length- to diameter ratio decides if the composites are called short or long fiber. If the length- to diameter ratio is greater than one, the composites are called short or long fiber composites. If this ratio is almost 100; it is called short fiber composites, while if the ratio is almost infinite; it is called long fiber composites. An example of short fiber composites is the fiberglass filler for boat panels. Long fiber composites usually uses the filler types carbon fiber or aramid fiber.

In laminate composites, the filler material is formed as a sheet. An example of this type of composites is Formica countertops, where the matrix is usually a type of polymer, while the filler can be many materials from craft paper to glass.

The resulting properties would be a combination of the constituent materials since the composites are nonhomogeneous. This means that the material properties in the composite materials would be dependent on tension, compression and bending (Rusmee, 2005).

2.3 Layered materials and their behaviour

The easiest form of anisotropy is by using plates of isotropic materials and stack them interleaved. This is the form of anisotropy used in the experiment part of this thesis.

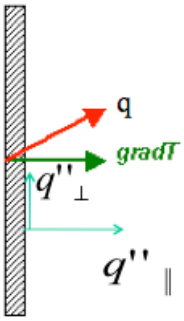

Figure 5: Thin plate anisotropy (Subbarao).

Figure 5 shows a thin plate, were the temperature gradient is perpendicular to the plate. Since the material is anisotropic, the heat flux, noted q, will be in the shown direction. However, the thermal conductivity perpendicular to the plate is calculated as the heat flux parallel to the temperature gradient, q''_{11}, divided by the temperature gradient. This means that the thermal conductivity of an anisotropic material should be calculated in both the axial and the radial direction (Subbarao).

The effective thermal conductivity for plates of the same material stacked at the top of each other will be relevant in the laboratory measurement. Both the radial and the axial thermal conductivity should be taken into account. The effective thermal conductivity is given by (Gustavsson, 1994):

$$k_{effective} = \sqrt{k_{axial} \cdot k_{radial}} \quad \text{[Eq. 22]}$$

However, it could be argued that the effective thermal conductivity should be looked at as vectors where the sum of the conductivity in axial and radial direction is the effective thermal conductivity. The thermal conductivity in axial and radial direction can be calculated as:

$$q_{rad} = -k_{rad} \frac{\partial T}{\partial x} \quad \text{[Eq. 23]}$$

$$q_{ax} = -k_{ax} \frac{\partial T}{\partial y} \quad \text{[Eq. 24]}$$

where k_{ax} is the axial thermal conductivity and k_{rad} is the radial thermal conductivity. When noting that the effective thermal conductivity should be looked at as vectors:

$$q_{effective} = \sqrt{q_{ax}^2 + q_{rad}^2} = k_{effective} \frac{\partial T}{\partial z} = \sqrt{(k_{ax} \frac{\partial T}{\partial y})^2 + (k_{rad} \frac{\partial T}{\partial x})^2} \quad \text{[Eq. 25]}$$

Since the temperature is assumed to be the same in all directions:

$$k_{effective} = \sqrt{k_{ax}^2 + k_{rad}^2} \quad \text{[Eq. 26]}$$

In anisotropic measurements done with plates with two different materials stacked interleaved with the same height, the thermal conductivity in the radial direction would ideally be the same as the average of the two reference materials. In the axial direction however, the thermal conductivity would be influenced by the thermal conductivity of air between the layers. The air interface together with the thermal contact resistance between the two materials will decrease the thermal conductivity. The heat will be moved more easily away from the sensor in the radial direction, due to both the air interface and thermal contact resistance between both the material and the sensor and between both the materials. The difference from equation 26 is that the height should be taken into account when calculation the effective thermal conductivity in radial direction:

$$k_{average} = \left(k_{rad,material\,1} + k_{rad,material\,2}\right) \cdot \delta \quad \text{[Eq. 27]}$$

If the plates do not have the same height, this should be taken into account:

$$k_{average} = \frac{h_{plate\,1}}{h_{total}} \cdot k_{material\,1} + \frac{h_{plate\,2}}{h_{total}} \cdot k_{material\,2} \quad \text{[Eq. 28]}$$

Part 2 Experiments

In this part, the transient plane source method will be discussed. This method is used when determining the thermal conductivity and specific heat of the samples. Later on, the instrumentation and sample setup are described. The different materials and their relevant properties are also explained.

1. Transient plane source method

The transient plane source method is a transitory method used to determine the thermal conductivity and specific heat. This is the method used in this experiment to find both the isotropic and the anisotropic thermal conductivity. However, in anisotropic measurements, the specific heat capacity must be known.

The method uses a round and plane heat source, which acts as a transient heat source and works simultaneously as a temperature sensor. The element consists of two insulating layers of Kapton, which has a double spiral inside. This spiral has an electrical conducting pattern of nickel foil, which is 10 μm thick. As shown in Figure 6, the element is located between two samples with the sensor faced in contact with the two sample surfaces (Solòrzano, Rodriguez-Perez, & de Saja, 2008).

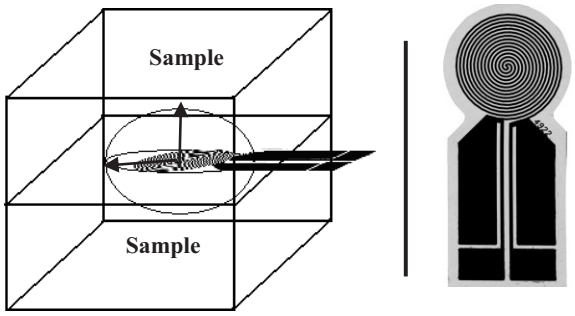

Figure 6: The sensor and the schematic setup of the experiment (Solòrzano, Reglero, Rodriguez-Perez, Lehmhus, Wichmann, & de Saja, 2007).

The sensor is exposed to constant electrical power. The sensors time-dependent resistance is calculated by:

$$R(t) = R_O\,[1 + \mathrm{TCR}\,(\Delta T_i + \Delta T_{ave}(\tau))] \qquad \text{[Eq.29]}$$

Where R_O is the disk resistance in the beginning of the recording, TCR is the temperature coefficient of resistance of the probe and ΔT_i is the constant temperature difference that develops momentarily over the thin insulating layers. The insulating material covers the two sides of Hot Disk sensor material (nickel) and makes the Hot Disk a good sensor. ΔT_{ave} (τ) is the temperature increase of the sample surface on the other side of the insulating layer.

The temperature increase recorded by the sensor is then given by:

$$\Delta T_i + \Delta T_{ave}(\tau) = \frac{1}{TCR}\left(\frac{R(t)}{R_o} - 1\right) \qquad \text{[Eq. 30]}$$

ΔT_i is a measure of "thermal contact" between the sample surface and the sensor. If $\Delta T_i = 0$, there are a perfect "thermal contact" realised by deposited thin film or an electrically insulating sample.

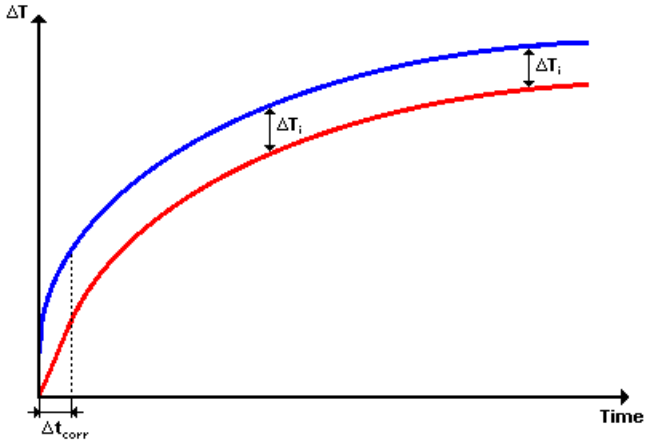

Figure 7: The temperature increases curve of sensor and sample (Hot Disk Thermal Constant Analyser, 2013).

In Figure 7, the blue curve represents the temperature increase in the sensor and the red curve represents the temperature increase of the sample surface.

ΔT_i will become constant after a very short time, and can be calculated as:

$$\Delta t_i = \frac{\delta^2}{\alpha_i} \qquad \text{[Eq. 31]}$$

Where the thickness of the insulating layer is δ and α_i is the thermal diffusivity of the material layer.

The temperature increase, which is time- dependent, is:

$$\Delta T_{ave}(\tau) = \frac{P_o}{\pi^{3/2} a\, k} \cdot D(\tau) \qquad \text{[Eq. 32]}$$

Where P_o is the sensors total power output, a is the radius of the disk, k is the thermal conductivity and D (τ) is a dimensionless time dependent function given by:

$$D(\tau) = \sqrt{\frac{t}{\Theta}} \qquad \text{[Eq. 33]}$$

Where t is the time from the beginning of the recording and Θ is the characteristic time given by (Hot Disk Thermal Constant Analyser, 2013):

$$\Theta = \frac{a^2}{\alpha} \qquad \text{[Eq. 34]}$$

In equation 34, α is the thermal diffusivity.

The thermal conductivity is defined as:

$$k = \rho \cdot C_p \cdot \alpha \quad \text{[Eq. 35]}$$

In equation 35, ρ is the input parameter in Hot Disk and C_p is from the measurements or from input and α is found from the measurements.

The probing depth, Δ, gives the distance that the heat flow penetrates in the material from any point of the disk surface. This is an important value of the transient plane method and is calculated by:

$$\Delta = \beta\sqrt{R^2 \frac{t}{\theta}} \rightarrow \Delta = R \cdot \sqrt{t} \quad \text{[Eq. 36]}$$

Where R is the sensor radius, t is measured time, β is an experimental parameter, which has a value close to 2, and θ is the characteristic time (Solòrzano, Rodriguez-Perez, & de Saja, 2008).

There are several advantages of the transient plane method. The method is easy to use and offers fast experiments. The thermal conductivity range is wide, and goes from 0.02 to 400 W/m·K. The methods offers flexibility in sample size, the sample preparation needs little effort and by only changing the sensor diameter, you can perform local and bulk measurements. However, the transient plane source method is a contact method, and thermal contact resistance has to be minimized (Solòrzano, Reglero, Rodriguez-Perez, Lehmhus, Wichmann, & de Saja, 2007).

1.1 Anisotropic TPS measurements

In anisotropic measurements, the specific heat capacity per unit volume is necessary to calculate the thermal properties. If these properties are constant in the a- and b-axis, but different from the c-axis this leads to a temperature increase:

$$\Delta T_s(\tau_a) = \frac{P_0}{\pi^{3/2} r (k_a k_c)^{1/2}} D(\tau_a) \quad \text{[Eq. 37]}$$

In this equation k_a is the thermal conductivity along the a-axis and k_c is the thermal conductivity along the c-axis.

$$\tau_a = \sqrt{\frac{t}{\theta_a}}, \theta_a = \frac{r^2}{\alpha_a} \quad \text{[Eq. 38]}$$

The thermal conductivity along the a-axis is calculated as:

$$k_a = C_p \alpha_a \quad \text{[Eq. 39]}$$

This means that the thermal conductivity along the a-axis can be calculated, since the specific heat is known. The thermal conductivity, k_c, can be obtained from equation 37. The thermal diffusivity along the c-axis is calculated from the standard relation.

1.2 Instrumentation and setup

The experimentation is done with two different methods, one method using a liquid oil bath and another using a room temperature measurement apparatus. However, the preparation before the measurements starts is the same for the different methods.

As explained later on, dimensions of the samples are important to calculate an accurate density. For this purpose, a sliding caliber and a scale are used. The scale used for measuring the weight of the materials is a Mettler AT261 Delta Range.

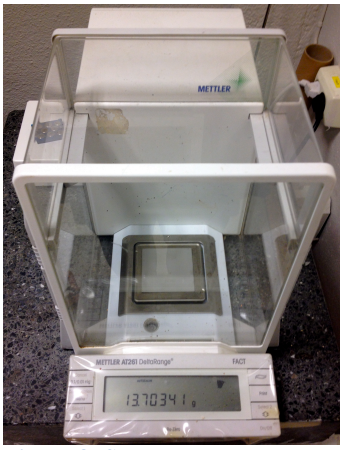

Figure 8: Scale.

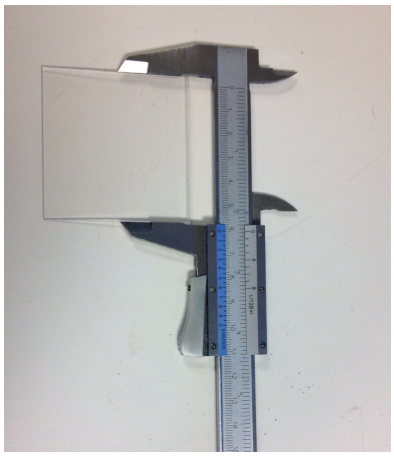

Figure 9: Sliding caliber.

1.2.1 Measurement at room temperature

The measurements at room temperature include Hot Disk Constants Analyser, Hot Disk sensor and room temperature sample holder. The system is put in a stable environment, because it detects temperature differences greater than 0.1 mK. The placement should be at an isothermal place, free from vibration and at near constant humidity. The TPS method is used in the Hot Disk Constant Analyser.

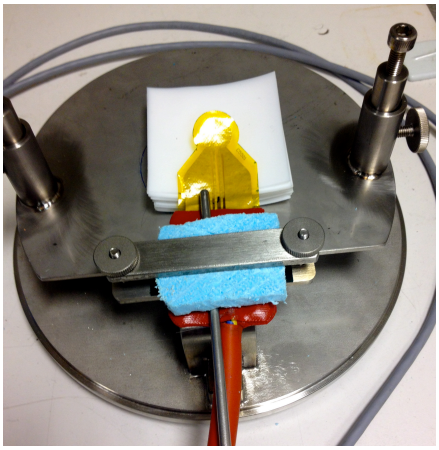

Figure 10: Sensor at the top of the sample.

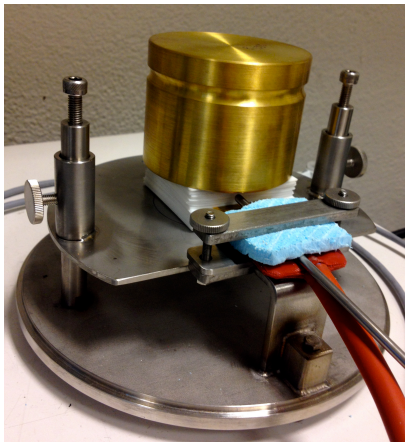

Figure 11: Position of scale and temperature sensor.

The red cable connected to the sensor is used. The cable with the sensor is introduced in the room temperature sample holder. One of the samples is put in the mounting table of the sample holder. Three screws adjust the height of the mounting table so that the sample is at the same level as the sensor. The middle of the sensor should be in the middle of the sample.

The second sample is placed at top of the sensor. A weight is put on the top of the construction to provide a good thermal contact. Figure 10 shows the room temperature sample holder, sensor and sample. The figures also show a temperature sensor. This is used to measure the temperature in the room when the experiment is running. The temperature sensor is the stainless steel rod, which is placed just beside the sample.

Finally, a black box is placed over the construction to prevent environmental impacts.

1.2.2 Liquid oil bath

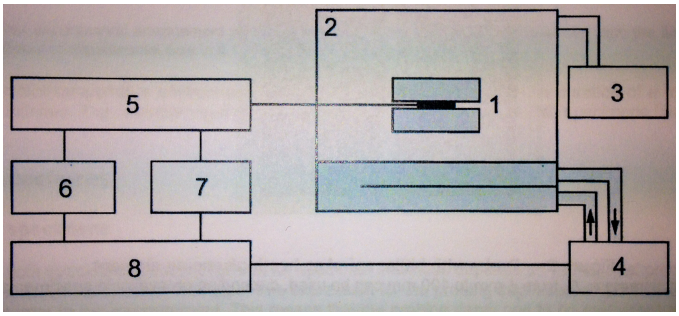

Figure 12: Schematic layout of the liquid oil bath apparatus (Hot Disk Thermal Constant Analyser, 2013).

Figure 12 shows the schematic setup of the experiment with the oil bath. An electrical current is sent through the probe to generate a temperature field and to produce a heat pulse. The temperature increase of the probe is measured as a function of time. In the figure, the numbers stand for:

1. Specimen with probe.
2. Chamber.
3. Vacuum pump
4. Thermostat
5. Bridge circuit
6. Voltmeter
7. Voltage source
8. Computer.

In the experiment the transient plane source (TPS) method is used (subchapter 1). The oil bath makes it possible to measure the thermal conductivity, specific heat and thermal diffusivity at various temperatures. This is necessary when measuring the Teflon samples, because it undergoes a phase change. The oil used in this experiment is silicone oil, SIL180. This oil can withstand temperatures from -40 °C to 200 °C.

The construction needed in this experiment is a rectangular container filled with silicone oil. The sample is placed in a rounded stainless steel cylinder with an open top, which is placed in the oil bath. In the bottom of the cylinder there is silicone paste, to ensure good thermal contact between the stainless steel cylinder and the sample.

When the sample is inside the cylinder, an insulating material is placed at the top of the cylinder. The cable is connected to the Thermal Constant Analyser. Figure 13 shows the finished setup.

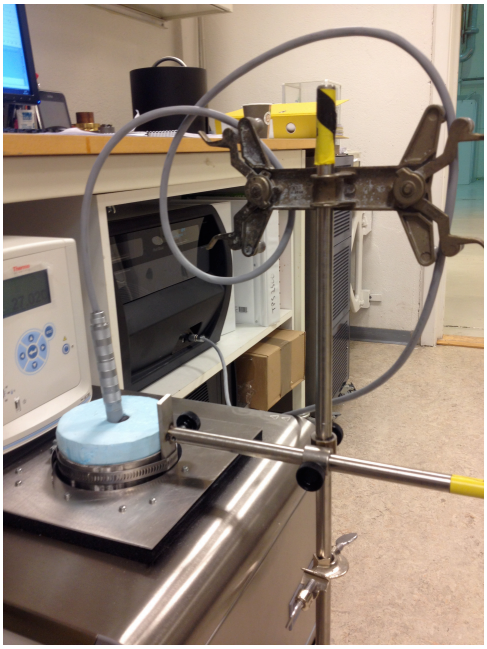

Figure 13: Installation of sample in oil bath.

1.2.3 Sample setup

In the first couple of experiments, the samples are made from 20 x 20 plates stacked with the same material. This is to get references to comparison and to see how the Hot Disk behaves under anisotropic conditions. In the later experiments, the plates where stacked interleaved with two materials.

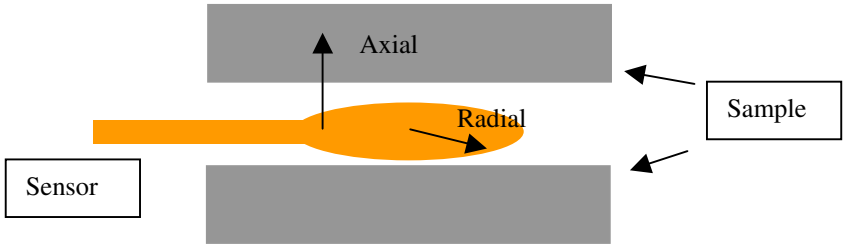

Figure 14: Setup for the sample (Lundstrøm, 2004).

Figure 14 shows the setup for the samples. The axial direction is the direction perpendicular to the plane of the sensor, while the radial direction is the direction plane to the sensor (Lundstrøm, 2004).

It is important to stack the plates tightly to prevent any air from getting in-between the plates and to achieve a good thermal contact. By putting a weight on top of the samples, there will be less air present, which would reduce the airs influence on the effective thermal conductivity.

When using the oil bath, a plate with an angle is used to setup the samples. The sensor is attached with two plates, screws and metal rods on the top of the angle. This is to ensure the sample from slipping off when put into the oil bath. See Figure 15, which shows the setup of the sample put in the oil bath and the room temperature holder respectively.

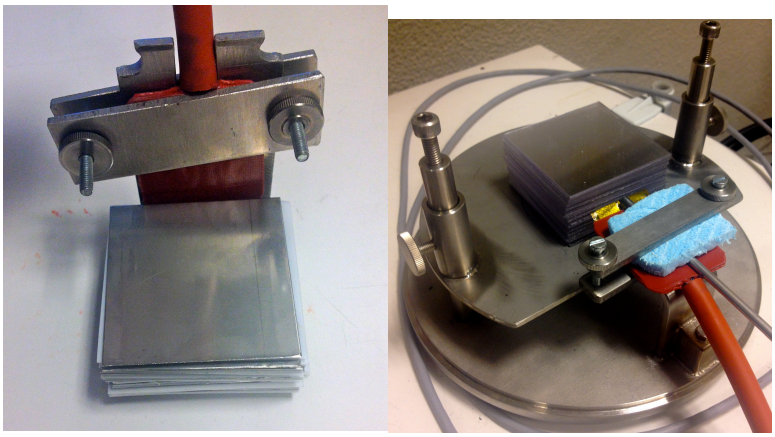

Figure 15: Setup of sample put in oil bath and the room temperature holder respectively.

1.3 Hot Disk Analysis software and input parameters

The tool used to analyse the results is the Hot Disk Thermal Analysis software.

There are several input parameters in the Hot Disk Analysis software that will severely affect the results. Some of these are sensor type, probing depth, power and measurement time. When an anisotropic material is tested, the specific heat has to be known.

Which sensor is being used is important in the experiment. The radius of the sensor must be much larger than the porosity or void structure of the sample if the material is not dense or homogenous. If the material is a metal, which has a structure variation that is at an atomic or molecular level, the Hot Disk sensors should have a radius from approximately 3.2 to 15 mm. If the materials have structure voids at mm level, a larger sensor should be used. The sensor number 5501 with a radius 6.403 mm is being used in this experiment.

The maximum available probing depth is a very important input parameter to prevent the measurements from being outside the samples range. The probing depth in the isotropic measurements is calculated by taking the diameter of the sample minus the diameter of the sample divided by 2. The probing depth calculated should be less than the height of the samples, if it is not, the height should be the probing depth. In the anisotropic measurement, both the axial and radial probing depth is to be decided. The maximum available axial probing depth is the height of the sample, while the maximum available radial probing depth is calculated the same way as the isotropic measurements.

It is important not to choose too high heating power, because this can lead to melting of the sensor. In this experiment various heat power are used to see how this affect the thermal conductivity of the samples. Too high heating power can lead to heating of the sample, which causes too high thermal conductivity.

The measurement time is also an important input parameter. The measurement time is normally low for materials with high thermal conductivity and specific heat, because the heat conduction is high. This means that the heat moves fast over the material, and a short measurement time is necessary to prevent the measurements from being outside the range. If the material is an isolation material, the heat moves slowly throughout the material, and a long measurement time will be necessary to ensure that the sample is measured properly.

2. Investigated materials

As mentioned, three different materials are used in this experiment. This is stainless steel 316L, Teflon and Lexan. These materials are chosen because they cover different thermal conductivity ranges. Stainless steel 316L and Teflon are also investigated thoroughly both through literature and previous isotropic experiments in the project thesis.

Reference materials are useful to give an indication about the correctness of the measurements in the laboratory. In appendix A the thermal conductivity, density and specific heat capacity calculations are shown.

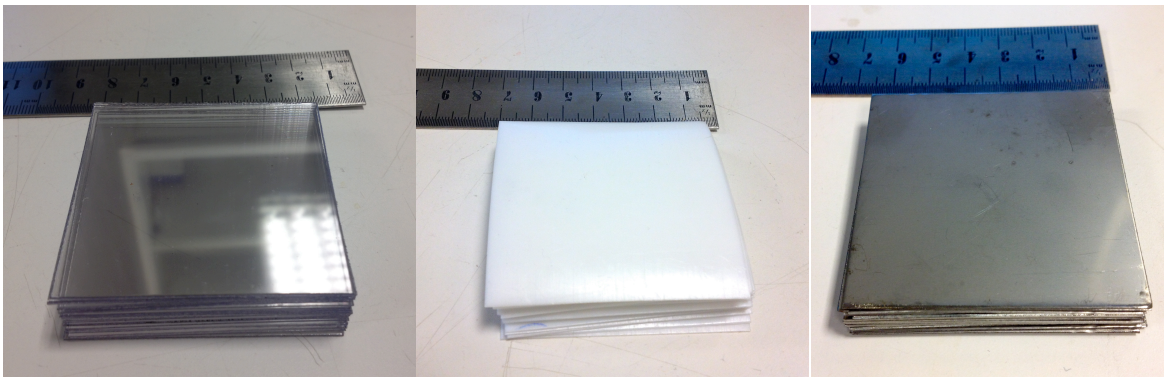

Figure 16: Materials; Lexan, Teflon and stainless steel respectively.

2.1 Dimensions

As can be seen from equation 41, the size of the materials influences the calculated density of the samples. Both stainless steel and Teflon are delivered as sheets with a height of 0.5 mm, while Lexan are delivered with a height of 0.8 mm.

Due to the fact that stainless steel were cut in the workshop at NTNU, some of the plates have a variation in weight, length and width. The average length and width of ten of each of the materials is calculated to get an approximate estimate. The sliding caliber and scale described in part 2, section 1 are being used for this purpose.

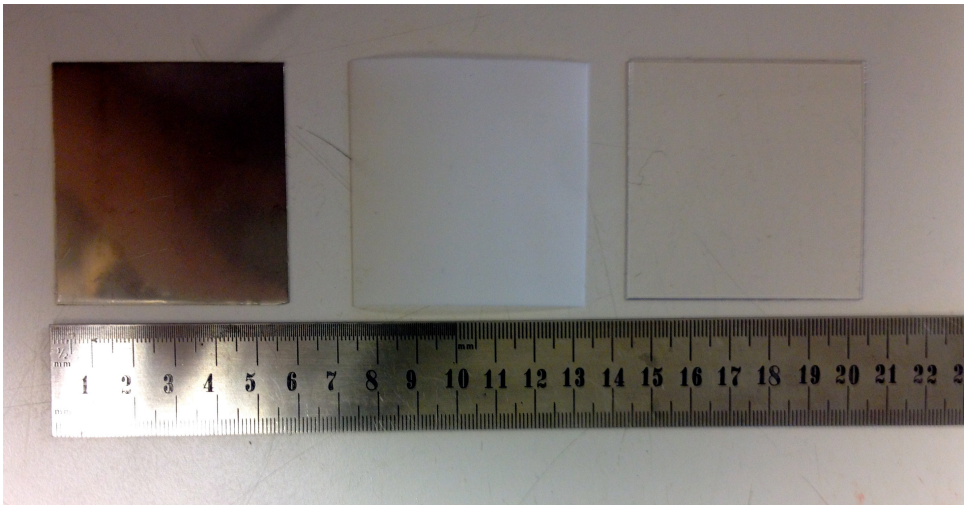

Figure 17: Dimension of the samples.

Table 1, Table 2 and Table 3 shows the measured dimensions of the three materials. However, Teflon was hard to measure due to the flexibility of the material. As can be seen from the tables, stainless steel deviates the most in length, width and weight.

Table 1: Measured dimensions of one plate of Teflon.

	Average	Standard deviation
Weight [g]	3.9854	0.02
height [mm]	0.5	0.00
length [mm]	60.22	0.28
width [mm]	60.15	0.28

Table 2: Measured dimensions of one plate of Lexan.

	Average	Standard deviation
Weight [g]	3.2345	0.03
height [mm]	0.8	0.00
length [mm]	60.02	0.39
width [mm]	60.02	0.24

Table 3: Measured dimensions of one plate of Stainless Steel 316L.

	Average	Standard deviation
Weight [g]	13.7755	0.30
height [mm]	0.5	0.00
length [mm]	59.41	0.85
width [mm]	59.68	0.95

2.2 Thermophysical properties

2.2.1 Thermal conductivity

The thermal conductivity and specific heat for stainless steel 316L and Teflon are calculated by an equation from the National Institute of Standards and Technology (NIST). The data range is from 3 - 400 K. According to NIST, the equation for thermal conductivity and specific heat are calculated as following:

$$k = 10^{a+b(log_{10}T)+c(log_{10}T)^2+d(log_{10}T)^3+e(log_{10}T)^4+f(log_{10}T)^5+g(log_{10}T)^6+h(log_{10}T)^7+i(log_{10}T)^8}$$ [Eq. 40]

In the equation, subscripts a to i are coefficients given in a table by NIST and T is the temperature given in kelvin. Figure 18 and Figure 19 shows how the thermal conductivity for Teflon and stainless steel varies with temperature.

As Teflon is a polymer, which is often used as an insulator, this material has a low thermal conductivity. This means that the heat is conducted poorly.

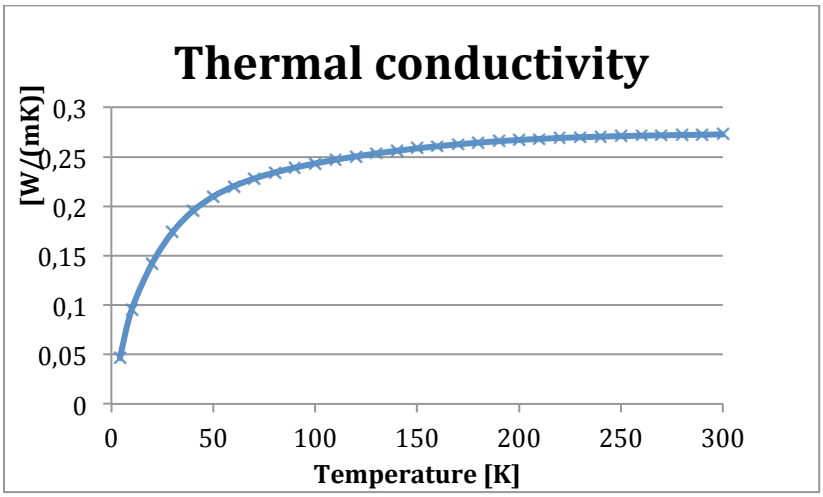

Figure 18: Thermal conductivity of Teflon as reference material.

Stainless steel 316L is a metal and the reference material used with the greatest thermal conductivity. However, as an impure material, the thermal conductivity will probably deviate some from the values measured in the laboratory.

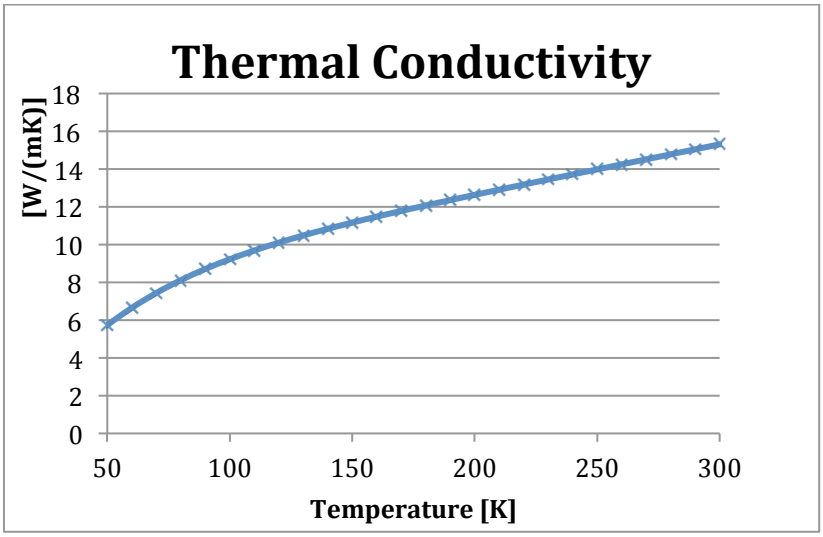

Figure 19: Thermal conductivity of Stainless steel as reference material.

The thermal properties of Lexan are only presented at room temperature. The reason for this is that Lexan is only measured at room temperature, and it was hard to find the temperature dependent thermal conductivity. The thermal conductivity is 0.19 W/m·K, which means that it conducts heat poorly.

2.2.2 Density

The respective densities of the investigated materials are found by dividing the measured mass by the calculated volume. The formula is applied on a selection of ten plates of each material. The average volume and weight will be used.

$$\rho = \frac{\Sigma m_i}{\Sigma V_i} \quad \text{[Eq. 41]}$$

Table 4: Density of the investigated materials.

	Density [kg/m^3]
Teflon	2200.52
Lexan	1122.35
SS 316L	7770.50

Table 4 shows the calculated density of the materials, but to get an accurate density with temperature change, the equation for linear thermal expansion is used. Seen from an atomic perspective, the thermal expansion is caused by an increase in average distance between the atoms. The linear thermal expansion is given by an equation from NIST:

$$y = a + bT + cT^2 + dT^3 + eT^4 \quad \text{[Eq. 42]}$$

Here subscript a to e are coefficients, while T is the temperature given in kelvin.

The linear thermal expansion is a percentage change in length from the original length, measured at 293 K. The linear expansion has the equation:

$$\Delta l = l_0 \cdot \alpha \cdot \Delta T \quad \text{[Eq. 43]}$$

This is related to density by looking at the volumetric expansion. The change in volume when the temperature changes can be calculated as:

$$\Delta V = V_0 \cdot 3 \cdot \alpha \cdot \Delta T = V_0 \cdot \beta \cdot \Delta T \quad \text{[Eq. 44]}$$

Here, $\Delta V = V_1 - V_0$ is the change in volume, ΔT is the change in temperature and β is the volumetric temperature expansion. This leads to a calculation of the final volume, V_1:

$$V_1 = V_0 \cdot \beta \cdot (t_1 - t_0) + V_0 = V_0(1 + \beta \cdot (t_1 - t_0)) \quad \text{[Eq. 45]}$$

The density when the temperature change is:

$$\rho_1 = \frac{m}{V_0(1+\beta\cdot(t_1-t_0))} = \frac{\rho_0}{1+\beta\cdot(t_1-t_0)} \quad \text{[Eq. 46]}$$

Where ρ_1 is final density and ρ_0 is initial density (Toolbox). Figure 20 and Figure 21 shows how the density varies with temperature for Teflon and stainless steel.

Teflon has a low density, which means that it has a low specific weight.

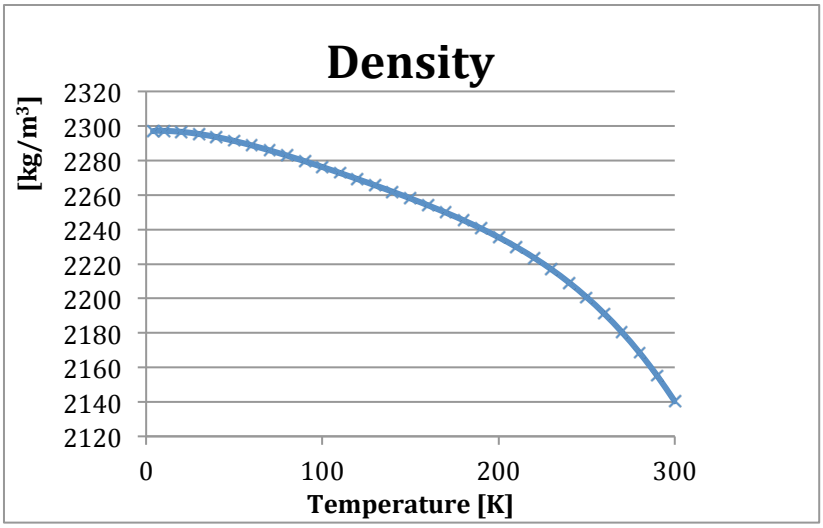

Figure 20: Density of Teflon as reference material.

Stainless steel 316L is a metal and has a high density. This means that it has a high specific weight. It can be seen that this density deviates a lot from the measured density. It will be necessary with an accurate uncertainty analysis of this property.

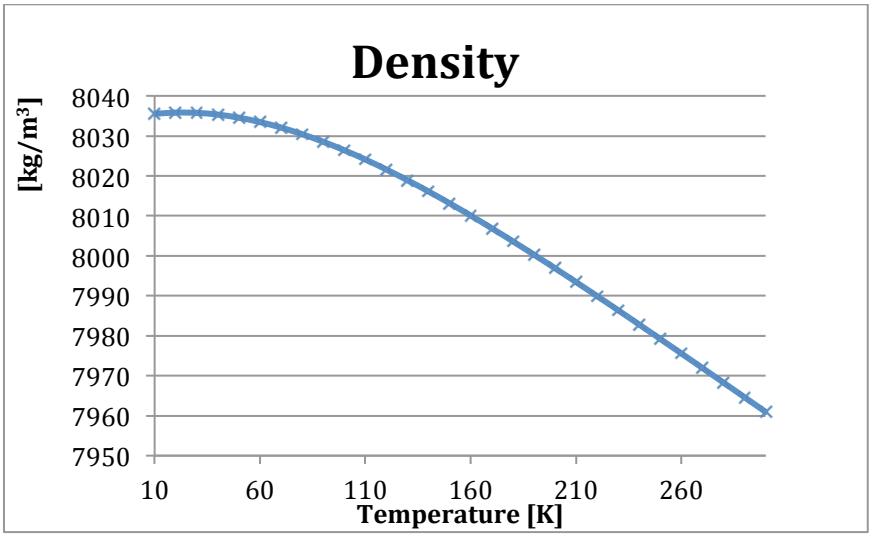

Figure 21: Density of stainless steel as reference material.

The thermal properties of Lexan are only presented at room temperature. The density is 1200 kg/m^3.

2.2.3 Specific Heat Capacity

The specific heat capacity is calculated with the same equation as the thermal conductivity. However, different coefficients are being used. To calculate the volumetric specific heat, which should be input in Hot Disk, the density is used. Figure 22 and Figure 23 shows how the volumetric specific heat varies with temperature for Teflon and stainless steel.

Teflon is as explain a polymer, which can be used as an insulator. This means that the material is a poor conductor of heat. The material also have a low heat storage capability.

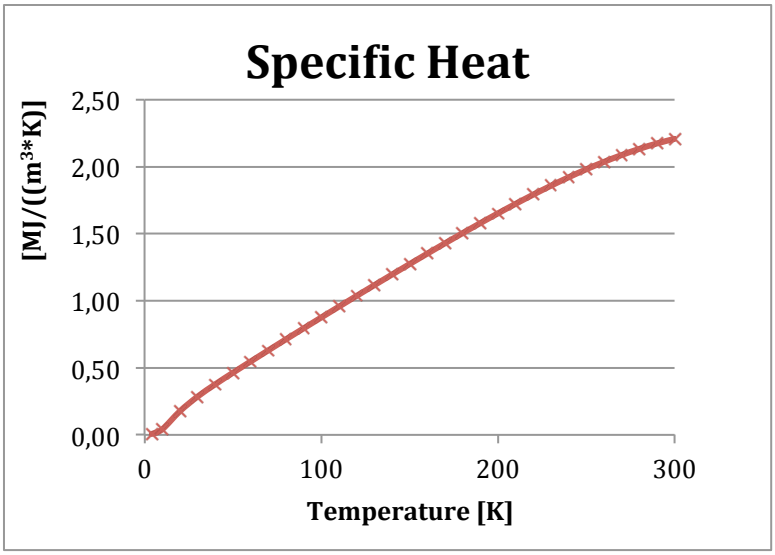

Figure 22: Specific heat of Teflon as reference material.

Stainless steel 316L is a metal and the reference material with the greatest specific heat. This is because metals are good conductors of heat, and also have a high heat storage capability. However, as an impure material, the specific heat will probably deviate some from the values measured in the laboratory.

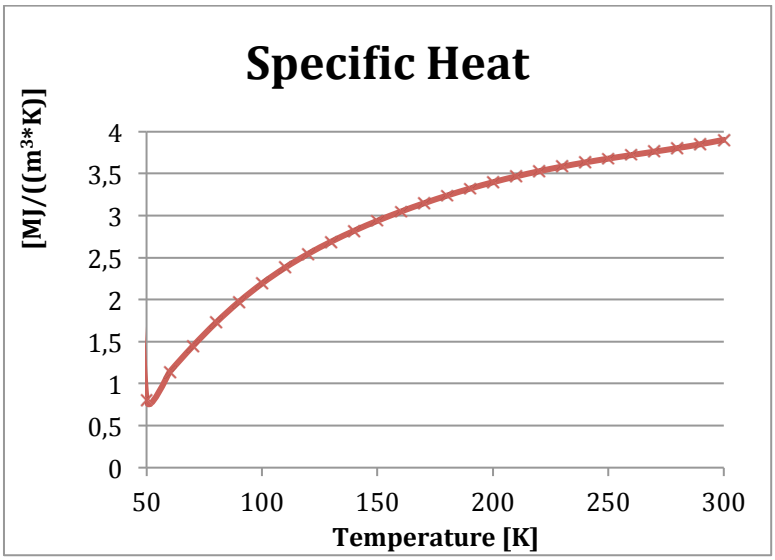

Figure 23: Specific heat of Stainless steel as reference material.

The thermal properties of Lexan are only presented at room temperature. The specific heat is 1260 J/kg·K. The volumetric specific heat is calculated as 1.512 MJ/m^{3}K.

3. Uncertainty analysis

The uncertainty analysis is important to get an idea of the accuracy of the results measured in the laboratory. The goal is that the measurements fit the theory within an uncertainty of 10 %.

The scale used for measuring the weight of the material is a Mettler AT261 Delta Range. It has a weighing capacity at 205 g and has a readability at 0,1 mg. The sliding caliber used has a resolution of 0,05 mm, yielding a reading of 0,025 mm. It is important to look at the uncertainty of the dimensions, since these are used to calculate the density. The volumetric specific heat is an input parameter in the laboratory, and it is important to investigate the uncertainty of the density, to see how this could influence the results.

The uncertainty of the measured volume, ΔV, is calculated as:

$$\frac{\Delta V}{V} = \sqrt{\left(\frac{\partial V}{\partial l}\cdot\frac{\Delta \mathrm{l}}{\mathrm{l}}\right)^2 + \left(\frac{\partial V}{\partial h}\cdot\frac{\Delta \mathrm{h}}{h}\right)^2 + \left(\frac{\partial V}{\partial w}\cdot\frac{\Delta \mathrm{w}}{w}\right)^2} \qquad \text{[Eq. 47]}$$

where l is the average length of a plate, h is the average height and w is the average width. $\Delta \mathrm{l}$, $\Delta \mathrm{h}$ and $\Delta \mathrm{w}$ is the measurement uncertainty.

The uncertainty of the calculated density, $\Delta\rho$, is calculated as:

$$\frac{\Delta\rho}{\rho} = \sqrt{\left(\frac{\partial \rho}{\partial m}\cdot\frac{\Delta \mathrm{m}}{m}\right)^2 + \left(\frac{\partial \rho}{\partial V}\cdot\frac{\Delta \mathrm{V}}{\mathrm{V}}\right)^2} \qquad \text{[Eq. 48]}$$

Table 5: Uncertainty of volume and density.

	$\frac{\Delta V}{V}$	ΔV	$\frac{\Delta\rho}{\rho}$	$\Delta\rho$
Teflon $_{\text{plate}}$	5.00 %	9.0055×10^{-8}	5.27 %	116.04
Lexan $_{\text{plate}}$	3.14 %	9.0717×10^{-8}	3.241 %	36.26
Stainless steel $_{\text{plate}}$	5.00 %	8.85×10^{-8}	5.263 %	409.6

Table 5 shows the uncertainty of the volume and density. The dimensions are taken from Table 1, Table 2 and Table 3, while the density is taken from Table 4.

The uncertainty of the volume of Lexan is smaller than the uncertainty of the volume of both steel and Teflon. The reason for this is that Lexan is 62.5 % higher than steel and Teflon, and it is easier to read the exact value when the dimensions are higher.

The uncertainty from the density calculations are larger than for the volume calculations. The cause for this is that the measurements of the density uses both the uncertainty from the sliding caliber and the scale.

The uncertainty of the thermal conductivity obtained from the manufacturer of Hot Disk is calculated from equation 35. This uncertainty can be calculated as:

$$\frac{\Delta k}{k} = \sqrt{\left(\frac{\partial k}{\partial \rho} \cdot \frac{\Delta \rho}{\rho}\right)^2 + \left(\frac{\partial k}{\partial Cp} \cdot \frac{\Delta Cp}{Cp}\right)^2 + \left(\frac{\partial k}{\partial \alpha} \cdot \frac{\Delta \alpha}{\alpha}\right)^2} \qquad \text{[Eq. 49]}$$

The uncertainty of the density is calculated previously, the reproducibility for the thermal diffusivity is $\pm$ 5 % and the reproducibility for the volumetric specific heat is $\pm$ 7 %.

Table 6: Uncertainty of thermal conductivity.

	$\frac{\Delta k}{k}$	Δk
Teflon $_{plate}$	10.09 %	0.026
Lexan $_{plate}$	9.19 %	0.019
Stainless steel $_{plate}$	10.08 %	1.47

It is clear from the tables that the uncertainty from the thermal conductivity increases as the uncertainty of the volume and density increase. The uncertainty of the thermal conductivity is inside the acceptable region.

The complete calculation can be seen in appendix G.

4. Comsol Multiphysics

Comsol Multiphysics is an analysis, solver and simulation software. It is especially useful when analysing multiphysics. In this thesis, Comsol Multiphysics is used to compare the simulated temperature increase in the sensor to the measurements in the laboratory.

The temperature distribution of numerical results from a book is compared to analytical results from simulation. A cylinder is simulated, and given thermophysical properties. A temperature is set to the top and the bottom of the cylinder, and the experiment is run through transient.

Later on, a sensor is implemented with a heat source on top of the cylinder. This is to compare the temperature increase in the sensor with the measurements from the laboratory. The input power is the same as the input power in Hot Disk. However, since only one of the two cylinders is simulated, the input power is divided by two. In the laboratory half of the heat goes up into the other cylinder, while the other half goes down into the cylinder simulated. In the simulation, the entire cylinder and sensor is insulated on the outer surfaces.

In this experiment, thermophysical properties are given to the material and to the sensor. The sensors material is Kapton. The dimensions of the sensor and the cylinder are put exactly as in the laboratory. The aim for this is to find the thermal contact resistance between the sensor and the material. This is done by simulating a thin layer between the cylinder and the sensor, and by giving the layer thermophysical properties. The temperature increase in the sensor from the measurements in the laboratory is compared to the increase in Comsol. The thermal conductivity of the thin resistance layer is changed until it matched the temperature increase in the laboratory.

Figure 24: Stacked interleaved materials simulated in Comsol, Steel and Lexan (Comsol).

Finally, the interleaved materials are simulated with a sensor as a heat source. Between each material and between the sensor and the material there is simulated a thin resistance layer. The goal is to get the temperature increase in the sensor to match the measurements in the laboratory. The resistance between two materials, and between the sensor and the material is changed until it matches. Figure 24 shows how the material is simulated in Comsol.

The results are shown in part 3 in subchapter 3-5.

Part 3: Discussion and results

First, the pure material plates stacked are compared with the reference. This is to see how well pure materials compare with the reference in anisotropic measurement. Later different materials are stacked interleaved.

Comsol Multiphysics is used to compare the temperature profile in the material analytical with a numerical calculation. The comparison between the numerical and analytical results will be important to learn how to use Comsol Multiphysics and to see how the simulated results compare.

In Comsol, a sensor is simulated with a cylinder. The temperature increase simulated is compared to the temperature increase in the sensor from the laboratory. At the end, the stacked materials are simulated with a sensor and compared to the results in the laboratory.

1. Comparison pure materials stacked with reference

In this experiment, the measurements were done anisotropic. 20 plates of the same material were stacked at the top of each other and compared to the reference materials. This is to see how the Hot Disk behaves at anisotropic measurements.

1.1 Teflon

Teflon is a synthetic fluoropolymer of tetrafluoroethylene. The energy transfer in polymers is accomplished by the vibration and rotation of chain molecules. Polymers are often used as insulators because of their low thermal conductivities.

Teflon measured at room temperature in the laboratory gave some strange values. This is because Teflon undergoes several phase changes from sub-ambient temperatures up to the melting point. When the temperature is below 19 °C, the structure is a well- ordered hexagonal one. This changes above 30 °C. The phase becomes a pseudo- hexagonal, which is a very disordered phase. This phase remains stable until the temperature reach the melting point around 330 °C. This means that the sample made of Teflon should be measured at temperatures below 19 °C.

Figure 25 shows how Teflon behaves with anisotropic stacked conditions at room temperature. At input power 0.15 W, the sample is probably overheated, which causes the axial thermal conductivity to be much higher than the radial one. When the heating power is lowered, the thermal conductivities are closer to each other. However, it does not make any sense that the axial thermal conductivity is that much higher than the radial one, even at lower power input. More naturally, the thermal conductivity should be higher in the radial direction. The reason for this is that the heat should be easier to transfer along the plates than through the plates. This results has probably something to do with the phase change above 19 °C. At room temperature, the average temperature is 21.13°C. At this temperature, the thermal conductivity is 0.27, while the specific heat is 2.18 MJ/m^{3}K. This is shown in Figure 18 and Figure 22. As can be seen, the thermal conductivity measured do not match the reference value.

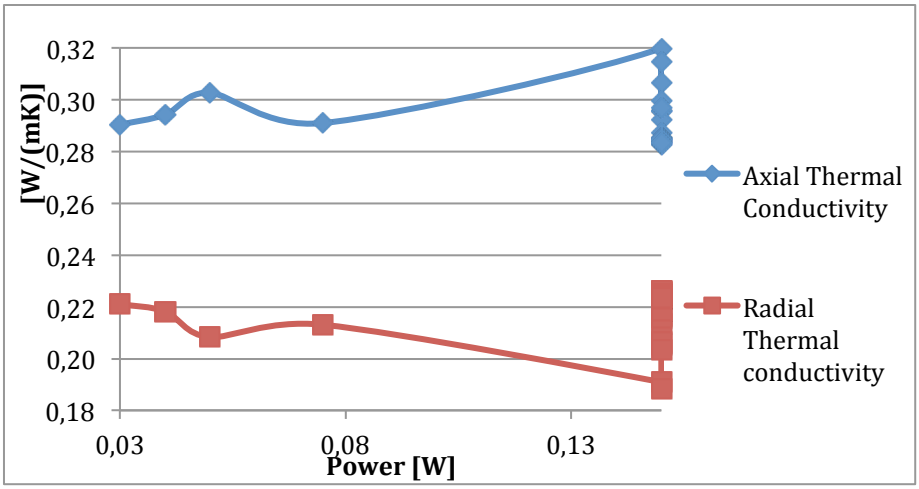

Figure 25: Teflon anisotropic measurement at room temperature.

Figure 26 shows how Teflon behaves with the oil bath at 0 °C. The reason for choosing 0 °C is to avoid the disordered phase. This shows that the radial thermal conductivity is higher than the axial thermal conductivity, as it should be. In the axial direction there will be the effect of thermal contact resistance, which leads to a lower thermal conductivity.

The average thermal conductivity is calculated with the average axial and radial thermal conductivities. The average values are calculated without the heating power 0.03 W, because as can be seen, this power is too low. A too low power means that the sensor is not heated enough before the measurement start. According to Gustavsson, the effective thermal conductivity in both radial in axial direction can be calculated. The effective thermal conductivity of an anisotropic material is given as:

$$k_{effective} = \sqrt{k_{axial} \cdot k_{radial}} = \sqrt{0.228 \cdot 0.3187} = 0.266$$

The reference value is 0.272 W/m^{2}K at 0 °C. The average thermal conductivity matches the reference value very well.

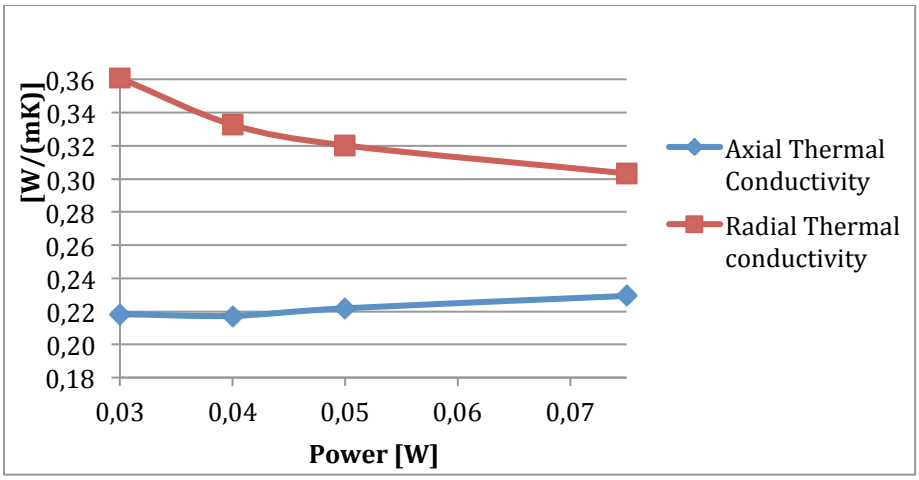

Figure 26: Teflon anisotropic measurement with oil bath.

1.2 Lexan

Polycarbonates, known by the trademark Lexan is a polymer like Teflon. It is known as a material with low thermal conductivity and density.

Figure 27 shows how the thermal conductivity of Lexan varies with power at room temperature. The value in axial direction is 10 % higher than the reference and in radial direction it is approximately 25 % higher. Hot Disk has an uncertainty of 10 %. A reason for the deviation could be an air interface between the plates of Lexan. This air interface causes a thermal contact resistance, but since the axial thermal conductivity and radial thermal conductivity are close in values, this is an indication that there is not much air between the layers. Air would cause the axial thermal conductivity to be lower. The effective thermal conductivity is calculated as:

$$k_{effective} = \sqrt{0{,}238 \cdot 0{,}217} = 0.227$$

The effective thermal conductivity causes a value 16.3 % higher than the reference value. This deviation can have something to do with the volumetric specific heat input. This has probably been set too high in Hot Disk, which causes the thermal conductivity to be too high.

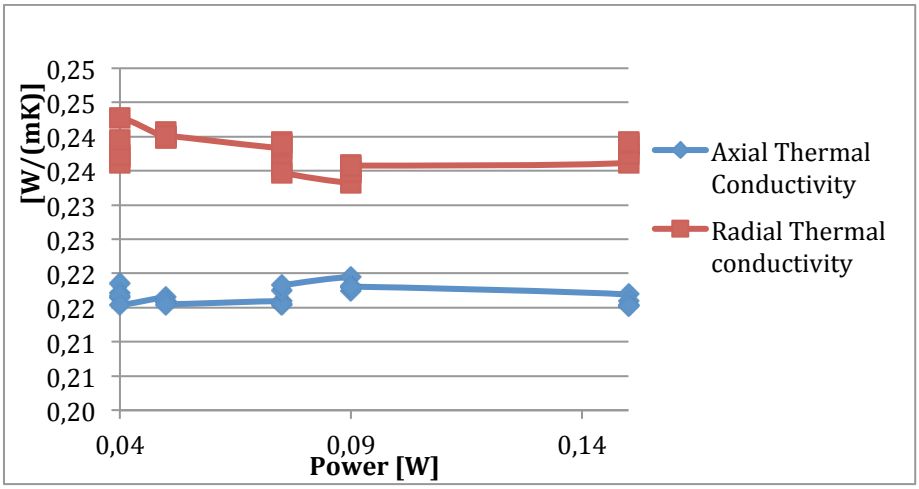

Figure 27: Lexan anisotropic measurement at room temperature.

1.3 Stainless steel 316L

Stainless steel 316L is one of the most stable stainless steels. It is a metal, and a good conductor of heat because of its high number of free electrons. If the metal is pure, the electron mechanism of heat transport is more efficient than the phonon contribution. The reason for this is that the electrons do not scatter as easy as the phonons, and have higher velocities. If the metal has impurities, as stainless steel 316L has, this will lead to a reduction in thermal conductivity. The efficiency of the electron motion will be lowered because the impurity will act as scattering centers.

At the anisotropic measurement the average room temperature during the measurement are 21.5 °C. At this temperature, the reference value of the thermal conductivity is 15.16, while the specific heat is 3.87 MJ/m^{3}K. This is shown in Figure 19 and Figure 23.

$$k_{isotropic} = \sqrt{{k_{axial}}^2 + {k_{radial}}^2} = \sqrt{0.4175^2 + 13.6257^2} = 13.63 \neq 15.16$$

According to the calculation the value does not match completely. This can be because it is hard to find the right reference of the thermal conductivity. The value at this temperature measured in the project thesis matches perfectly. In the project thesis the value was measured with two stainless steel cylinders.

The effect of air between the layers should be taken into account when dealing with the stainless steel plates. This is the stiffest of the materials, and there will be more air present in between the plates.

$$\frac{Height\ steel\ plate}{k_{stål}} + \frac{Height\ air(x)}{k_{air}} = \frac{Height\ of\ the\ entire\ stack}{Total\ conductivity}$$

$$Height\ air\ (x) = k_{air}\left(\frac{height\ entire\ stack}{k_{total}} - \frac{height\ steel\ plate}{k_{steel}}\right)$$

$$Height\ air\ (x) = 0.025 \cdot \left(\frac{10\times10^{-3}m}{13.63} - \frac{0{,}5\times10^{-3}m}{15.16}\right)$$

$$Height\ air\ (x) = 1.75\times10^{-5}\ m = 0.0175\ mm$$

This calculation shows how much air there are between each plate. However, this is a simplification of the calculation, but as can be seen, there is a bit air present between the plates. This causes a thermal contact resistance, which will influence the results.

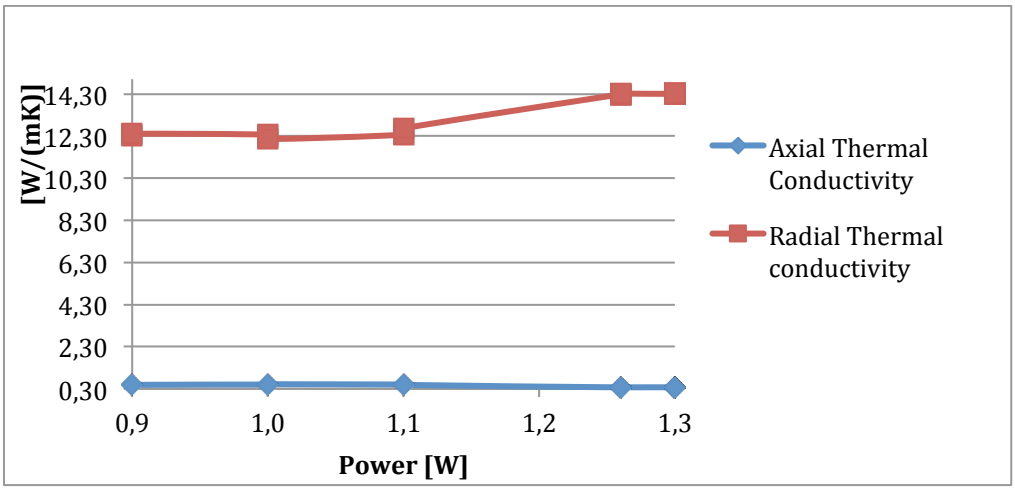

Figure 28: Stainless steel anisotropic measurement at room temperature.

2. Comparison stacked materials

2.1 Steel and Teflon stacked

The first measurements were done with steel and Teflon stacked interleaved. Steel was closest to the sensor. Later on, the Teflon plates were closest to the sensor. These experiments were done in the oil bath, because of the phase change of Teflon.

These anisotropic measurements were ran a couple of times, because it was difficult to find the right input parameters. The sample required lower measurement time than assumed. As can be seen from equation 36, the characteristic time and the measured time are interrelated. With too high measured time, the characteristic time would be too high if the probing depth and resistance is constant. However, this could also lead to an increase in probing depth and a decrease in characteristic time. This will interfere with the results and cause a thermal diffusivity decrease following:

$$\Delta p = 2\sqrt{\alpha \cdot t} \qquad \text{[Eq. 50]}$$

This will also lead to an decrease in thermal conductivity following:

$$\alpha = \frac{k}{\rho \cdot C_p} \qquad \text{[Eq. 51]}$$

With this in mind, different input parameters, shown in Table 7, are used. These parameters gave a characteristic time inside the acceptable region.

Table 7: Input parameters Steel and Teflon stacked.

Input power [W]	0.4 / 0.6 / 0.8 / 2 / 1.1
Measurement time [s]	20
Specific Heat [MJ/m^{3}K]	3.023

Figure 29 shows how the thermal conductivity varies with the input power for the steel and Teflon stacked interleaved with steel closest to the sensor at 0 °C, while Figure 30 shows the thermal conductivity of Teflon and steel with Teflon closest to the sensor. The curve of the radial and axial thermal conductivity is almost completely straight except for a 1.0 W and 1.1 W. This means that this input power is too high, and the sensor is heated.

As assumed, the axial thermal conductivity in both cases is low because the heat transfers more slowly through the plates. However, the radial thermal conductivity should be the average of the thermal conductivity of steel and Teflon:

$$k_{average} = \frac{k_{steel} + k_{teflon}}{2} = \frac{14.5 + 0.27}{2} = 7.385 \ \frac{W}{mK}$$

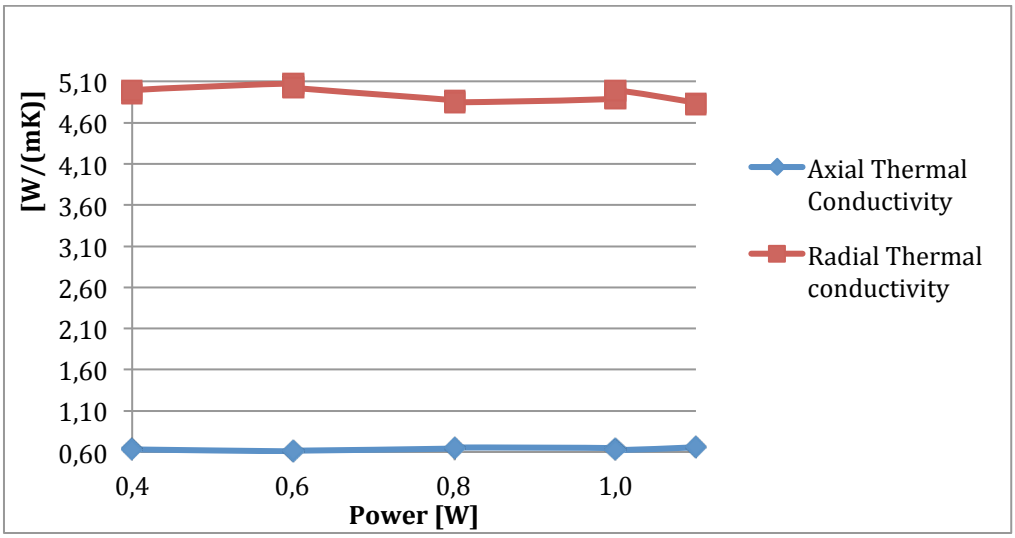

Figure 29: Steel and Teflon stacked interleaved at 0 °C.

According to the figures, the measurements with steel closest to the sensor give a too low radial thermal conductivity, while the measurements with Teflon closest to the sensor give a too high thermal conductivity. It seems strange that the measurements with Teflon closest to the sensor gave a higher thermal conductivity, but this is probably linked to the probing depth. Since Teflon has a lower thermal conductivity than steel, the measurements with Teflon closest to the sensor give a probing depth almost 3 mm lower than with steel closest to the sensor. This is because the heat moves more slowly across the Teflon plate.

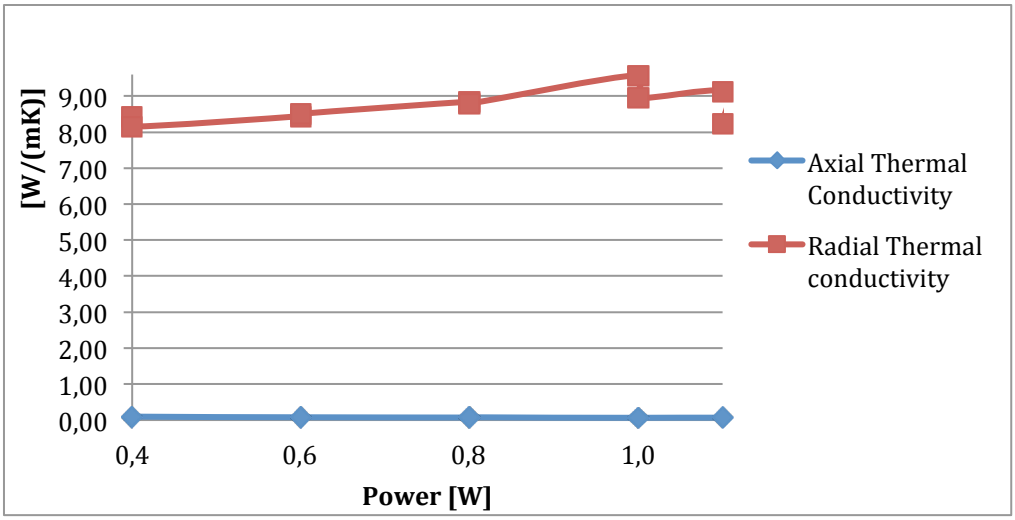

Figure 30: Teflon and Steel stacked interleaved at 0°C.

2.2 Steel and Lexan stacked

The first measurements done were with steel and Lexan stacked interleaved. Steel was closest to the sensor. Later on, the Lexan plates were closest to the sensor. These experiments were done at room temperature.

As can be seen in Table 8, the same input power and measurement time as for steel and Teflon were being used. This is because Lexan has approximately the same thermal properties as Teflon.

Table 8: Input parameters Steel and Lexan stacked.

Input power [W]	0.4 / 0.6 / 0.8 / 2 / 1.1
Measurement time [s]	20
Specific Heat [MJ/m^{3}K]	2.689

Figure 31 shows how the thermal conductivity varies with input power for steel and Lexan stacked interleaved with steel closest to the sensor at room temperature, while Figure 32 shows the thermal conductivity with Lexan closest to the sensor. The curve of the radial thermal conductivity is almost completely flat, which indicate that the input power is correct without heating of the sensor.

The axial thermal conductivity in both cases are low, because the heat transfer is slower through the plates. However, the radial thermal conductivity in both cases should be the average of the thermal conductivity of steel and Lexan:

$$k_{average} = \frac{k_{steel} \cdot h_{steel} + k_{lexan} \cdot h_{lexan}}{total\ height}$$

$$k_{average} = 15 \cdot \frac{0.5\ mm}{1.3\ mm} + 0.19 \cdot \frac{0.8\ mm}{1.3\ mm} = 5.84 \frac{W}{mK}$$

In this average thermal conductivity, the plates different height must be taken into account. The Lexan plate is 62.5 % higher than the steel plate, and this causes the low thermal conductivity of Lexan to influence the average thermal conductivity more than steel.

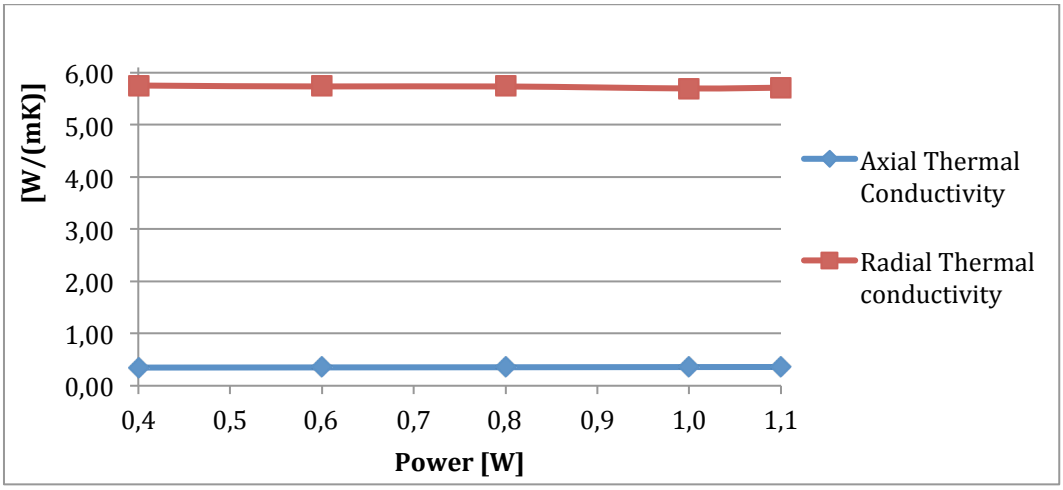

Figure 31: Steel and Lexan stacked interleaved at room temperature.

According to the figures, the measurements with steel closest to the sensor give a very similar radial thermal conductivity to the ideal, and the measurements with Lexan closest to the sensor give a too high thermal conductivity. The axial thermal conductivity is low, as it should be.

The results with Lexan closest to the sensor are similar to the measurements with Teflon and steel. They seem strange, but the deviation has probably something to do with the probing depth. In the radial direction, the probing depth of Lexan closest to the sensor is almost 2 mm higher than with steel closest to the sensor.

Ideally, an infinite time and dimension of the samples should be used to ensure more accurate results. The results are too dependent of the probing depth because of transient measurement. The heat would only reach as far as the time input in Hot Disk allows it. These results indicate that there are more steel layers in the measurement. This can be calculated by:

$$\Delta p = 11.83\ mm$$

$$\Delta p = \frac{11.83\ mm}{1.3\ mm} = 9.1$$

This means that there are more than 9 of both the steel and Lexan stacked at top of each other. It is solved analytically, and calculated that there are 10 layers of Lexan and 9 layers of steel. This will influence the results from the laboratory, and this should lead to lower thermal conductivity. However, this calculation is an approximate, and it could be a fewer layers of both steel and Lexan. The probing depth used is the average probing depth.

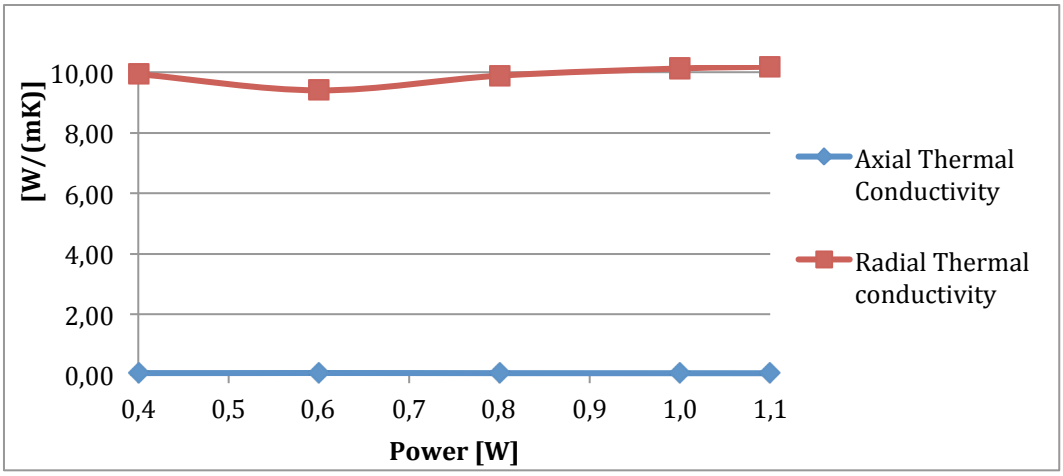

Figure 32: Lexan and Steel stacked interleaved at room temperature.

Both the experiment of steel and Teflon stacked interleaved and Lexan and steel interleaved could be improved by improving the setup of the samples. The setup did not ensure a good pressure distribution. The pressure is mostly oriented at the edges of the material, and a lot of air could be in the middle of the sample. To ensure a better pressure distribution, a screw clamp with a small stainless steel piece is used. Figure 33 shows schematic how the setup was before, and how it is improved.

This gave a small improvement, however, an even better way of distributing the pressure should be investigated.

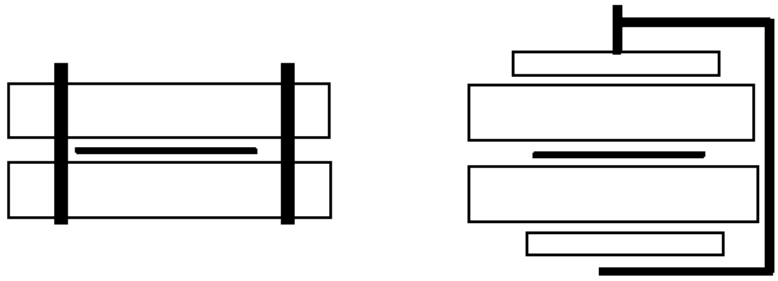

Figure 33: Setup for better power distribution.

3. Comparison analytical and numerical results

The aim is to compare the temperature profile in a simulation with the numerical results from calculation. To do this, Comsol Multiphysics is used to simulate a cylinder and setting a temperature at the bottom. The initial temperature is 273.15 K. The temperature profile is shown in Figure 34.

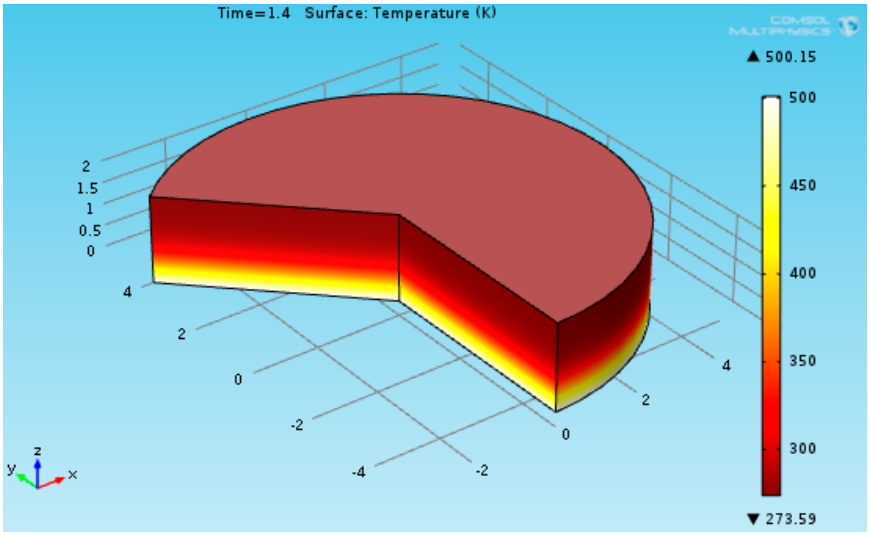

Figure 34: Temperature profile Teflon cylinder Comsol Multiphysics (Comsol).

The numerical solution can be done in two ways. This is either by using the one term approximation solution or by using the semi-infinite solution.

The one term approximation uses a midterm temperature chart. This chart is shown in appendix B, and it uses the Biot number and error function. The Biot number, which is a dimensionless quantity, gives the ratio of heat transfer inside and at the surface of a body. The Biot number is calculated as:

$$Bi = \frac{hL}{k} = \frac{heat\ convection}{heat\ conduction} \qquad \text{[Eq. 52]}$$

where h is the heat transfer coefficient, L is the characteristic length and k is the thermal conductivity. The heat transfer coefficient can be calculated by Newton`s law of cooling as:

$$q = h \cdot A \cdot (T_s - T_\infty) \qquad \text{[Eq. 53]}$$

where q is the heat transferred per unit time, h is the heat transfer coefficient, A is the heat transfer area of the surface and dT describes the temperature difference between the surface and the bulk fluid. The heat transfer coefficient describes temperature loss between the gas or fluid and the solid, but in this simulation there is no temperature loss. The reason for this is that the surface of the body is suddenly brought to the infinite temperature at t= 0 and kept at this temperature at all times. This causes the heat transfer coefficient to be infinite, which also causes the Biot number to be infinite at all the materials.

Fourier number gives the dimensionless time, and it is the value to be read out of the chart. Fourier number is calculated by:

$$Fo = \tau = \frac{\alpha t}{L^2} = \frac{diffusive\ transport\ rate}{storage\ rate}$$ [Eq. 54]

where α is the thermal diffusivity, t is the time and L is the characteristic length. To calculated the measuring time:

$$t = \frac{Fo \cdot L^2}{\alpha}$$ [Eq. 55]

Table 9: Biot number, Fourier number and time.

	$Teflon_{273K}$	$Steel_{273K}$	$Steel_{293K}$	$Lexan_{293K}$
Bi	∞	∞	∞	∞
1/Bi	0	0	0	0
Fo	2.95	2.95	2.95	2.95
2·L [mm]	4	4	4	4
α [m^2/s]	1.29×10^{-7}	3.86×10^{-6}	3.896×10^{-6}	1.257×10^{-7}
t [s]	91.47	3.06	3.03	93.87

However, in this calculation, the semi-infinite solution is used. The semi-infinite solution uses the complementary error function directly. Since the specific surface temperature is constant, the complementary error function is calculated as:

$$\frac{T(x,t)-T_i}{T_S-T_i} = erfc\left(\frac{x}{2\sqrt{\alpha t}}\right)$$ [Eq. 56]

Figure 35 shows how the temperature is distributed in the plate. At the outlet of the plate, the complementary error function should be 0.001. This means that the temperature variation is 0,001:

$$\frac{T(2\ mm)-T_i}{T_S-T_i} = 0.001$$ [Eq. 57]

When the complementary error function is 0.001, it can be seen from a table that:

$$\eta = 2.3311 = \frac{x}{2\sqrt{\alpha t}}$$ [Eq. 58]

At the start of the plate, there will be no error, which causes the complementary error function to be 1.

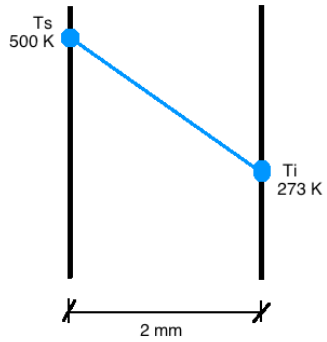

Figure 35: Temperature distribution in a thin plate.

Table 10 shows the calculated time with semi-infinite solution. This is the time used in the Comsol Multiphysics simulations.

Table 10: Time calculation at semi-infinite solution.

	$Teflon_{273K}$	$Steel_{273K}$	$Lexan_{293K}$
α [m^2/s]	1.29×10^{-7}	3.86×10^{-6}	1.257×10^{-7}
t [s]	1.43	0.04845	1.464

Figure 36 shows the temperature profiles of the numerical and the analytical calculations. These graphs are located exactly at the top of each other, which means that the temperature profiles are similar. Both Lexan and stainless steel results are shown in appendix C.

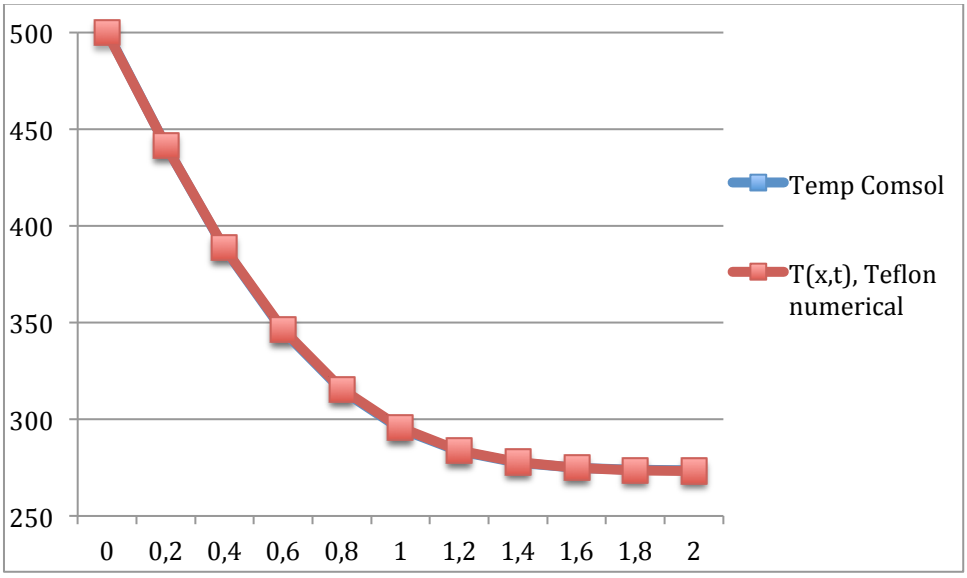

Figure 36: Temperature profile for Lexan numerical results and Comsol Multiphysics.

4. Comparison temperature increase in sensor TPS method and Comsol Multiphysics, cylinders.

The sensor from the transient plane source method is simulated with a cylinder of a pure material in Comsol Multiphysics. The temperature increase indicated in this sensor, is compared to the temperature increase in the sensor of the experiments in the laboratory.

Teflon, stainless steel and PMMA were investigated. PMMA was used instead of Lexan because Lexan was only available in small, thin plates. However, only the simulation of the steel cylinder is shown, the rest is implemented in appendix D. In this appendix, the thermal properties for the sensor, the resistive layer and the material is shown.

The sensor is implemented as a heat source with an input power equal to the one used the laboratory. However, the power is divided by a factor of two, because half of the power input in Hot Disk would be used to heat up the other cylinder. In Comsol, the sensor is insulated on all sides, except for against the material.

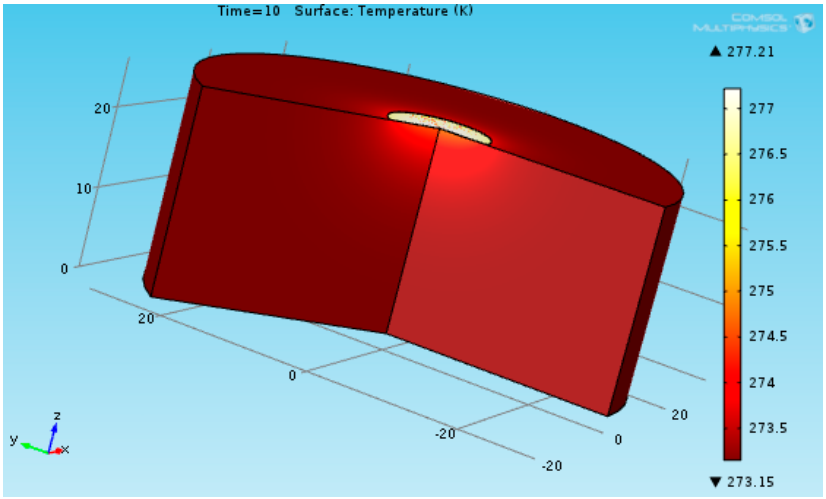

Figure 37: Temperature increase in Comsol Multiphysics simulation of Stainless Steel after 10 seconds (Comsol).

The thermal contact resistance between the sensor and the cylinder is an important parameter, which will influence the temperature increase in the sensor. The sensor acts both as a heat source and a resistance thermometer. The thermal contact resistance is calculated as:

$$R''_{t,c} = \frac{\delta}{k_r} = \frac{T_A - T_B}{q''_x} \qquad \text{[Eq. 59]}$$

where δ is the thickness of the layer and k is the thermal conductivity of the layer. This effect will be important in composite systems, because the thermal contact resistance causes the temperature drop across the interface between two materials. The thermal contact resistance is due to surface roughness effects. Figure 38 shows temperature drop due to thermal contact resistance. As can be seen in the figure, contact spots are interspersed with gaps, which often are filled with air. Heat transfer over the surface will be due to conduction across the actual spot where the surfaces contact each other and due to conduction and/or radiation across the gaps. This means that the contact resistance is due to both the contact spots and the gaps. In very rough surfaces, the contact resistance is mostly due to the gaps (Incropera, DeWitt, Bergmann, & Lavine, 2006).

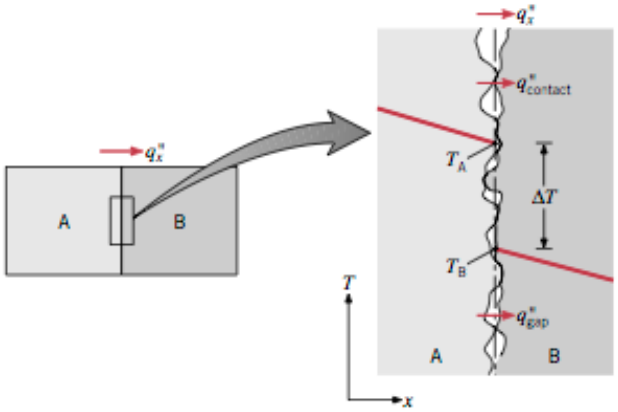

Figure 38: Temperature drop due to thermal contact resistance (Incropera, DeWitt, Bergmann, & Lavine, 2006).

Increasing the area of the contact spots may reduce the thermal contact resistance. This increase can be done by increasing the joint pressure and/or reducing the roughness of the adjacent surfaces (Incropera, DeWitt, Bergmann, & Lavine, 2006).

Table 11: Thermal contact resistance for Teflon, Steel and PMMA.

	Teflon	Steel	PMMA
Thickness [m]	1×10^{-5}	1×10^{-5}	1×10^{-5}
Th. cond. resistive layer [W/mK]	3.5×10^{-3}	0.32×10^{-1}	0.35×10^{2}
Thermal resistance [m^2K/W]	2.86×10^{-3}	3.125×10^{-4}	2.857×10^{-7}

In the experiment in the laboratory, the contact spots is interspersed with air filled gaps, and this causes a thermal contact resistance between the material and the sensor. The resistance is decreased when the thermal conductivity of the material is greater than air. Since air has a very low thermal conductivity, all the materials investigated have a higher conductivity. However, PMMA has a very smooth surface, and this causes a low thermal contact resistance. According to Incropera (2008), the thermal resistance of stainless steel should be in the range of $6\text{-}25\cdot10^{-4}$ m^2K/W at a contact pressure 100 kN/m^2. However, the contact pressure should be further looked into.

The contact pressure is calculated as:

$$P = \frac{F}{A} = \frac{9.81*m}{A_{sensor}+A_{cylinder}} \qquad \text{[Eq. 60]}$$

It is important to remember to take into account the entire surface area of the sensor. The mass is both the mass of the cylinder and the mass of the weight on top of the cylinder.

Table 12: Contact pressure for Teflon, steel and PMMA cylinders.

	Teflon	Steel	PMMA
Mass $_{cylinder}$ [kg]	0.156	0.585	0.086
Mass $_{weight}$ [kg]	1.8366	2.563	0.5
Area $_{sensor}$ [m^2]	1×10^{-3}	8.258×10^{-4}	8.258×10^{-4}
Area $_{cylinder}$ [m^2]	2.88×10^{-3}	2.88×10^{-3}	2.88×10^{-3}
Contact pressure [kN/m^2]	5.04	32.35	1.59

Since stainless steel is the heaviest material, and it is the one with the highest contact pressure. It is seen that this contact pressure is lower than 100 kN/m^2. This should give a higher thermal contact resistance than the reference value from the book written by Incropera and DeWitt.

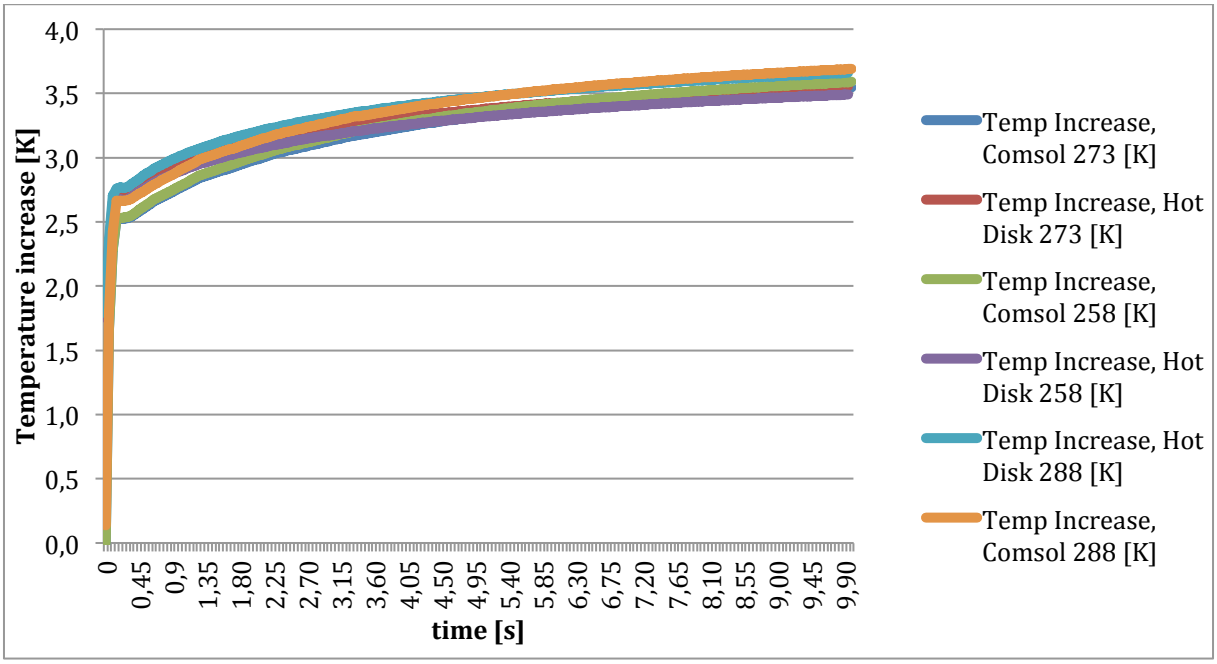

Figure 39: Temperature increase comparison between Hot Disk and Comsol for Stainless Steel.

It is also investigated how the input parameters in Comsol Multiphysics can manipulate the results. As discussed, the thermal contact resistance will influence the temperature increase, and an increase or decrease in this value will change the front part of the curve. However, a change in the thermal conductivity of the material investigated will change the curve at the end of the transient measurement. Figure 40 shows how the thermal conductivity and resistance between the sensor and the material affects the temperature increase. When the resistance is decreased or increased by 50 % it is seen that the front part of the curve is greatly affected. This means that a change in resistance between the sensor and the material causes a change at the start of the measurements. An increase in resistance causes an accelerated temperature increase, while a decrease causes a lower curve. This means that a high thermal resistance between the material and the sensor causes a higher temperature increase in the sensor. This is because the high resistance in the thermal contact resistance layer causes the heat to move more slowly across the layer.

When changing the thermal conductivity of the material, the latter part of the curve is affected the most. The reason for this is that at the start of the simulation, the heat has not pushed through the contact layer to the material, and there will be no changes. The thermophysical properties of the material will then not affect the temperature increase. However, after 10 seconds, an increase in thermal conductivity causes a lower temperature increase. This is because when the material conducts heat better, the heat is conducted faster away from the sensor where the temperature increase is measured.

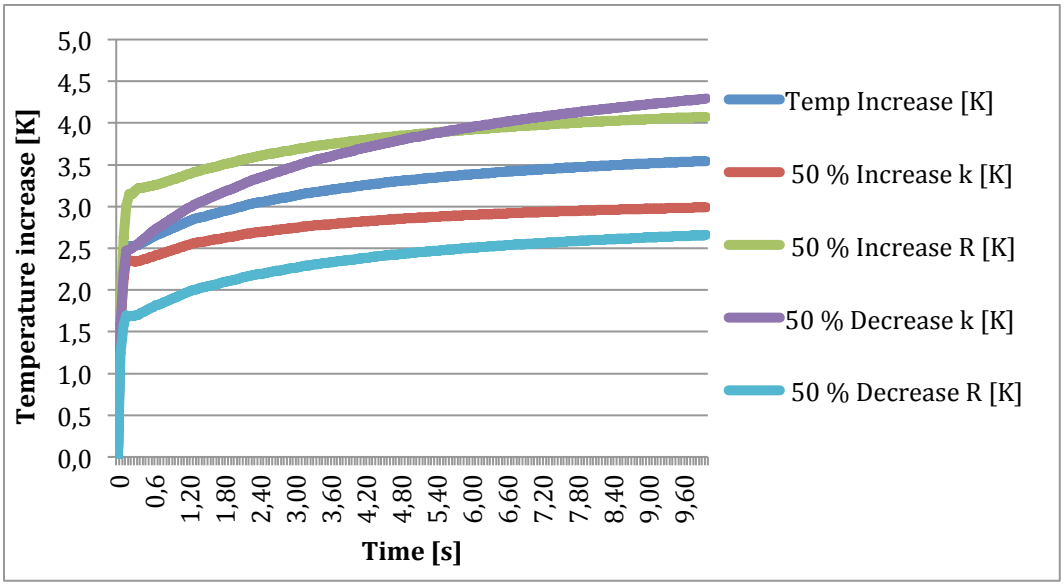

Figure 40: How the thermal conductivity and resistance changes the temperature increase in Comsol.

5. Comparison temperature increase in sensor TPS method and Comsol Multiphysics, stacked materials

A sensor is simulated with stacked materials, and the temperature increase in this sensor is compared to the temperature increase measured in Hot Disk. This is to see how these matches, and to understand what's the cause of the deviation from the laboratory. The temperature increase from the sensor in the laboratory can be hard to interpret in highly anisotropic materials.

In Comsol Multiphysics, many different material combinations are tested. These are simulations with steel closest to the sensor stacked with Teflon, Teflon closest to the sensor stacked with steel, Lexan closest to the sensor stacked with steel and steel closest to the sensor stacked with Lexan. However, only the two simulations with steel and Teflon are shown. The rest is implemented in appendix E. In this appendix, the thermal properties for the sensor, the resistive layer and the material is shown.

It is important to see how many layers should be implemented in the simulation, so that the heat does not reach further then what is simulated. Equation 54 is used to calculate this. However, the smallest length is chosen. This is because the material with the lowest thermal conductivity will determine how far the heat will reach before it stops.

Table 13: How far the temperature will reach in the material.

	Lexan $_{293\ K}$	Steel $_{293\ K}$	Steel $_{273\ K}$	Teflon $_{273\ K}$
Fo	2.95	2.95	2.95	2.95
α [m^2/s]	1.257×10^{-7}	3.896×10^{-6}	3.86×10^{-6}	1.29×10^{-7}
Time [s]	20	20	20	20
L [mm]	0.923	5.14	5.12	0.935

Table 13 shows how far the heat will reach in the material. This calculation shows that there should be two layers of each material of both the simulation of steel and Lexan (0.8 mm), and steel and Teflon (0.5 mm).

The sensor is implemented as a heat source with an input power equal to the one used the laboratory. However, the power is divided by a factor of two, because half of the power input in Hot Disk would be used to heat up the other half of the material. In Hot Disk, the sensor is insulated on all sides, apart from against the material.

Table 14: Thermal conductivity and thermal contact resistance Steel and Teflon stacked.

	Teflon/Steel	Steel/Teflon
Thickness $_{sensor/material}$ [m]	1×10^{-5}	1×10^{-5}
Th. cond. Resistive $_{sensor/material}$ [W/m·K]	0.9×10^{-2}	2×10^{-2}
Thermal resistance $_{sensor/material}$ [m^2K/W]	1.11×10^{-3}	5×10^{-4}
Thickness $_{material/material}$ [m]	1×10^{-5}	1×10^{-5}
Th. cond. Resistive $_{material/material}$ [W/m·K]	2.3×10^{-2}	1×10^{2}
Thermal resistance $_{material/material}$ [m^2K/W]	4.35×10^{-4}	1×10^{-7}

Table 14 shows the thermal conductivity and thermal contact resistance for steel and Teflon stacked. When a further look at the simulations with steel closest to the sensor is done, it can be seen that the resistance between steel and the sensor is much larger than between Teflon and steel. Between these two materials, there are no thermal contact resistance.

The simulations with Teflon closest to the sensor shows that the thermal contact resistance between the sensor and Teflon is bigger than between the two materials. The measurements with Teflon closest to the sensor gave a much larger thermal contact resistance between the two materials than with steel closest to the sensor. This has probably something to do with the cutting of the materials. Some of the steel plates had some irregularities at the edges, and this will influence the thermal contact pressure.

The thermal contact resistance between the sensor and the materials in the two different cases are closer in value. The reason for this is that the same weight is put on the top of the samples. But since Teflon has a rougher surface, this thermal contact resistance is larger.

At the start of the simulation, the thermal contact resistance between the sensor and material found in the previous subchapter is used. However, this proved not to be accurate. The reason for this is that the surface of the plates is smoother than the cylinders. It was clear that thermal contact resistance between the sensor and the materials should be changed when Teflon closest to the sensor was investigated. Teflon, which is a polymer, is an insulating material, and the heat only reached this material.

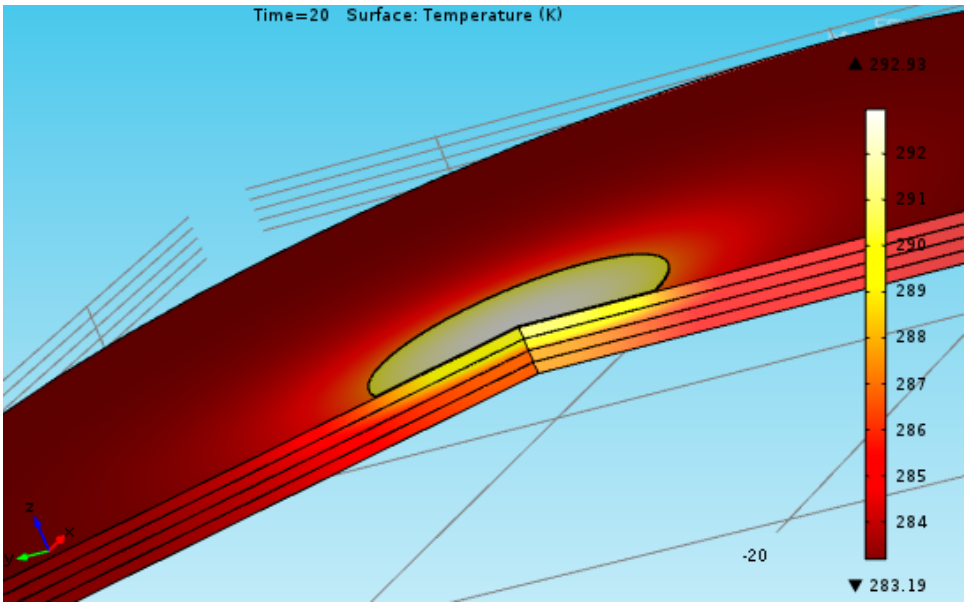

Figure 41: Temperature profile of Steel and Teflon stacked (Comsol).

Figure 41 shows the temperature profile of steel and Teflon stacked with steel closest to the sensor at the end of the transient measurements. Figure 42 shows the temperature increase in the simulated sensor compared to the measured increase in the laboratory experiment. The curves ends up ends at the same point, but they deviate some in the middle. This means that the thermal conductivity between the two materials is a bit high. A decrease in thermal conductivity of this layer leads to an increase in thermal contact resistance. When the thermal contact resistance increases, the temperature in the sensor will increase. This is obvious because when the heat is conducted slower, a larger temperature will be at the sensor.

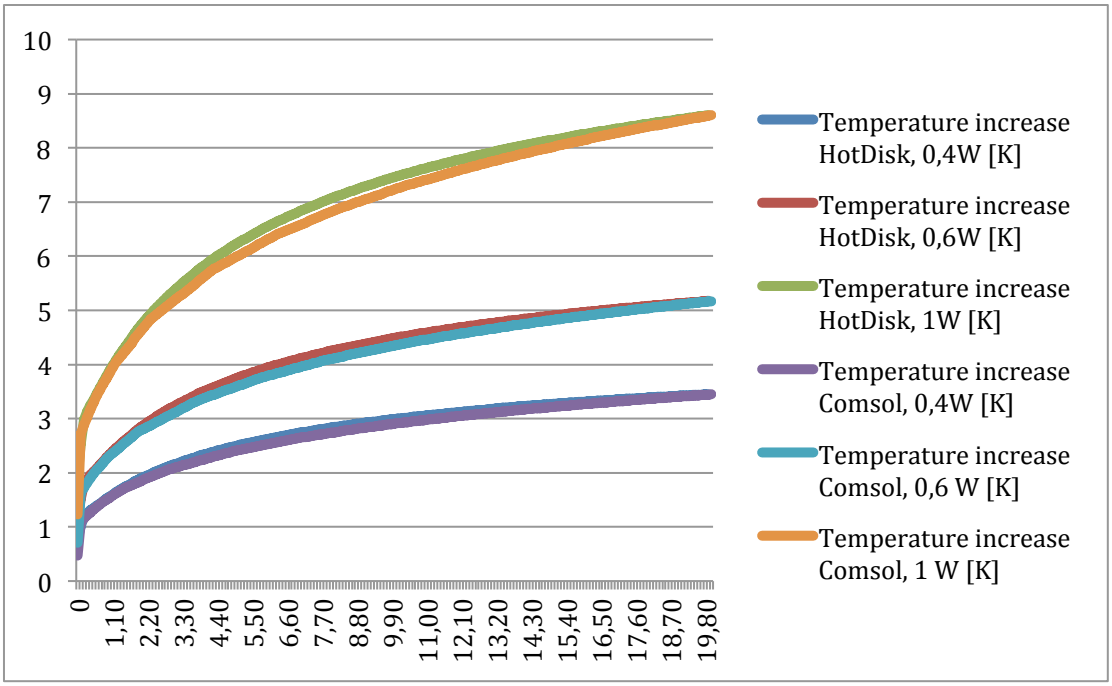

Figure 42: Temperature increase comparison Steel and Teflon stacked.

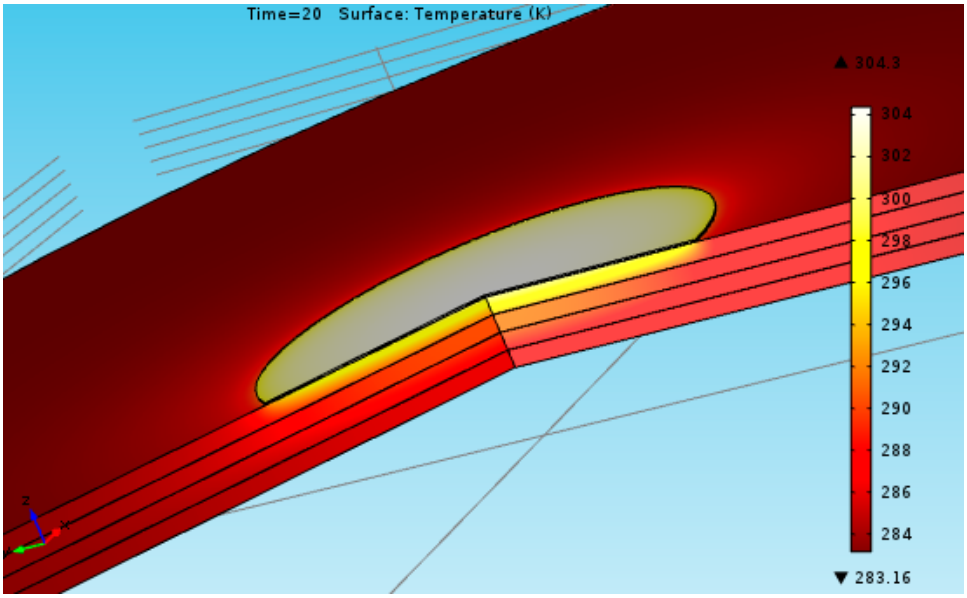

Figure 43: Temperature profile of Teflon and Steel stacked (Comsol).

Figure 43 shows the temperature profile of Teflon and steel stacked with Teflon closest to the sensor at the end of the transient measurements. When comparing it to Figure 41, it can be seen that the heat will not penetrate as far into the stack with Teflon closest to the sensor. This is because of the low conductance of Teflon. More of the heat from the sensor is used to heat up the sensor, and will not go down into the material.

Figure 44 shows the temperature increase in the sensor simulated compared to the increase measured in the experiment in the laboratory. The curves matches very well at heating power 0.4 W and 0.6 W. However, at 1.0 W there is a larger deviation. This is because at this high power, the sensor in the measurement in the laboratory was heated too much, thus, this large power should not be used.

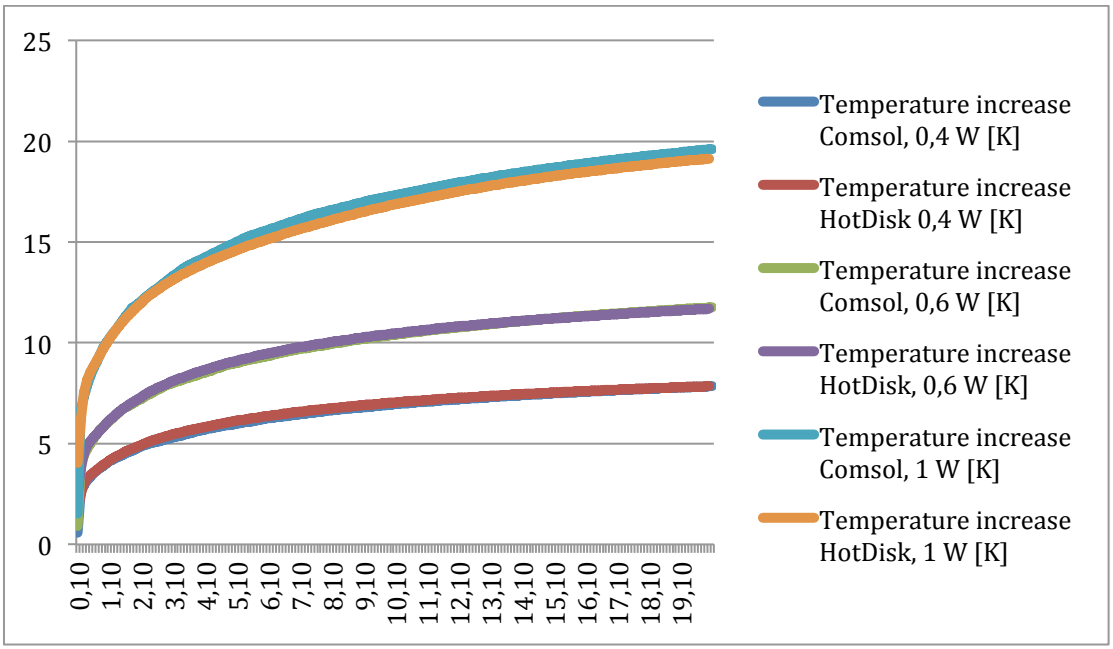

Figure 44: Temperature increase comparison Teflon and Steel stacked.

Table 15 shows the thermal conductivity and thermal contact resistance for the measurement with steel and Lexan stacked. The thermal contact resistance between both the sensor and the material, and between the two different materials are higher for steel stacked closest to the sensor. This is reasonable for the sensor, because the surface of steel is rougher than the surface of Lexan. The temperature profile and temperature increase comparison is shown in appendix F.

Table 15: Thermal conductivity and thermal contact resistance Steel and Lexan stacked.

	Lexan/Steel	Steel/Lexan
Thickness $_{sensor/material}$ [m]	1×10^{-5}	1×10^{-5}
Th. cond. Resistive $_{sensor/material}$ [W/m·K]	0.9×10^{-1}	2×10^{-2}
Thermal resistance $_{sensor/material}$ [m^2K/W]	1.11×10^{-4}	5×10^{-4}
Thickness $_{material/material}$ [m]	1×10^{-5}	1×10^{-5}
Th. cond. Resistive $_{material/material}$ [W/m·K]	5×10^{2}	3×10^{-1}
Thermal resistance $_{material/material}$ [m^2K/W]	2×10^{-8}	3.33×10^{-5}

To evaluate how well the data points measured in the laboratory fits the Comsol Multiphysics simulated values; two and two values are compared and multiplied by the time difference.

$$Res = (\sum T_{measured} - \sum T_{simulated}) * \Delta t$$

For the measurements with steel and Teflon with steel closest to the sensor the greatest deviation is between 0.1 and 0.2 seconds for input power 0.4 W. This means that the resistance between the sensor and steel probably should be a little higher. For heating power 0.6 W, the largest deviation is between 6.7 and 6.9 seconds. For heating power 1.0 W, the largest deviation is between 7.3 and 7.5 W. Both these deviations means that the resistance between the steel and Teflon layer should be a little larger. The smallest deviation for all the input powers is at the end of the measurements.

For the measurements with Teflon and steel with Teflon closest to the sensor, the greatest deviation is at the start of the recording for input power 0.4 W and 0.6 W. This probably means that there should be a larger thermal contact resistance between the material and the sensor. The input power of 1.0 W has the largest deviation. As explained, the cause is probably that the power heats the sensor too much.

The complete results for the curve fit quality are shown in appendix F.

6. Discussion

The laboratory results of the stacked interleaved plates are surprising. Since the layered materials can be modelled in series, there is an assumption that the radial thermal conductivity is the average of the two materials. This proved not to be correct. This would only be true if the time and dimensions of the sample is infinite. Since the measurements are transient, the heat only moves to a certain point, which causes the thermal conductivity to be too high or too low.

There are different parameters that affect the thermal conductivity of the anisotropic materials measured in the laboratory. Transient measurements mean that the heat only reaches the probing depth after a certain time. The order of which material is closest to the sensor will have something to say when investigating the probing depth. The heat moves faster over the steel plates than the Teflon plates, since steel conducts heat better than Teflon. This means that the probing depth for Teflon closest to the sensor is lower in the radial direction than with steel closest to the sensor. The measurements with steel closest to the sensor will include more plates, which leads to a more accurate estimation of the thermal conductivity.

It is clear that the thermal conductivity of air influences the thermal conductivity of the anisotropic materials. It was tried to improve the setup with a better pressure to make sure the plates got pressed closer together. This made the results a little better, but a better setup should be used in later experiments.

The temperature increase in the sensor is simulated in Comsol Multiphysics and compared to the results in the laboratory for a cylinder. When the temperature increase is investigated it shows that the air between the gaps on the surface can cause a large thermal contact resistance between the sensor and the cylinder. For the cylinders, Teflon has the highest thermal contact resistance between the sensor and the material. One of the reasons for this is that Teflon has a rough surface. The PMMA cylinder has almost no thermal contact resistance. The surface of this cylinder is very smooth, and a heavy weight is used on top of the construction of the samples to make the resistance less.

However, in the stacked materials, there are thermal contact resistance both between the material and the sensor and between the two materials. Investigation of the temperature increase curve in Comsol Multiphysics made it clear that it was important to investigate the thermal conductivity of the material, the resistance layer between the sensor and the material and the resistance layer between each material. It was not only important what material was closest to the sensor, but also which one of the plates it was. Some of the steel plates had irregularities near the edges, and this will influence the thermal contact resistance.

7. Further work

It seemed like the measurement time in the experiments done in this thesis is too short. This causes the measurements to be too dependent on the order the materials are stacked in. However, if the measurement times were higher, there would be a need for a lot more layers. Too few layers cause the order and probing depth of the materials to be important. This is not desirable, and for further investigation a larger time and sample size should be used.

It could also be interesting to investigate more anisotropic materials. This could for example be by stacking steel plates interleaved with thin aluminium foil. This would make the air interface smaller, and this should be looked into.

It was attempted to create a setup that ensured a better pressure distribution to the material. This improved the results a little. A way to create a better thermal contact between the layered materials should be investigated further. The plates should be pressed more tightly together to prevent as much air as possible to get in between them. This would ensure that the thermal conductivity of the air would not influence the results as much, resulting in a more accurate effective thermal conductivity.

8. Conclusion

When the pure materials are stacked and measured anisotropic, it is seen that the axial and radial thermal conductivity of these materials behaves exactly as expected. There are, however, some deviation in the Lexan measurements. The cause of this is that a wrong volumetric specific heat parameter is set as input in the analysis software. This leads to a higher thermal conductivity than the reference value. The uncertainty of the thermal conductivity of the plates is within the goal of 10 %.

Investigation of anisotropic materials gave some unexpected values. It was only steel and Lexan, with steel closest to the sensor, that gave the correct thermal conductivity in radial direction. However, when Lexan was closest to the sensor, the radial thermal conductivity got way too high. The same results were shown when Teflon and steel was investigated. When steel was closest to the sensor, the radial thermal conductivity got lower than expected, while with Teflon closest to the sensor, the radial thermal conductivity got higher. In the axial direction, the thermal conductivity is low in every case.

The temperature increase in the sensor was simulated in Comsol Multiphysics. The resistance between the sensor and the material, and between the two materials, were adjusted until the results matched the measurement from the laboratory. A too high input power made it impossible to match the temperature increase from the simulation with the temperature increase from the laboratory. Also, it was clear that the materials should be cut more accurately. There was some deviations that probably was the consequence of irregularities along the edge of the sample.

It is unclear if the transient plane source method could be used to further investigation of anisotropic materials. There are some great deviations in the stacked materials, but a better pressure distribution and more precisely cut samples should be tested before a conclusive answer could be given.

9. References

Bouguerra, A., Ait-Mokhtar, A., & Diop, M. (2001). *Measurement of thermal conductivity, thermal diffusivity and heat capacity of highly porous building materials using transient plane source technique.* France.

Canada, N. R. (2010, September 26). *Nanotechnology for High Performance Thermal Insulation*. Retrieved May 27, 2014 from http://archive.nrc-cnrc.gc.ca/: http://archive.nrc-cnrc.gc.ca/eng/projects/irc/thermal-insulation.html

Cengel, Y., Turner, R., & Cimbala, J. (2008). *Fundamentals of Thermal- Fluid Science.* McGraw-Hill.

Chen, G., Borca-Tasciuc, D., & Yang, R. (n.d.). *Nanoscale heat transfer.* Retrieved May 3, 2014 from http://spot.colorado.edu: http://spot.colorado.edu/~yangr/Publications/Yang_Encyclopedia.pdf

Fitzpatrick, R. (2006 йил 2-2). *farside.ph.utexas.edu*. Retrieved 2013 йил 3-11 from Conduction electrons in a metal: http://farside.ph.utexas.edu/teaching/sm1/lectures/node86.html

Hot Disk Thermal Constant Analyser. (2013).

HotDisk. (2014). *Anisotropy 100:1-1000:1*. Retrieved February 11, 2014 from http://www.hotdiskinstruments.com/: http://www.hotdiskinstruments.com/applications/examples/anisotropy.html

Incropera, DeWitt, Bergmann, & Lavine. (2006). Chapter 2: One-Dimensional, Steady-State Conduction. In Incropera, DeWitt, Bergmann, & Lavine, *Fundamentals of Heat and Mass Transfer* (pp. 101-110). USA: John Wiley & Sons.

Johansson, P., Adl-Zarrabi, B., & Hagentoft, C.-E. (2012, September 24). *Using transient plane source sensor for determination of thermal properties of vacuum insulation panels*. Retrieved March 11, 2014 from www.sciencedirect.com: www.elsevier.com/locate/foar

Lundstrøm, D. (2004). *Measure Anisotropic thermal conductivity and diffusivity in fiber enforced polymers with the Hot Disk Thermal Constants Analyser*. Retrieved February 20, 2014 from http://www.hotdiskinstruments.com/: http://www.hotdiskinstruments.com/images/stories/pdf/Nr%203%20Application%20note%20-%20ANI%20A4.PDF

NIST. (n.d.). *Material Properties 316 Stainless (UNS S31600)*. Retrieved March 3, 2014 from http://cryogenics.nist.gov/: http://cryogenics.nist.gov/MPropsMAY/316Stainless/316Stainless_rev.htm

Peles, Y. (n.d.). *Chapter 2: Heat Conduction Equation*. Retrieved December 14, 2013 from http://wwwme.nchu.edu.tw/: http://wwwme.nchu.edu.tw/Enter/html/lab/lab516/Heat%20Transfer/chapter_2.pdf

Perkowitz, S. (2013, June 14). *Fermi surface*. Retrieved May 4, 2014 from http://global.britannica.com/: http://global.britannica.com/EBchecked/topic/204790/Fermi-surface

Rehman, A. (2012, September 13). *Heat conduction Rate equation*. Retrieved December 14, 2013 from http://www.bestinnovativesource.com/: http://www.bestinnovativesource.com/2012/09/13/heat-conduction-rate-equation/

Rusmee, P. (2005, September). *High Strength Composites*. Retrieved February 17, 2013 from http://www.mech.utah.edu/: http://www.mech.utah.edu/~rusmeeha/labNotes/composites.html

Schroeder, D. V. (2000). *An Introduction to Thermal Physics.* Addison- Wesley.

Sobhan, C., & Peterson, G. (2008). *Microscale and Nanoscal Heat Transfer.* Boca Raton: Taylor & Francis Group - LLC.

Solòrzano, E., Reglero, J., Rodriguez-Perez, M., Lehmhus, D., Wichmann, M., & de Saja, J. (2007). *An experimental study on the thermal conductivity of aluminium foams by using the transient plane source method.* Spain.

Solòrzano, E., Rodriguez-Perez, M., & de Saja, J. (2008). *Thermal Conductivity of Cellular Metals Measured by the Transient Plane Source Method.* Weinheim: Wiley-Vch Verlag.

Subbarao, P. (n.d.). *Equation of Heat Conduction.* Retrieved February 12, 2014 from web.iitd.ac.in: web.iitd.ac.in/~pmvs/mel2422008/mel242-9.ppt

Toolbox, E. (n.d.). *Cubical expansion when changing temperature*. Retrieved March 3, 2014 from http://www.engineeringtoolbox.com/: http://www.engineeringtoolbox.com/volumetric-temperature-expansion-d_315.html

Ziman, J. (1967). *The Thermal Properties of Materials.* Scientific American.

Appendix A: Reference values

A.1 Teflon

				Linear expansion	
Thermal conductivity		Heat Capacity		(L(T)-L(293K))	Volume
T [K]	k [W/m*K]	[J/kg*K]	[kJ/kgK*]	[m/m]	[m^3]
4	0,045994855	2,232330528	0,002232331	-2,127E-02	6,791E-05
10	0,095453092	18,02353607	0,018023536	-2,127E-02	6,791E-05
20	0,14217365	76,79180457	0,076791805	-2,119E-02	6,792E-05
30	0,173826575	124,3391686	0,124339169	-2,102E-02	6,796E-05
40	0,195277091	164,4150204	0,16441502	-2,078E-02	6,801E-05
50	0,209922153	202,0761948	0,202076195	-2,047E-02	6,808E-05
60	0,220289986	238,9734008	0,238973401	-2,012E-02	6,816E-05
70	0,228011897	275,5847021	0,275584702	-1,973E-02	6,824E-05
80	0,234078944	312,0375061	0,312037506	-1,931E-02	6,834E-05
90	0,239078511	348,3635585	0,348363559	-1,886E-02	6,843E-05
100	0,243354847	384,5740713	0,384574071	-1,840E-02	6,853E-05
110	0,247108375	420,6778896	0,42067789	-1,791E-02	6,864E-05
120	0,250455252	456,6822225	0,456682222	-1,742E-02	6,875E-05
130	0,253462807	492,5889857	0,492588986	-1,691E-02	6,886E-05
140	0,256170634	528,3909575	0,528390958	-1,639E-02	6,897E-05
150	0,258603163	564,0689123	0,564068912	-1,585E-02	6,909E-05
160	0,260777138	599,5898744	0,599589874	-1,529E-02	6,921E-05
170	0,262706019	634,9063278	0,634906328	-1,470E-02	6,934E-05
180	0,264402505	669,9561653	0,669956165	-1,407E-02	6,948E-05
190	0,26587992	704,6631871	0,704663187	-1,339E-02	6,962E-05
200	0,267152886	738,9380012	0,738938001	-1,265E-02	6,978E-05
210	0,268237574	772,6792185	0,772679219	-1,185E-02	6,996E-05
220	0,269151696	805,7748655	0,805774865	-1,095E-02	7,015E-05
230	0,269914361	838,1039583	0,838103958	-9,957E-03	7,037E-05
240	0,270545849	869,5381988	0,869538199	-8,840E-03	7,061E-05
250	0,271067365	899,9437579	0,899943758	-7,583E-03	7,089E-05
260	0,271500787	929,1831217	0,929183122	-6,165E-03	7,119E-05
270	0,271868436	957,1169736	0,957116974	-4,562E-03	7,154E-05
280	0,272192867	983,6060913	0,983606091	-2,750E-03	7,194E-05
290	0,272496701	1008,513235	1,008513235	-7,031E-04	7,238E-05
300	0,272802484	1031,705004	1,031705004	1,607E-03	7,289E-05

Density	Specific Heat				
[kg/m^3]	[MJ/m^{3}K]		Material	Teflon	
2297,26	0,01		a	-2125	
2297,26	0,04		b	-0,8201	
2296,66	0,18		c	0,06161	
2295,40	0,29		d	-0,0003171	
2293,61	0,38		e	6,85E-07	
2291,38	0,46				
2288,80	0,55				
2285,94	0,63				
2282,86	0,71				
2279,63	0,79		mass (@293)	[kg]	0,156
2276,26	0,88		r (293)	[m]	0,0298
2272,80	0,96		h (293)	[m]	0,026
2269,25	1,04		V (293)	[m^3]	7,25364E-05
2265,61	1,12				
2261,88	1,20				
2258,03	1,27				
2254,03	1,35				
2249,84	1,43				
2245,40	1,50				
2240,65	1,58				
2235,51	1,65				
2229,90	1,72				
2223,72	1,79				
2216,87	1,86				
2209,24	1,92				
2200,71	1,98				
2191,17	2,04				
2180,49	2,09				
2168,54	2,13				
2155,19	2,17				
2140,33	2,21				

A.2 Lexan

A.3 Stainless steel 316L

				Linear expansion	
Thermal Conductivity		Heat Capacity		(L(T)-L(293))	Volume
Temp [K]	k [W/m*K]	Cp [J/kg*K]	[kJ/kg*K]	[m/m]	[m^3]
10	0,903857571	159,22083	0,15922083	-0,002986144	7,27146E-05
20	2,168622406	403,7077743	0,403707774	-0,002999542	7,27117E-05
30	3,468572587	626,4720747	0,626472075	-0,00299675	7,27123E-05
40	4,670281	827,2387182	0,827238718	-0,00297888	7,27162E-05
50	5,730166936	100,2389711	0,100238971	-0,002947003	7,27232E-05
60	6,646641427	141,7745878	0,141774588	-0,002902151	7,27331E-05
70	7,434751536	179,8645818	0,179864582	-0,002845313	7,27456E-05
80	8,114319471	214,70219	0,21470219	-0,002777438	7,27605E-05
90	8,704844967	245,8015512	0,245801551	-0,002699432	7,27777E-05
100	9,223590217	273,0234813	0,273023481	-0,002612163	7,27969E-05
110	9,685093439	296,6753307	0,296675331	-0,002516455	7,2818E-05
120	10,10128078	317,3112907	0,317311291	-0,002413092	7,28407E-05
130	10,48179376	335,5314436	0,335531444	-0,002302818	7,2865E-05
140	10,83436242	351,8599306	0,351859931	-0,002186334	7,28907E-05
150	11,16515436	366,6958622	0,366695862	-0,002064301	7,29175E-05
160	11,4790756	380,3103827	0,380310383	-0,001937338	7,29455E-05
170	11,78001966	392,8670117	0,392867012	-0,001806025	7,29744E-05
180	12,07106923	404,4507094	0,404450709	-0,001670898	7,30041E-05
190	12,35465738	415,097761	0,415097761	-0,001532454	7,30346E-05
200	12,63269588	424,822691	0,424822691	-0,001391148	7,30657E-05
210	12,90667672	433,6406394	0,433640639	-0,001247394	7,30973E-05
220	13,17775271	441,5847692	0,441584769	-0,001101566	7,31294E-05
230	13,44680137	448,7188578	0,448718858	-0,000953994	7,31619E-05
240	13,7144757	455,1455575	0,455145557	-0,000804971	7,31947E-05
250	13,98124475	461,0110392	0,461011039	-0,000654745	7,32278E-05
260	14,24742608	466,5068957	0,466506896	-0,000503526	7,32611E-05
270	14,51321188	471,870294	0,471870294	-0,00035148	7,32945E-05
280	14,77869006	477,3834326	0,477383433	-0,000198734	7,33282E-05
290	15,04386145	483,3733819	0,483373382	-4,53738E-05	7,33619E-05
300	15,30865382	490,2133824	0,490213382	0,000108557	7,33958E-05

Density	Specific Heat				
[kg/m^3]	[MJ/m^{3}K]		Material	Steel	
8035,52526	1,279423001		a	-295,54	
8035,851189	3,244135598		b	-0,39811	
8035,783265	5,034193814		c	0,0092683	
8035,348576	6,647151456		d	-0,000020261	
8034,573306	0,805377361		e	1,7127E-08	
8033,48271	1,1389437				
8032,101096	1,444690504				
8030,451807	1,72415559				
8028,557205	1,973431815				
8026,438661	2,191406226		mass (@293)	[kg]	0,5843
8024,116547	2,380557431		r(293)	[m]	0,03
8021,610222	2,545347493		h (293)	[m]	0,02595
8018,938029	2,690605853		V (293)	[m^3]	7,337E-05
8016,117291	2,820550474				
8013,164308	2,938394195				
8010,09435	3,046322047				
8006,921661	3,145655386				
8003,659457	3,237085745				
8000,319928	3,320914889				
7996,914237	3,397270626				
7993,452525	3,466285864				
7989,943911	3,528237537				
7986,396498	3,583646715				
7982,817375	3,633343864				
7979,212619	3,678505101				
7975,587304	3,720666474				
7971,9455	3,761724267				
7968,290278	3,803929765				
7964,623719	3,849887103				
7960,946914	3,902562713				

Appendix B: Temperature Charts for Induction and Constant Temperature Heating

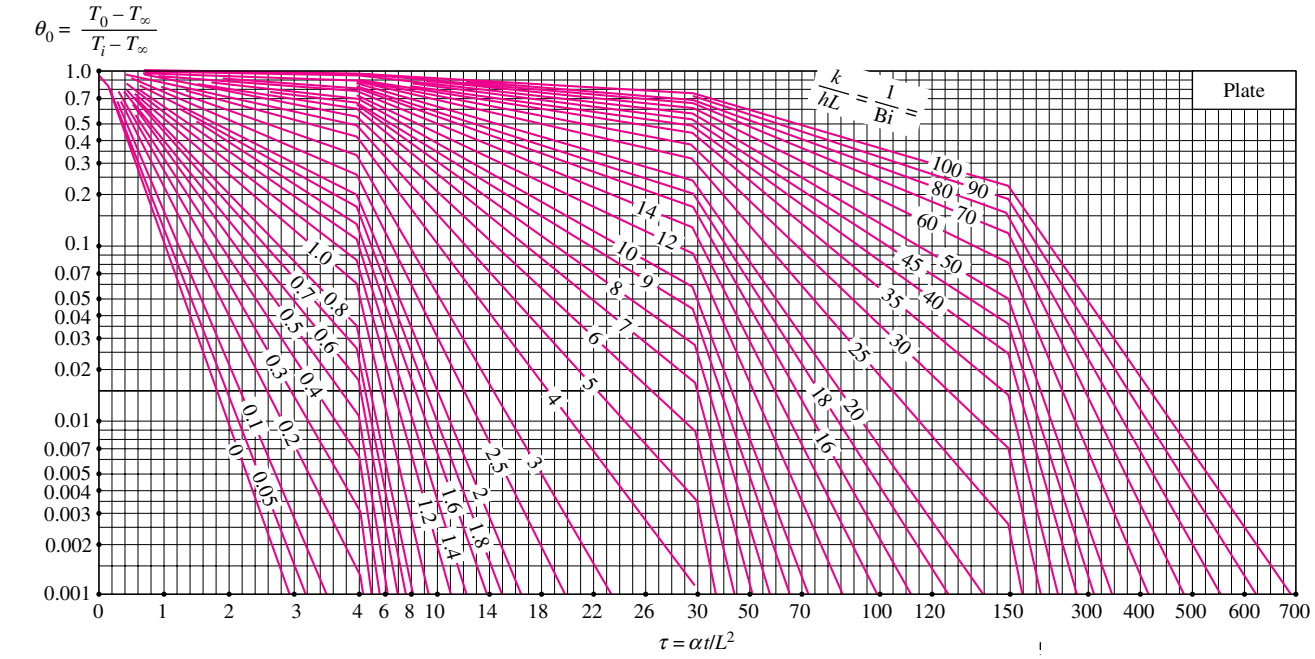

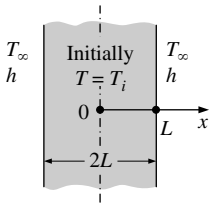

Appendix C: Temperature profile numerical results compared to Comsol Multiphysics

C.1 Semi- infinite solution

C.1.1 Teflon

After 1,40 s in Comsol	
mm	Temp Comsol
0	500,15
0,2	441,37
0,4	388,48
0,6	345,76
0,8	314,86
1	294,93
1,2	283,47874
1,4	277,61869
1,6	274,93993
1,8	273,87024
2	273,59362

Analytical results from book					
	Thermal diffusivity	0,000000129	m^2/s	Initial temperature	273
	Time	1,43	s	Surface temperature	500
x [mm]	x [m]	n	erfc(n)	T(x,t), Teflon numerical	
0	0	0	1	500	
0,2	0,0002	0,232829029	0,7420	441,4230223	
0,4	0,0004	0,465658057	0,5102	388,8134118	
0,6	0,0006	0,698487086	0,3232	346,376786	
0,8	0,0008	0,931316114	0,1878	315,6332901	
1	0,001	1,164145143	0,0997	295,6300277	
1,2	0,0012	1,396974171	0,0482	283,9409125	
1,4	0,0014	1,6298032	0,0212	277,8062135	
1,6	0,0016	1,862632228	0,0084	274,9146495	
1,8	0,0018	2,095461257	0,0030	273,6906055	
2	0,002	2,328290285	0,0010	273,225253	

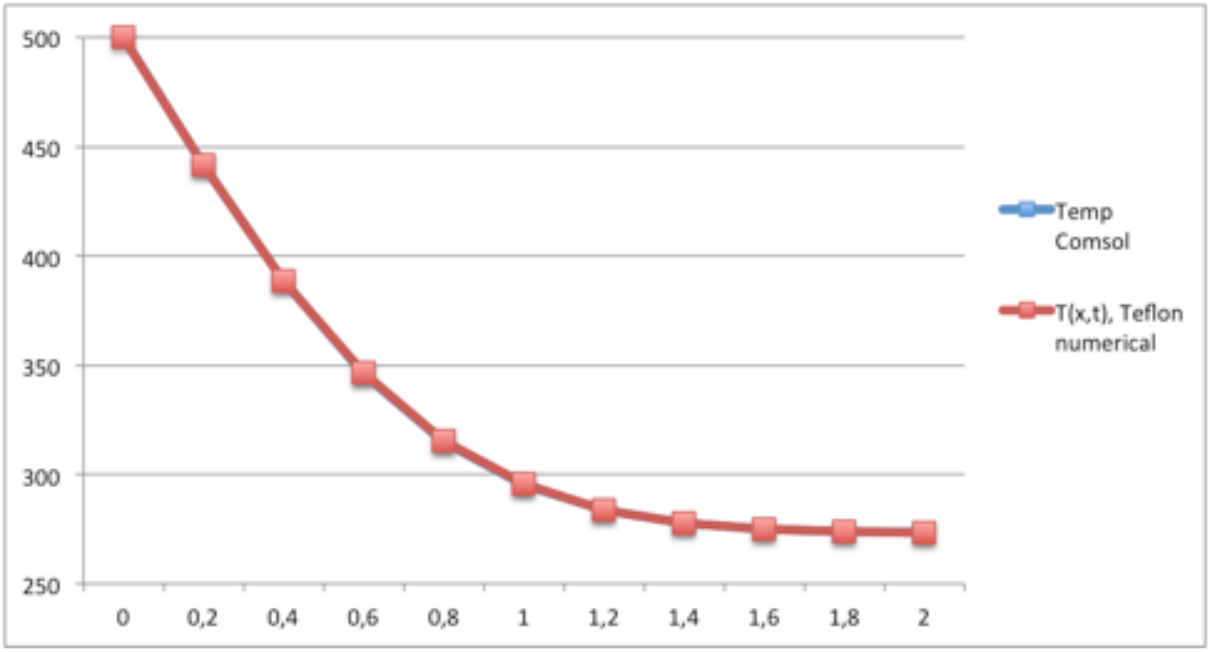
500
450
400
350
300
250
0
0,2
0,4
0,6
0,8
1
1,2
1,4
1,6
1,8
2
Temp Comsol
T(x,t), Teflon numerical

C.1.2 Stainless Steel

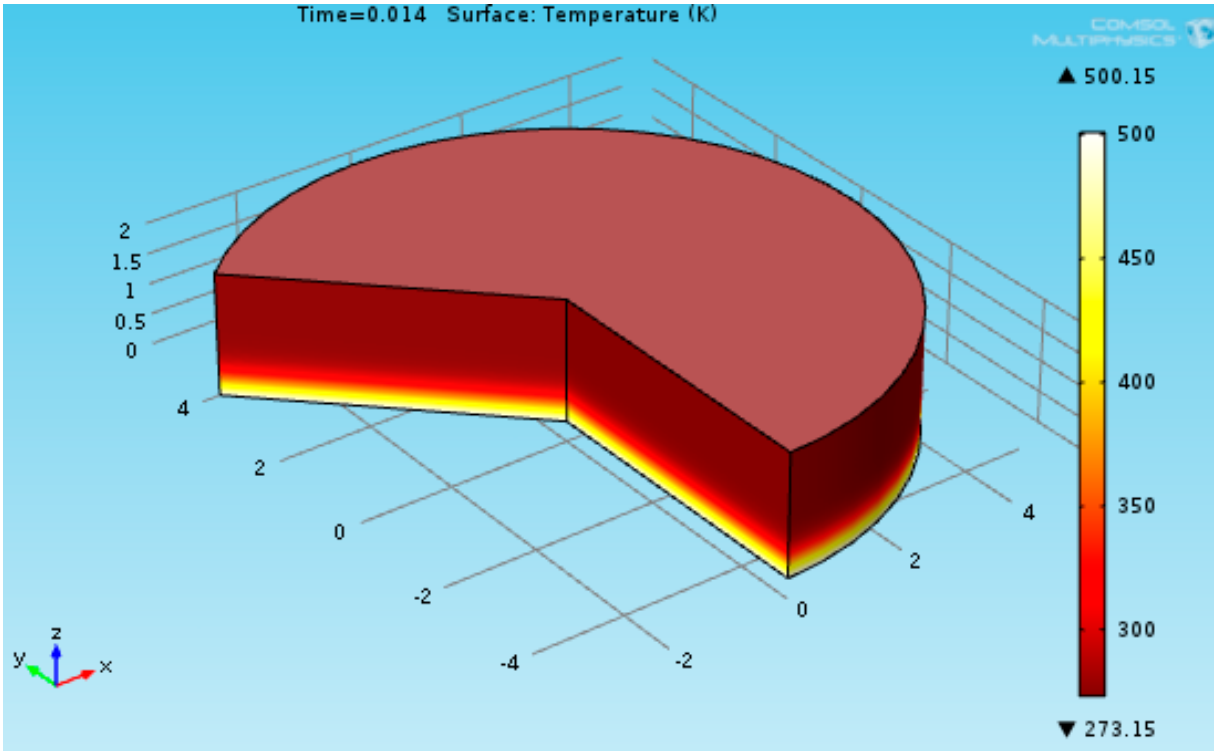

After 0,048 s in Comsol	
mm	Temp Comsol
0	500,15
0,2	441,97094
0,4	389,50077
0,6	346,93216
0,8	315,93319
1	295,74356
1,2	284,01115
1,4	277,92096
1,6	275,09394
1,8	273,94792
2	273,64851

Analytical results from book					
	Thermal diffusivity	0,0000038	m^2/s	Initial temperature	273
	Time	0,0484	s	Surface temperature	500
x [mm]	x [m]	n	erfc(n)	T(x,t), Steel numerical	
0	0	0	1	500	
0,2	0,0002	0,233176898	0,7416	441,338626	
0,4	0,0004	0,466353796	0,5096	388,66999	
0,6	0,0006	0,699530695	0,3225	346,212796	
0,8	0,0008	0,932707593	0,1872	315,483766	
1	0,001	1,165884491	0,0992	295,515366	
1,2	0,0012	1,399061389	0,0479	283,865187	
1,4	0,0014	1,632238287	0,0210	277,762594	
1,6	0,0016	1,865415186	0,0083	274,892569	
1,8	0,0018	2,098592084	0,0030	273,680735	
2	0,002	2,331768982	0,0010	273,221343	

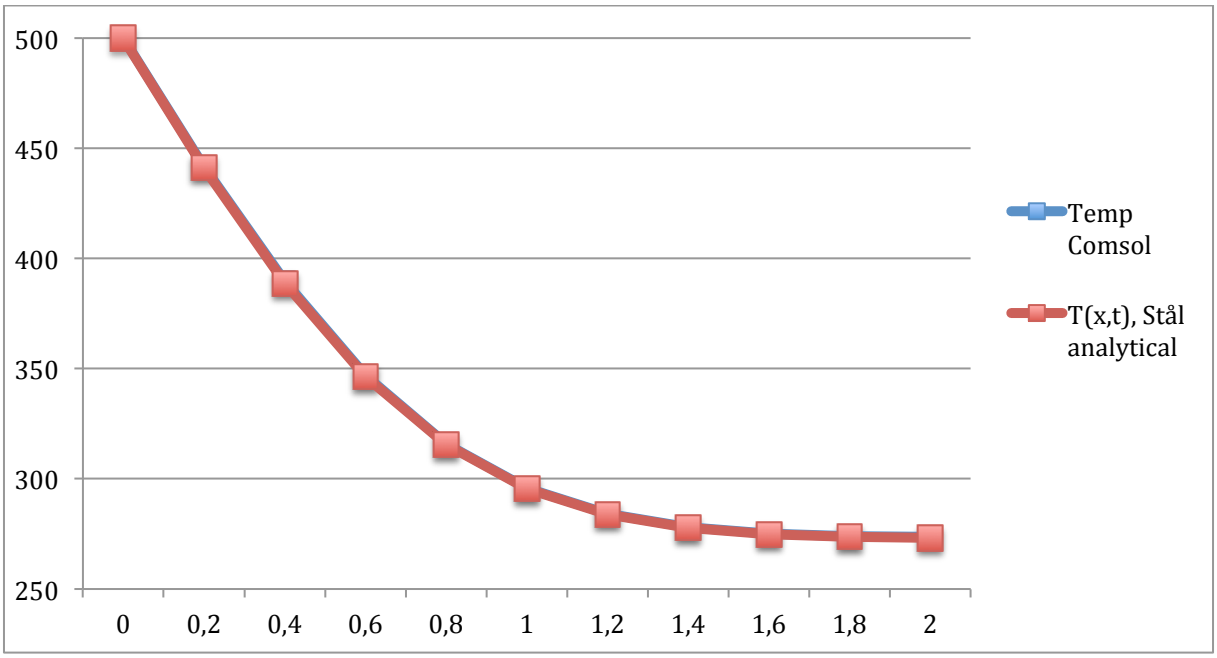

C.1.3 Lexan

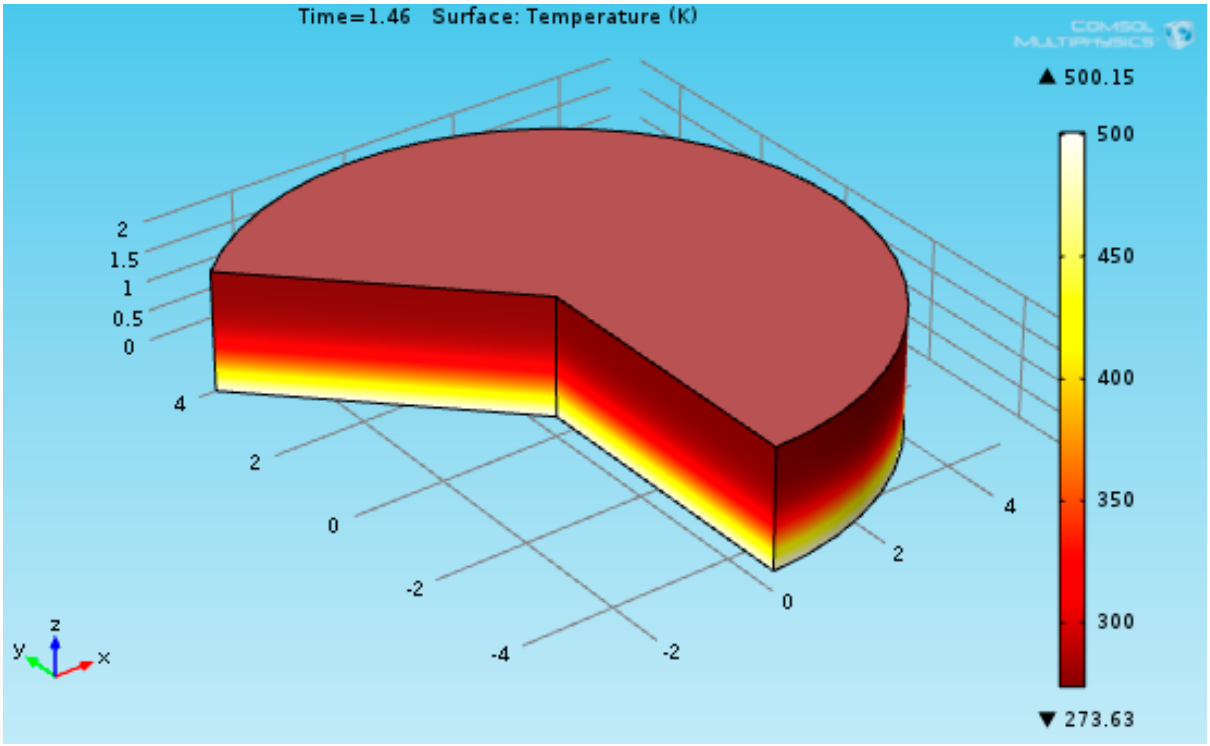

After 1,46 s in Comsol	
mm	Temp Comsol
0	500,15
0,2	441,73358
0,4	389,09516
0,6	346,46575
0,8	315,50667
1	295,41751
1,2	283,79786
1,4	277,7993
1,6	275,03162
1,8	273,91629
2	273,62607

Analytical results from book					
	Thermal diffusivity	1,257E-07	m_2/s	Initial temperature	273
	Time	1,464	s	Surface temperature	500
x [mm]	x [m]	n	Erfc (n)	T (x,t), Lexan numerical	
0	0	0	1	500	
0,2	0,0002	0,233110493	0,7417	441,3547361	
0,4	0,0004	0,466220986	0,5097	388,6973607	
0,6	0,0006	0,699331479	0,3227	346,244082	
0,8	0,0008	0,932441972	0,1873	315,5122794	
1	0,001	1,165552465	0,0993	295,5372182	
1,2	0,0012	1,398662958	0,0479	283,8796084	
1,4	0,0014	1,631773451	0,0210	277,7708944	
1,6	0,0016	1,864883944	0,0084	274,8967668	
1,8	0,0018	2,097994437	0,0030	273,6826095	
2	0,002	2,33110493	0,0010	273,2220851	

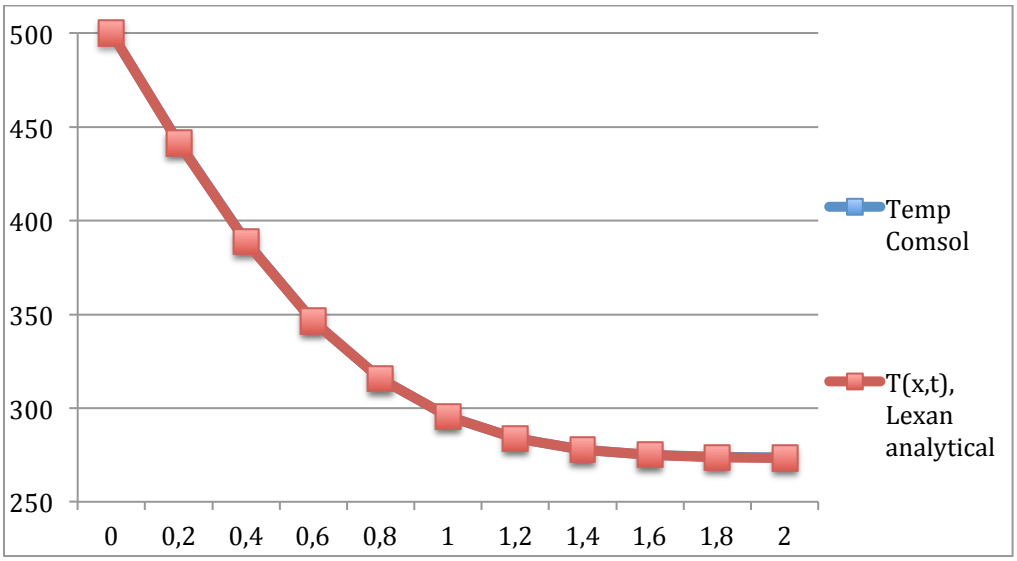

Appendix D: Comparison temperature increase in sensor TPS method and Comsol Multiphysics, cylinder

D.1 Teflon

D.1.1 Input parameters Comsol Multiphysics 253 K

Area sensor	4,934E-07	m^2
Thermal properties at initial temperature T=253 K		
Teflon		
k=	0,31	W/m*K
Cp=	870,2	J/kg*K
Density=	2150	kg/m^3
Thermal properties of sensor		
Kapton		
k=	0,12	W/m*K
Cp=	1090	J/kg*K
Density=	1420	kg/m^3
Width=	9,868	mm
Height=	0,05	mm
Thermal properties of the resistance layer for Teflon		
k=	$3,5*10^{-3}$	
Cp=	1	
Density=	1	
Width=	9,868	mm
Height=	0,01	mm

Input power sensor= 4 903 239,5 W/m^3

D.1.2 Input parameters Comsol Multiphysics 263 K

Area sensor	4,934E-07	m^2
Thermal properties at initial temperature T=263 K		
Teflon		
k=	0,31	W/m*K
Cp=	881,4	J/kg*K
Density=	2150	kg/m^3
Thermal properties of sensor		
Kapton		
k=	0,12	W/m*K
Cp=	1090	J/kg*K
Density=	1420	kg/m^3
Width=	9,868	mm
Height=	0,05	mm
Thermal properties of the resistance layer for Teflon		
k=	$3,5*10^{-3}$	
Cp=	1	
Density=	1	
Width=	9,868	mm
Height=	0,01	mm

Input power sensor= 4 903 239,5 W/m^3

D.1.3 Input parameters Comsol Multiphysics 273 K

Area sensor	4,934E-07	m^2
Thermal properties at initial temperature T=273 K		
Teflon		
k=	0,31	W/m*K
Cp=	914,4	J/kg*K
Density=	2150	kg/m^3
Thermal properties of sensor		
Kapton		
k=	0,12	W/m*K
Cp=	1090	J/kg*K
Density=	1420	kg/m^3
Width=	9,868	mm
Height=	0,05	mm
Thermal properties of the resistance layer for Teflon		
k=	$3,5*10^{-3}$	
Cp=	1	
Density=	1	
Width=	9,868	mm
Height=	0,01	mm

Input power sensor= 4 903 239,5 W/m^3

D.1.4 Temperature increase comparison Comsol and HotDisk Teflon cylinder

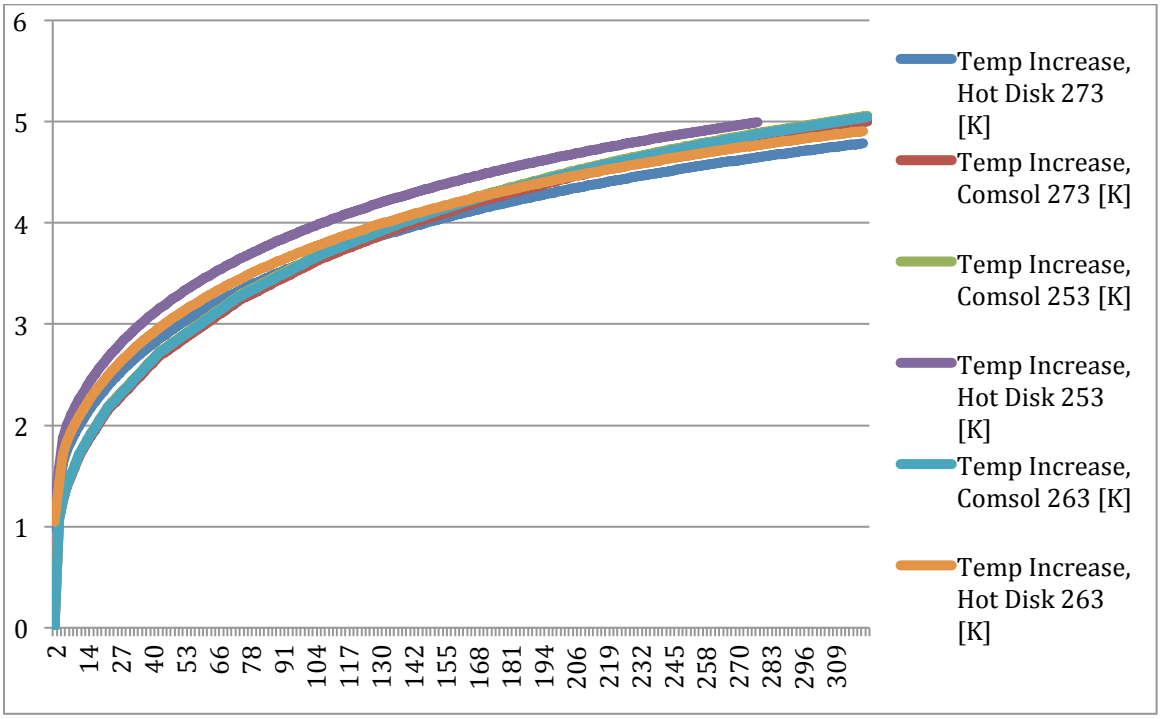

D.2 PMMA

D.2.1 Input parameters Comsol Multiphysics 248 K

Area sensor	3,2015E-07	m^2
Thermal properties at initial temperature T=248 K		
PMMA		
k=	0,195	W/m*K
Cp=	1202,2	J/kg*K
Density=	1177	kg/m^3
Thermal properties of sensor		
Kapton		
k=	0,12	W/m*K
Cp=	1090	J/kg*K
Density=	1420	kg/m^3
Width=	6,403	mm
Height=	0,05	mm
Thermal properties of the resistance layer for Teflon		
k=	$0,35*10^2$	
Cp=	1	
Density=	1	
Width=	6,403	mm
Height=	0,01	mm

Input power sensor= 4 270 176,4 W/m^3

D.2.2 Input parameters Comsol Multiphysics 263 K

Area sensor	3,2015E-07	m^2
Thermal properties at initial temperature T=263 K		
PMMA		
k=	0,201	W/m*K
Cp=	1228,5	J/kg*K
Density=	1177	kg/m^3
Thermal properties of sensor		
Kapton		
k=	0,12	W/m*K
Cp=	1090	J/kg*K
Density=	1420	kg/m^3
Width=	6,403	mm
Height=	0,05	mm
Thermal properties of the resistance layer for Teflon		
k=	$0,35*10^2$	
Cp=	1	
Density=	1	
Width=	6,403	mm
Height=	0,01	mm

Input power sensor= 4 270 176,4 W/m^3

D.2.3 Input parameters Comsol Multiphysics 278 K

Area sensor	3,2015E-07	m^2
Thermal properties at initial temperature T=278 K		
PMMA		
k=	0,202	W/m*K
Cp=	1271,9	J/kg*K
Density=	1177	kg/m^3
Thermal properties of sensor		
Kapton		
k=	0,12	W/m*K
Cp=	1090	J/kg*K
Density=	1420	kg/m^3
Width=	6,403	mm
Height=	0,05	mm
Thermal properties of the resistance layer for Teflon		
k=	$0,35*10^2$	
Cp=	1	
Density=	1	
Width=	6,403	mm
Height=	0,01	mm

Input power sensor= 4 270 176,4 W/m^3

D.2.4 Temperature increase comparison Comsol and HotDisk PMMA cylinder

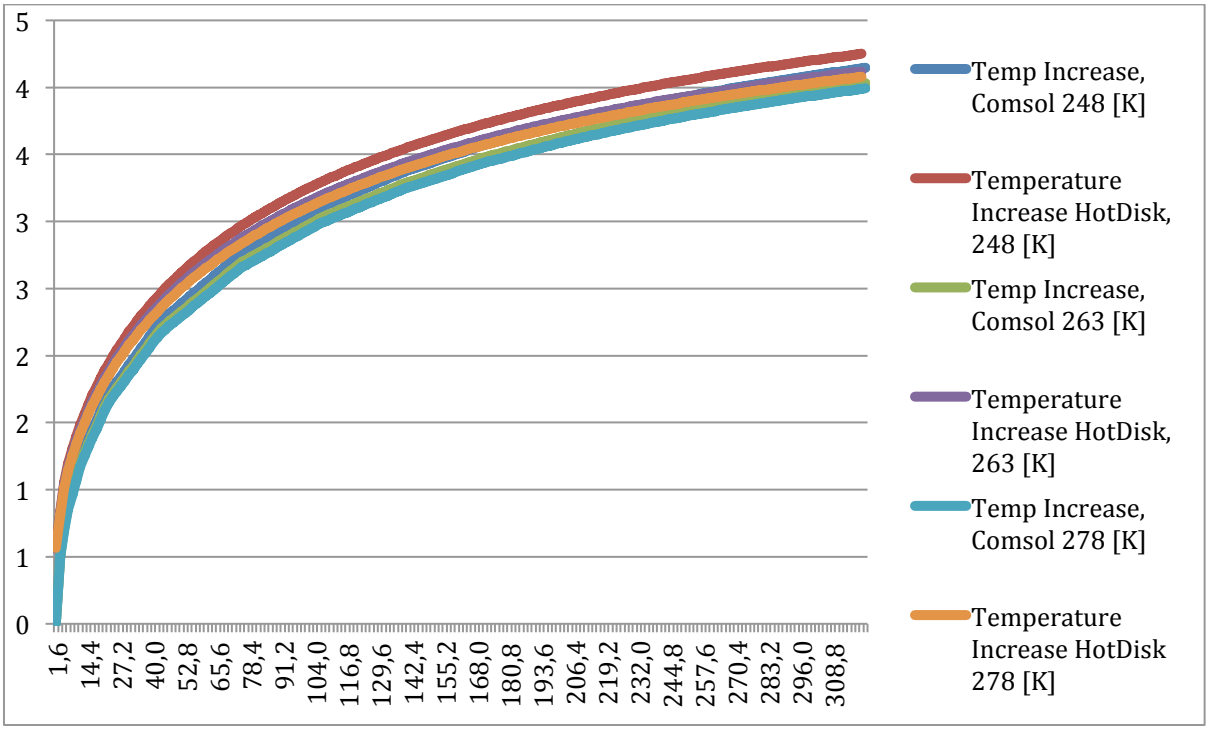

D.3 Stainless steel

D.3.1 Input parameters Comsol Multiphysics 258 K

Area sensor	3,2015E-07	m^2
Thermal properties at initial temperature T=258 K		
Stainless Steel 316L		
k=	13,2	W/m*K
Cp=	454,8	J/kg*K
Density=	7975	kg/m^3
Thermal properties of sensor		
Kapton		
k=	0,12	W/m*K
Cp=	1090	J/kg*K
Density=	1420	kg/m^3
Width=	6,403	mm
Height=	0,05	mm
Thermal properties of the resistance layer for Stainless Steel		
k=	$0,32*10^{-1}$	
Cp=	1	
Density=	1	
Width=	6,403	mm
Height=	0,01	mm

Input power sensor= 85 403 527,44 W/m^3

D.3.2 Input parameters Comsol Multiphysics 273 K

Area sensor	3,2015E-07	m^2
Thermal properties at initial temperature T=273 K		
Stainless Steel 316L		
k=	13,6	W/m*K
Cp=	469	J/kg*K
Density=	7975	kg/m^3
Thermal properties of sensor		
Kapton		
k=	0,12	W/m*K
Cp=	1090	J/kg*K
Density=	1420	kg/m^3
Width=	6,403	mm
Height=	0,05	mm
Thermal properties of the resistance layer for Stainless Steel		
k=	$0,32*10^{-1}$	
Cp=	1	
Density=	1	
Width=	6,403	mm
Height=	0,01	mm

Input power sensor= 90 605 378,7 W/m^3

D.3.3 Input parameters Comsol Multiphysics 288 K

Area sensor	3,2015E-07	m^2
Thermal properties at initial temperature T=288 K		
Stainless Steel 316L		
k=	13,6	W/m*K
Cp=	457,05	J/kg*K
Density=	7975	kg/m^3
Thermal properties of sensor		
Kapton		
k=	0,12	W/m*K
Cp=	1090	J/kg*K
Density=	1420	kg/m^3
Width=	6,403	mm
Height=	0,05	mm
Thermal properties of the resistance layer for Stainless Steel		
k=	$0,32*10^{-1}$	
Cp=	1	
Density=	1	
Width=	6,403	mm
Height=	0,01	mm

Input power sensor= 95 496 671,59 W/m^3

D.3.4 Temperature increase comparison Comsol and HotDisk Stainless steel cylinder

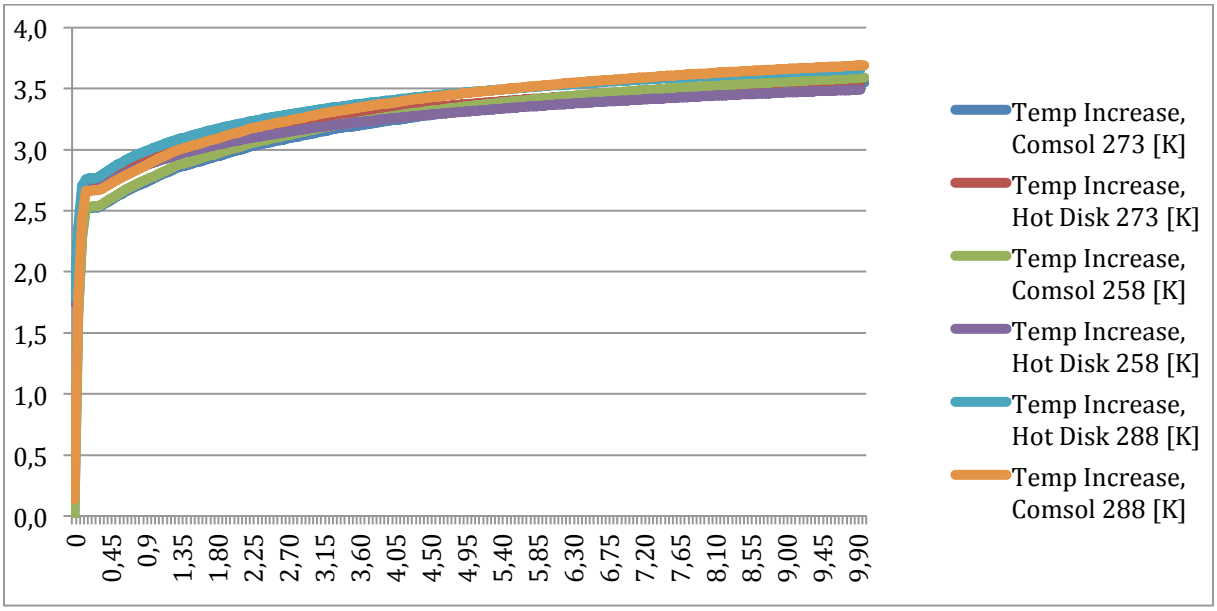

Appendix E: Comparison temperature increase in sensor TPS method and Comsol Multiphysics, stacked materials

E.1 Steel and Teflon stacked

E.1.1 Input parameters Comsol Multiphysics 0,4 W, 0,6 W and 1 W.

Thermal properties at initial temperature T=283 K		
Stainless Steel 316L		
k=	13,6	W/m*K
Cp=	460	J/kg*K
Density=	7975	kg/m^3
Thermal properties at initial temperature T=283		
Teflon		
k=	0,27	W/m*K
Cp=	965,6	J/kg*K
Density=	2150	kg/m^3
Thermal properties of sensor		
Kapton		
k=	0,12	W/m*K
Cp=	1090	J/kg*K
Density=	1420	kg/m^3
Width=	6,403	mm
Height=	0,05	mm
Thermal properties of the resistance layer sensor and Stainless Steel		
k=	2*10^(-2)	
Cp=	1	
Density=	1	
Width=	6,403	mm
Height=	0,01	mm
Thermal properties of the resistance layer Teflon and Stainless Steel		
k=	1*10^2	
Cp=	1	
Density=	1	
Width=	6,403	mm
Height=	0,01	mm

Input power$_{0,4\ W}$= 31 055 828, 16 W/m^3
Input power$_{0,6\ W}$= 46 583 742, 24 W/m^3
Input power$_{1\ W}$= 77 639 570, 4 W/m^3

E.2 Teflon and Steel stacked

E.2.1 Input parameters Comsol Multiphysics 0,4 W, 0,6 W and 1 W.

Thermal properties at initial temperature T=283 K		
Stainless Steel 316L		
k=	13,6	W/m*K
Cp=	460	J/kg*K
Density=	7975	kg/m^3
Thermal properties at initial temperature T=283		
Teflon		
k=	0,27	W/m*K
Cp=	965,6	J/kg*K
Density=	2150	kg/m^3
Thermal properties of sensor		
Kapton		
k=	0,12	W/m*K
Cp=	1090	J/kg*K
Density=	1420	kg/m^3
Width=	6,403	mm
Height=	0,05	mm
Thermal properties of the resistance layer sensor and Teflon		
k=	0,9*10^(-2)	
Cp=	1	
Density=	1	
Width=	6,403	mm
Height=	0,01	m
Thermal properties of the resistance layer Teflon and Stainless Steel		
k=	2,3*10^(-2)	
Cp=	1	
Density=	1	
Width=	6,403	mm
Height=	0,01	mm

Input $power_{0,4\ W}$= 31 055 828, 16 W/m^3
Input $power_{0,6\ W}$= 46 583 742, 24 W/m^3
Input $power_{1\ W}$= 77 639 570, 4 W/m^3

E.3 Steel and Lexan stacked

E.3.1 Input parameters Comsol Multiphysics 0,6 W, 0,8 W and 1 W.

Thermal properties at initial temperature T=293 K		
Stainless Steel 316L		
k=	15	W/m*K
Cp=	483,37	J/kg*K
Density=	7964,6	kg/m^3
Thermal properties at initial temperature T=293		
Lexan		
k=	0,19	W/m*K
Cp=	1200	J/kg*K
Density=	1260	kg/m^3
Thermal properties of sensor		
Kapton		
k=	0,12	W/m*K
Cp=	1090	J/kg*K
Density=	1420	kg/m^3
Width=	6,403	mm
Height=	0,05	mm
Thermal properties of the resistance layer sensor and Stainless Steel		
k=	2*10^(-2)	
Cp=	1	
Density=	1	
Width=	6,403	mm
Height=	0,01	mm
Thermal properties of the resistance layer Lexan and Stainless Steel		
k=	3*10^(-1)	
Cp=	1	
Density=	1	
Width=	6,403	mm
Height=	0,01	mm

Input $power_{0,6\ W}$= 46 583 742,24 W/m^3
Input $power_{0,8\ W}$= 62 111 656,32 W/m^3
Input $power_{1W}$= 77 639 570,4 W/m^3

E.3.2 Temperature profile after 20 seconds, 1 W.

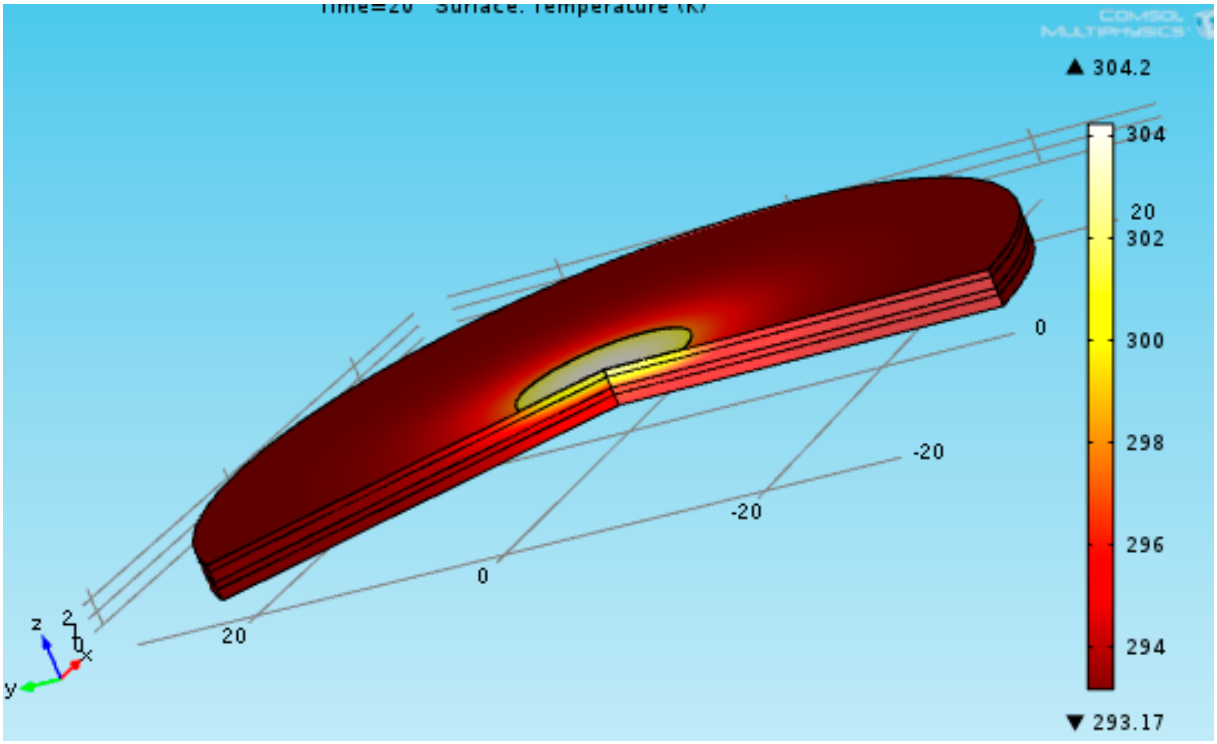

E.3.2 Temperature increase comparison

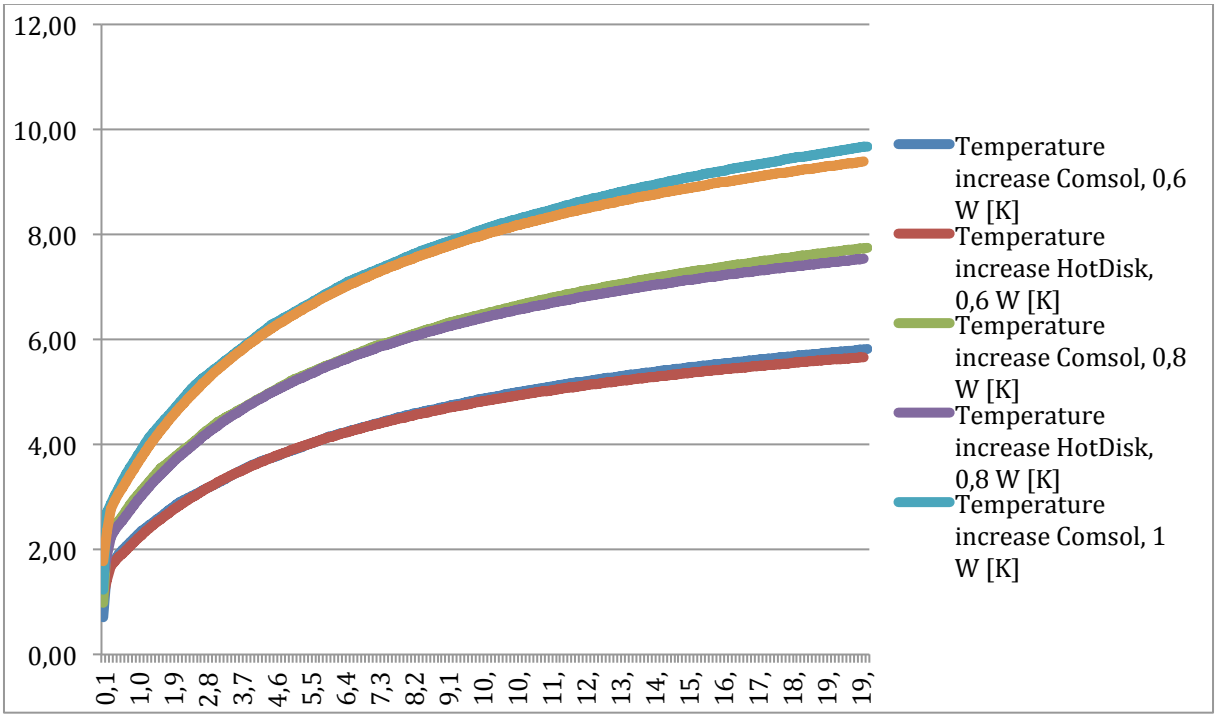

E.4 Lexan and Steel stacked

E.4.1 Input parameters Comsol Multiphysics 0,6 W, 0,8 W and 1 W.

Thermal properties at initial temperature T=293 K		
Stainless Steel 316L		
k=	15	W/m*K
Cp=	483,37	J/kg*K
Density=	7964,6	kg/m^3
Thermal properties at initial temperature T=293		
Lexan		
k=	0,19	W/m*K
Cp=	1200	J/kg*K
Density=	1260	kg/m^3
Thermal properties of sensor		
Kapton		
k=	0,12	W/m*K
Cp=	1090	J/kg*K
Density=	1420	kg/m^3
Width=	6,403	mm
Height=	0,05	mm
Thermal properties of the resistance layer sensor and Lexan		
k=	0,9*10^(-1)	
Cp=	1	
Density=	1	
Width=	6,403	mm
Height=	0,01	mm
Thermal properties of the resistance layer Lexan and Stainless Steel		
k=	5*10^2	
Cp=	1	
Density=	1	
Width=	6,403	mm
Height=	0,01	mm

Input $power_{0,6\ W}$= 46 583 742,24 W/m^3
Input $power_{0,8\ W}$= 62 111 656,32 W/m^3
Input $power_{1W}$= 77 639 570,4 W/m^3

E.4.2 Temperature profile after 20 seconds, 1 W.

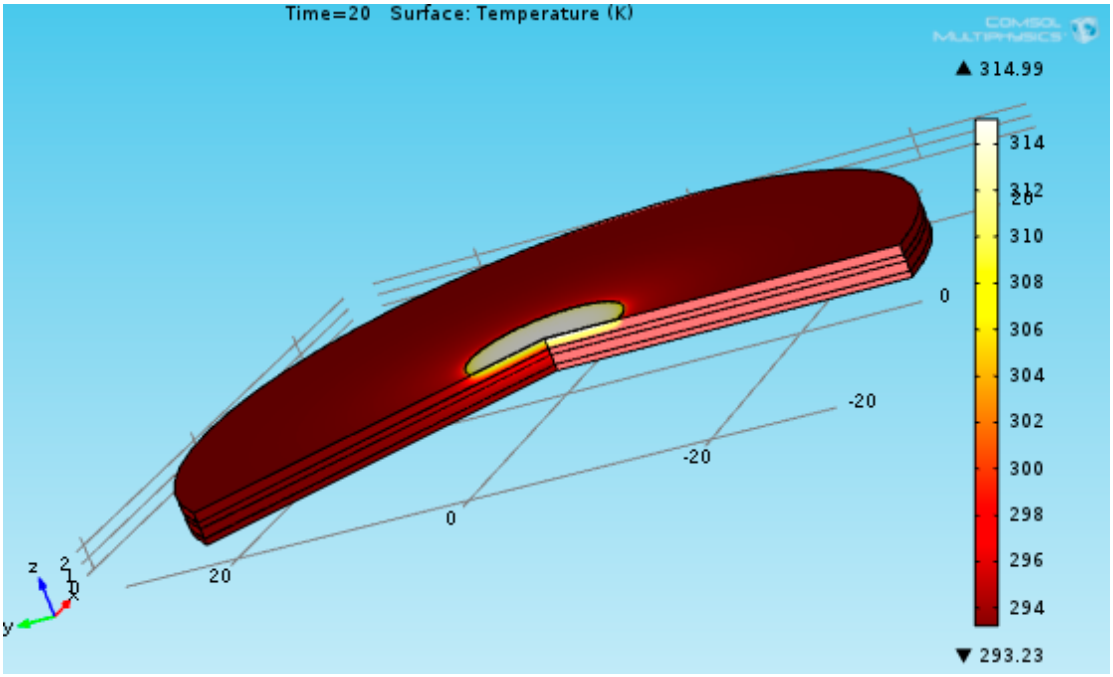

E.4.3 Temperature increase comparison

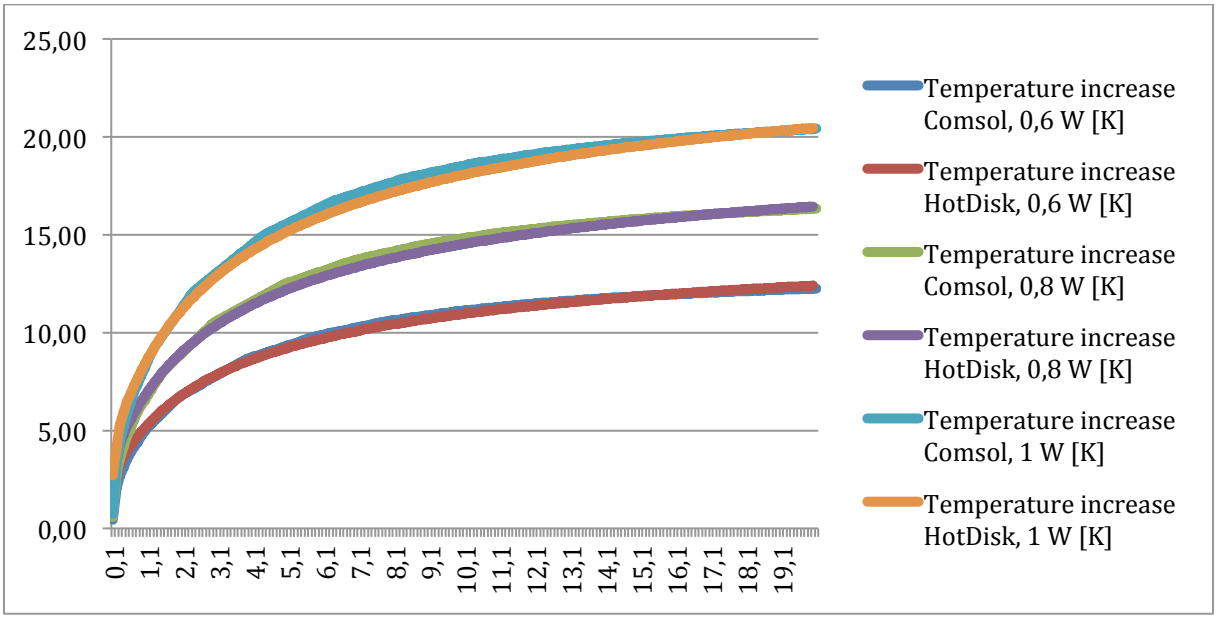

Appendix F: Curve fit quality

F.1 Temperature increase Teflon Steel

t [s]	0,4 W Comsol	0,4 W HotDisk	Curve fit	0,6 W Comsol	0,6 W HotDisk	Curve fit	1 W Comsol	1 W HotDisk	Curve fit
0,10	2,65	1,63	-0,1476	3,98	2,43	-0,2255	6,65	4,05	-0,3788
0,20	2,94	2,48	-0,0602	4,42	3,71	-0,0918	7,36	6,17	-0,1529
0,30	3,17	3,03	-0,0206	4,74	4,53	-0,0319	7,87	7,53	-0,0550
0,40	3,35	3,29	-0,0144	5,01	4,90	-0,0211	8,37	8,16	-0,0398
0,50	3,53	3,45	-0,0165	5,24	5,13	-0,0256	8,74	8,55	-0,0422
0,60	3,66	3,58	-0,0164	5,46	5,31	-0,0355	9,08	8,85	-0,0514
0,70	3,78	3,70	-0,0154	5,69	5,49	-0,0374	9,42	9,13	-0,0618
0,80	3,90	3,82	-0,0147	5,83	5,66	-0,0316	9,76	9,42	-0,0656
0,90	4,01	3,94	-0,0148	5,98	5,84	-0,0269	10,02	9,70	-0,0594
1,00	4,13	4,05	-0,0135	6,13	6,00	-0,0239	10,23	9,96	-0,0518
1,10	4,22	4,16	-0,0091	6,27	6,16	-0,0228	10,45	10,20	-0,0477
1,20	4,29	4,26	-0,0041	6,42	6,31	-0,0236	10,66	10,43	-0,0466
1,30	4,36	4,35	-0,0004	6,57	6,45	-0,0258	10,88	10,64	-0,0481
1,40	4,43	4,44	0,0024	6,71	6,58	-0,0233	11,09	10,85	-0,0519
1,50	4,51	4,52	0,0042	6,80	6,70	-0,0164	11,31	11,04	-0,0577
1,60	4,58	4,60	0,0052	6,88	6,82	-0,0107	11,52	11,22	-0,0634
1,70	4,65	4,68	0,0054	6,97	6,93	-0,0060	11,72	11,39	-0,0616
1,80	4,72	4,75	0,0050	7,06	7,04	-0,0024	11,84	11,55	-0,0543
1,90	4,80	4,82	0,0039	7,14	7,14	0,0004	11,96	11,70	-0,0485
2,00	4,87	4,88	0,0030	7,23	7,24	0,0023	12,08	11,85	-0,0440
2,10	4,93	4,95	0,0046	7,31	7,33	0,0035	12,20	11,99	-0,0408
2,20	4,97	5,01	0,0082	7,40	7,42	0,0039	12,33	12,13	-0,0388
2,30	5,02	5,06	0,0114	7,49	7,51	0,0037	12,45	12,26	-0,0379
2,40	5,06	5,12	0,0142	7,57	7,59	0,0028	12,57	12,38	-0,0381
2,50	5,10	5,17	0,0165	7,66	7,67	0,0014	12,69	12,50	-0,0392
2,60	5,14	5,23	0,0185	7,74	7,75	-0,0006	12,82	12,62	-0,0412
2,70	5,18	5,28	0,0202	7,83	7,82	-0,0028	12,94	12,73	-0,0441
2,80	5,22	5,32	0,0215	7,91	7,89	-0,0020	13,06	12,83	-0,0478
2,90	5,26	5,37	0,0225	7,96	7,96	0,0015	13,18	12,93	-0,0522
3,00	5,30	5,42	0,0233	8,02	8,03	0,0046	13,31	13,03	-0,0573
3,10	5,34	5,46	0,0237	8,07	8,10	0,0073	13,43	13,13	-0,0629
3,20	5,38	5,50	0,0240	8,12	8,16	0,0095	13,55	13,22	-0,0692
3,30	5,42	5,54	0,0240	8,17	8,22	0,0115	13,67	13,31	-0,0739
3,40	5,46	5,58	0,0237	8,22	8,28	0,0131	13,77	13,40	-0,0745
3,50	5,51	5,62	0,0232	8,27	8,34	0,0144	13,85	13,48	-0,0731
3,60	5,55	5,66	0,0226	8,32	8,40	0,0153	13,93	13,56	-0,0722
3,70	5,59	5,70	0,0217	8,38	8,45	0,0160	14,00	13,64	-0,0716
3,80	5,63	5,73	0,0206	8,43	8,51	0,0164	14,08	13,72	-0,0715
3,90	5,67	5,77	0,0194	8,48	8,56	0,0165	14,16	13,80	-0,0718

4,00	5,71	5,80	0,0183	8,53	8,61	0,0164	14,23	13,87	-0,0723
4,10	5,75	5,84	0,0185	8,58	8,66	0,0161	14,31	13,94	-0,0732
4,20	5,77	5,87	0,0196	8,63	8,71	0,0155	14,38	14,01	-0,0744
4,30	5,80	5,90	0,0206	8,68	8,76	0,0146	14,46	14,08	-0,0759
4,40	5,83	5,93	0,0215	8,74	8,81	0,0136	14,54	14,15	-0,0776
4,50	5,85	5,96	0,0222	8,79	8,85	0,0124	14,61	14,22	-0,0796
4,60	5,88	5,99	0,0228	8,84	8,90	0,0110	14,69	14,28	-0,0817
4,70	5,91	6,02	0,0232	8,89	8,94	0,0095	14,76	14,35	-0,0841
4,80	5,93	6,05	0,0236	8,94	8,98	0,0095	14,84	14,41	-0,0868
4,90	5,96	6,08	0,0238	8,97	9,03	0,0109	14,92	14,48	-0,0896
5,00	5,99	6,11	0,0239	9,01	9,07	0,0120	14,99	14,54	-0,0927
5,10	6,01	6,13	0,0239	9,04	9,11	0,0130	15,07	14,60	-0,0959
5,20	6,04	6,16	0,0238	9,08	9,15	0,0139	15,14	14,66	-0,0993
5,30	6,07	6,18	0,0236	9,11	9,19	0,0146	15,22	14,72	-0,1019
5,40	6,09	6,21	0,0234	9,15	9,22	0,0152	15,29	14,77	-0,1025
5,50	6,12	6,23	0,0230	9,18	9,26	0,0156	15,34	14,83	-0,1020
5,60	6,15	6,26	0,0225	9,22	9,30	0,0158	15,39	14,88	-0,1017
5,70	6,17	6,28	0,0219	9,25	9,33	0,0159	15,45	14,94	-0,1016
5,80	6,20	6,31	0,0213	9,29	9,37	0,0159	15,50	14,99	-0,1016
5,90	6,22	6,33	0,0205	9,32	9,40	0,0158	15,55	15,04	-0,1017
6,00	6,25	6,35	0,0199	9,36	9,44	0,0156	15,61	15,10	-0,1020
6,10	6,28	6,37	0,0198	9,39	9,47	0,0153	15,66	15,15	-0,1023
6,20	6,30	6,40	0,0202	9,43	9,50	0,0148	15,71	15,20	-0,1027
6,30	6,32	6,42	0,0205	9,46	9,54	0,0142	15,76	15,25	-0,1032
6,40	6,34	6,44	0,0208	9,50	9,57	0,0135	15,82	15,30	-0,1039
6,50	6,36	6,46	0,0210	9,53	9,60	0,0127	15,87	15,35	-0,1046
6,60	6,38	6,48	0,0211	9,57	9,63	0,0118	15,92	15,40	-0,1054
6,70	6,39	6,50	0,0212	9,60	9,66	0,0109	15,98	15,45	-0,1063
6,80	6,41	6,52	0,0212	9,64	9,69	0,0108	16,03	15,50	-0,1073
6,90	6,43	6,54	0,0211	9,66	9,72	0,0115	16,08	15,54	-0,1084
7,00	6,45	6,56	0,0209	9,69	9,75	0,0120	16,14	15,59	-0,1096
7,10	6,47	6,58	0,0208	9,72	9,78	0,0125	16,19	15,64	-0,1109
7,20	6,49	6,60	0,0205	9,74	9,81	0,0129	16,24	15,69	-0,1122
7,30	6,51	6,62	0,0202	9,77	9,83	0,0132	16,30	15,73	-0,1130
7,40	6,53	6,63	0,0199	9,79	9,86	0,0134	16,34	15,78	-0,1127
7,50	6,55	6,65	0,0195	9,82	9,89	0,0136	16,38	15,82	-0,1116
7,60	6,57	6,67	0,0190	9,84	9,91	0,0136	16,42	15,87	-0,1107
7,70	6,59	6,69	0,0185	9,87	9,94	0,0136	16,46	15,91	-0,1098
7,80	6,61	6,70	0,0179	9,90	9,96	0,0135	16,50	15,96	-0,1090
7,90	6,63	6,72	0,0173	9,92	9,99	0,0134	16,54	16,00	-0,1082
8,00	6,65	6,74	0,0168	9,95	10,01	0,0131	16,58	16,04	-0,1076
8,10	6,67	6,75	0,0167	9,97	10,04	0,0128	16,62	16,09	-0,1070
8,20	6,69	6,77	0,0169	10,00	10,06	0,0124	16,66	16,13	-0,1065
8,30	6,70	6,79	0,0171	10,03	10,09	0,0120	16,70	16,17	-0,1061
8,40	6,72	6,80	0,0172	10,05	10,11	0,0115	16,74	16,21	-0,1057

8,50	6,73	6,82	0,0174	10,08	10,13	0,0110	16,78	16,26	-0,1055
8,60	6,75	6,83	0,0174	10,10	10,16	0,0104	16,82	16,30	-0,1053
8,70	6,76	6,85	0,0175	10,13	10,18	0,0098	16,86	16,34	-0,1051
8,80	6,78	6,86	0,0174	10,15	10,20	0,0096	16,90	16,38	-0,1051
8,90	6,79	6,88	0,0174	10,18	10,22	0,0098	16,94	16,42	-0,1052
9,00	6,80	6,89	0,0173	10,20	10,25	0,0100	16,98	16,46	-0,1053
9,10	6,82	6,91	0,0172	10,22	10,27	0,0102	17,02	16,50	-0,1054
9,20	6,83	6,92	0,0170	10,24	10,29	0,0102	17,06	16,54	-0,1057
9,30	6,85	6,93	0,0168	10,26	10,31	0,0102	17,10	16,58	-0,1057
9,40	6,86	6,95	0,0166	10,28	10,33	0,0102	17,14	16,61	-0,1049
9,50	6,88	6,96	0,0164	10,30	10,35	0,0101	17,17	16,65	-0,1037
9,60	6,89	6,98	0,0161	10,32	10,37	0,0100	17,20	16,69	-0,1026
9,70	6,91	6,99	0,0157	10,34	10,39	0,0099	17,24	16,73	-0,1016
9,80	6,92	7,00	0,0154	10,36	10,41	0,0096	17,27	16,76	-0,1006
9,90	6,94	7,01	0,0150	10,38	10,43	0,0094	17,30	16,80	-0,0998
10,00	6,95	7,03	0,0146	10,40	10,45	0,0091	17,33	16,83	-0,0990
10,10	6,97	7,04	0,0143	10,42	10,47	0,0087	17,36	16,87	-0,0982
10,20	6,98	7,05	0,0142	10,44	10,49	0,0083	17,39	16,90	-0,0976
10,30	6,99	7,07	0,0140	10,47	10,51	0,0079	17,43	16,94	-0,0970
10,40	7,01	7,08	0,0138	10,49	10,52	0,0074	17,46	16,97	-0,0965
10,50	7,02	7,09	0,0137	10,51	10,54	0,0069	17,49	17,01	-0,0961
10,60	7,03	7,10	0,0135	10,53	10,56	0,0063	17,52	17,04	-0,0957
10,70	7,05	7,11	0,0134	10,55	10,58	0,0058	17,55	17,08	-0,0954
10,80	7,06	7,13	0,0132	10,57	10,60	0,0056	17,58	17,11	-0,0952
10,90	7,07	7,14	0,0131	10,59	10,61	0,0057	17,62	17,14	-0,0950
11,00	7,08	7,15	0,0129	10,60	10,63	0,0058	17,65	17,17	-0,0949
11,10	7,10	7,16	0,0128	10,62	10,65	0,0058	17,68	17,21	-0,0949
11,20	7,11	7,17	0,0126	10,64	10,67	0,0058	17,71	17,24	-0,0949
11,30	7,12	7,18	0,0125	10,65	10,68	0,0058	17,74	17,27	-0,0949
11,40	7,13	7,19	0,0124	10,67	10,70	0,0058	17,77	17,30	-0,0947
11,50	7,14	7,20	0,0122	10,69	10,71	0,0057	17,80	17,33	-0,0944
11,60	7,15	7,22	0,0121	10,70	10,73	0,0056	17,83	17,36	-0,0941
11,70	7,17	7,23	0,0120	10,72	10,75	0,0054	17,86	17,39	-0,0938
11,80	7,18	7,24	0,0119	10,74	10,76	0,0052	17,89	17,42	-0,0935
11,90	7,19	7,25	0,0118	10,75	10,78	0,0050	17,92	17,45	-0,0932
12,00	7,20	7,26	0,0117	10,77	10,79	0,0048	17,95	17,48	-0,0929
12,10	7,21	7,27	0,0115	10,79	10,81	0,0045	17,97	17,51	-0,0926
12,20	7,22	7,28	0,0113	10,80	10,82	0,0042	18,00	17,54	-0,0924
12,30	7,23	7,29	0,0112	10,82	10,84	0,0038	18,03	17,57	-0,0921
12,40	7,24	7,30	0,0110	10,84	10,85	0,0034	18,06	17,60	-0,0919
12,50	7,25	7,31	0,0109	10,85	10,87	0,0030	18,08	17,62	-0,0916
12,60	7,26	7,32	0,0107	10,87	10,88	0,0026	18,11	17,65	-0,0914
12,70	7,27	7,33	0,0105	10,89	10,90	0,0022	18,14	17,68	-0,0911
12,80	7,28	7,34	0,0103	10,90	10,91	0,0018	18,16	17,71	-0,0909
12,90	7,29	7,35	0,0102	10,92	10,93	0,0016	18,19	17,73	-0,0906

13,00	7,31	7,36	0,0100	10,93	10,94	0,0013	18,21	17,76	-0,0904
13,10	7,32	7,36	0,0098	10,95	10,96	0,0011	18,24	17,79	-0,0902
13,20	7,33	7,37	0,0097	10,96	10,97	0,0009	18,26	17,81	-0,0900
13,30	7,34	7,38	0,0095	10,98	10,98	0,0006	18,29	17,84	-0,0897
13,40	7,34	7,39	0,0094	10,99	11,00	0,0003	18,31	17,87	-0,0895
13,50	7,35	7,40	0,0092	11,01	11,01	0,0001	18,34	17,89	-0,0894
13,60	7,36	7,41	0,0091	11,02	11,02	-0,0001	18,36	17,92	-0,0893
13,70	7,37	7,42	0,0090	11,04	11,04	-0,0004	18,39	17,94	-0,0891
13,80	7,38	7,43	0,0088	11,05	11,05	-0,0006	18,41	17,97	-0,0890
13,90	7,39	7,44	0,0087	11,07	11,06	-0,0008	18,44	17,99	-0,0889
14,00	7,40	7,44	0,0085	11,08	11,08	-0,0011	18,46	18,02	-0,0888
14,10	7,41	7,45	0,0084	11,09	11,09	-0,0013	18,48	18,04	-0,0887
14,20	7,42	7,46	0,0082	11,11	11,10	-0,0016	18,51	18,06	-0,0886
14,30	7,43	7,47	0,0080	11,12	11,11	-0,0018	18,53	18,09	-0,0885
14,40	7,44	7,48	0,0078	11,13	11,13	-0,0020	18,55	18,11	-0,0884
14,50	7,45	7,49	0,0077	11,15	11,14	-0,0022	18,58	18,14	-0,0884
14,60	7,46	7,49	0,0075	11,16	11,15	-0,0025	18,60	18,16	-0,0884
14,70	7,47	7,50	0,0074	11,17	11,16	-0,0027	18,62	18,18	-0,0883
14,80	7,47	7,51	0,0072	11,19	11,17	-0,0029	18,65	18,20	-0,0883
14,90	7,48	7,52	0,0070	11,20	11,19	-0,0032	18,67	18,23	-0,0882
15,00	7,49	7,53	0,0069	11,21	11,20	-0,0034	18,69	18,25	-0,0882
15,10	7,50	7,53	0,0067	11,23	11,21	-0,0037	18,71	18,27	-0,0882
15,20	7,51	7,54	0,0066	11,24	11,22	-0,0039	18,73	18,29	-0,0882
15,30	7,52	7,55	0,0064	11,25	11,23	-0,0042	18,75	18,31	-0,0882
15,40	7,52	7,56	0,0063	11,27	11,24	-0,0045	18,78	18,33	-0,0882
15,50	7,53	7,56	0,0061	11,28	11,26	-0,0047	18,80	18,36	-0,0883
15,60	7,54	7,57	0,0060	11,29	11,27	-0,0049	18,82	18,38	-0,0884
15,70	7,55	7,58	0,0059	11,30	11,28	-0,0052	18,84	18,40	-0,0884
15,80	7,56	7,59	0,0057	11,32	11,29	-0,0055	18,86	18,42	-0,0885
15,90	7,56	7,59	0,0056	11,33	11,30	-0,0057	18,88	18,44	-0,0886
16,00	7,57	7,60	0,0054	11,34	11,31	-0,0060	18,90	18,46	-0,0887
16,10	7,58	7,61	0,0053	11,35	11,32	-0,0062	18,92	18,48	-0,0888
16,20	7,59	7,61	0,0051	11,36	11,33	-0,0064	18,94	18,50	-0,0888
16,30	7,60	7,62	0,0050	11,38	11,34	-0,0067	18,96	18,52	-0,0890
16,40	7,60	7,63	0,0048	11,39	11,35	-0,0069	18,98	18,54	-0,0891
16,50	7,61	7,64	0,0047	11,40	11,36	-0,0071	19,00	18,55	-0,0892
16,60	7,62	7,64	0,0045	11,41	11,37	-0,0073	19,02	18,57	-0,0894
16,70	7,63	7,65	0,0044	11,42	11,38	-0,0076	19,04	18,59	-0,0895
16,80	7,63	7,66	0,0042	11,43	11,40	-0,0078	19,06	18,61	-0,0896
16,90	7,64	7,66	0,0041	11,44	11,41	-0,0080	19,08	18,63	-0,0897
17,00	7,65	7,67	0,0039	11,46	11,42	-0,0083	19,10	18,65	-0,0897
17,10	7,66	7,68	0,0037	11,47	11,43	-0,0086	19,11	18,67	-0,0898
17,20	7,66	7,68	0,0036	11,48	11,44	-0,0088	19,13	18,68	-0,0899
17,30	7,67	7,69	0,0034	11,49	11,45	-0,0090	19,15	18,70	-0,0900
17,40	7,68	7,70	0,0033	11,50	11,46	-0,0092	19,17	18,72	-0,0901

17,50	7,69	7,70	0,0031	11,51	11,46	-0,0095	19,19	18,74	-0,0902
17,60	7,69	7,71	0,0030	11,52	11,47	-0,0097	19,21	18,75	-0,0904
17,70	7,70	7,71	0,0029	11,53	11,48	-0,0100	19,22	18,77	-0,0905
17,80	7,71	7,72	0,0027	11,54	11,49	-0,0102	19,24	18,79	-0,0906
17,90	7,71	7,73	0,0026	11,55	11,50	-0,0104	19,26	18,81	-0,0907
18,00	7,72	7,73	0,0025	11,57	11,51	-0,0107	19,28	18,82	-0,0908
18,10	7,73	7,74	0,0024	11,58	11,52	-0,0109	19,30	18,84	-0,0909
18,20	7,73	7,75	0,0022	11,59	11,53	-0,0111	19,31	18,86	-0,0910
18,30	7,74	7,75	0,0020	11,60	11,54	-0,0113	19,33	18,87	-0,0911
18,40	7,75	7,76	0,0019	11,61	11,55	-0,0116	19,35	18,89	-0,0912
18,50	7,75	7,76	0,0017	11,62	11,56	-0,0118	19,36	18,91	-0,0913
18,60	7,76	7,77	0,0016	11,63	11,57	-0,0120	19,38	18,92	-0,0913
18,70	7,77	7,78	0,0014	11,64	11,58	-0,0122	19,40	18,94	-0,0914
18,80	7,77	7,78	0,0012	11,65	11,59	-0,0124	19,41	18,96	-0,0916
18,90	7,78	7,79	0,0011	11,66	11,59	-0,0127	19,43	18,97	-0,0917
19,00	7,79	7,79	0,0009	11,67	11,60	-0,0129	19,45	18,99	-0,0918
19,10	7,79	7,80	0,0008	11,68	11,61	-0,0131	19,46	19,00	-0,0919
19,20	7,80	7,80	0,0006	11,69	11,62	-0,0133	19,48	19,02	-0,0921
19,30	7,81	7,81	0,0005	11,70	11,63	-0,0136	19,50	19,04	-0,0922
19,40	7,81	7,81	0,0004	11,71	11,64	-0,0138	19,51	19,05	-0,0924
19,50	7,82	7,82	0,0002	11,72	11,65	-0,0140	19,53	19,07	-0,0925
19,60	7,83	7,83	0,0001	11,72	11,65	-0,0142	19,54	19,08	-0,0928
19,70	7,83	7,83	-0,0001	11,73	11,66	-0,0145	19,56	19,10	-0,0930
19,80	7,84	7,84	-0,0002	11,74	11,67	-0,0147	19,58	19,11	-0,0932
19,90	7,84	7,84	-0,0004	11,75	11,68	-0,0149	19,59	19,12	-0,0934
20,00	7,85	7,85		11,76	11,69		19,61	19,14	
Max			0,0240			0,0165			-0,0379
Min			-0,1476			-0,2255			-0,3788

F.2 Temperature increase Steel Teflon

t [s]	Comsol 0,4 W	HotDisk 0,4 W	Curve fit	Comsol 0,6 W	HotDisk 0,6 W	Curve fit	Comsol 1 W	HotDisk 1 W	Curve fit
0,1	0,47	0,77	0,0232	1,63	1,17	-0,0660	2,72	1,93	-0,1128
0,2	1,09	1,02	-0,0027	1,73	1,53	-0,0223	2,88	2,54	-0,0397
0,3	1,15	1,19	0,0088	1,82	1,79	-0,0042	3,03	2,98	-0,0089
0,4	1,21	1,26	0,0083	1,90	1,88	-0,0040	3,17	3,13	-0,0081
0,5	1,27	1,31	0,0065	1,98	1,96	-0,0057	3,30	3,25	-0,0123
0,6	1,32	1,34	0,0046	2,05	2,02	-0,0070	3,43	3,35	-0,0147
0,7	1,37	1,39	0,0033	2,12	2,08	-0,0078	3,53	3,46	-0,0138
0,8	1,42	1,43	0,0030	2,19	2,15	-0,0085	3,64	3,57	-0,0127
0,9	1,46	1,48	0,0038	2,26	2,21	-0,0081	3,74	3,68	-0,0120
1	1,50	1,52	0,0043	2,32	2,28	-0,0061	3,84	3,79	-0,0120
1,1	1,54	1,56	0,0045	2,36	2,34	-0,0039	3,95	3,89	-0,0113
1,2	1,58	1,60	0,0043	2,41	2,40	-0,0021	4,04	3,99	-0,0082
1,3	1,62	1,64	0,0039	2,46	2,46	-0,0008	4,11	4,08	-0,0043

1,4	1,66	1,67	0,0032	2,51	2,51	0,0001	4,18	4,17	-0,0011
1,5	1,69	1,71	0,0036	2,56	2,56	0,0007	4,26	4,26	0,0016
1,6	1,72	1,74	0,0051	2,61	2,61	0,0008	4,33	4,34	0,0036
1,7	1,75	1,78	0,0065	2,66	2,66	0,0007	4,40	4,42	0,0052
1,8	1,77	1,81	0,0077	2,71	2,71	0,0007	4,47	4,50	0,0062
1,9	1,80	1,84	0,0087	2,75	2,76	0,0022	4,55	4,58	0,0067
2	1,82	1,87	0,0095	2,78	2,80	0,0048	4,62	4,65	0,0068
2,1	1,85	1,90	0,0101	2,82	2,85	0,0071	4,69	4,73	0,0065
2,2	1,87	1,93	0,0106	2,85	2,89	0,0092	4,77	4,80	0,0057
2,3	1,90	1,95	0,0110	2,88	2,93	0,0111	4,84	4,87	0,0072
2,4	1,92	1,98	0,0112	2,91	2,97	0,0127	4,89	4,93	0,0110
2,5	1,95	2,00	0,0112	2,94	3,01	0,0142	4,93	5,00	0,0145
2,6	1,97	2,03	0,0111	2,97	3,04	0,0154	4,98	5,06	0,0176
2,7	2,00	2,05	0,0109	3,00	3,08	0,0164	5,02	5,12	0,0204
2,8	2,02	2,08	0,0105	3,03	3,12	0,0173	5,07	5,18	0,0229
2,9	2,05	2,10	0,0108	3,06	3,15	0,0180	5,12	5,24	0,0251
3	2,07	2,12	0,0118	3,09	3,19	0,0185	5,16	5,29	0,0270
3,1	2,08	2,15	0,0129	3,13	3,22	0,0188	5,21	5,35	0,0287
3,2	2,10	2,17	0,0138	3,16	3,25	0,0190	5,25	5,40	0,0300
3,3	2,12	2,19	0,0147	3,19	3,28	0,0190	5,30	5,45	0,0312
3,4	2,13	2,21	0,0154	3,22	3,31	0,0189	5,35	5,51	0,0320
3,5	2,15	2,23	0,0161	3,25	3,34	0,0186	5,39	5,56	0,0327
3,6	2,17	2,25	0,0167	3,28	3,37	0,0182	5,44	5,60	0,0331
3,7	2,18	2,27	0,0172	3,31	3,40	0,0181	5,49	5,65	0,0334
3,8	2,20	2,29	0,0176	3,34	3,43	0,0190	5,53	5,70	0,0334
3,9	2,22	2,30	0,0179	3,36	3,46	0,0202	5,58	5,74	0,0332
4	2,23	2,32	0,0181	3,38	3,48	0,0213	5,62	5,79	0,0328
4,1	2,25	2,34	0,0183	3,40	3,51	0,0223	5,67	5,83	0,0322
4,2	2,27	2,36	0,0184	3,42	3,54	0,0232	5,72	5,88	0,0315
4,3	2,28	2,37	0,0184	3,44	3,56	0,0239	5,76	5,92	0,0320
4,4	2,30	2,39	0,0184	3,47	3,59	0,0246	5,80	5,96	0,0337
4,5	2,31	2,41	0,0183	3,49	3,61	0,0252	5,83	6,00	0,0352
4,6	2,33	2,42	0,0181	3,51	3,63	0,0257	5,86	6,04	0,0366
4,7	2,35	2,44	0,0179	3,53	3,66	0,0261	5,89	6,08	0,0379
4,8	2,36	2,45	0,0176	3,55	3,68	0,0264	5,92	6,12	0,0390
4,9	2,38	2,47	0,0176	3,57	3,70	0,0266	5,96	6,15	0,0399
5	2,39	2,48	0,0180	3,59	3,72	0,0268	5,99	6,19	0,0407
5,1	2,41	2,50	0,0185	3,61	3,75	0,0268	6,02	6,23	0,0414
5,2	2,42	2,51	0,0188	3,63	3,77	0,0268	6,05	6,26	0,0420
5,3	2,43	2,53	0,0191	3,65	3,79	0,0267	6,08	6,30	0,0424
5,4	2,44	2,54	0,0193	3,68	3,81	0,0266	6,12	6,33	0,0428
5,5	2,45	2,55	0,0195	3,70	3,83	0,0263	6,15	6,36	0,0430
5,6	2,47	2,57	0,0197	3,72	3,85	0,0260	6,18	6,40	0,0430
5,7	2,48	2,58	0,0198	3,74	3,87	0,0259	6,21	6,43	0,0430
5,8	2,49	2,59	0,0199	3,76	3,89	0,0262	6,25	6,46	0,0429

5,9	2,50	2,60	0,0199	3,77	3,91	0,0266	6,28	6,49	0,0426
6	2,52	2,62	0,0199	3,79	3,92	0,0271	6,31	6,52	0,0423
6,1	2,53	2,63	0,0199	3,81	3,94	0,0274	6,34	6,55	0,0418
6,2	2,54	2,64	0,0198	3,82	3,96	0,0277	6,37	6,58	0,0413
6,3	2,55	2,65	0,0197	3,84	3,98	0,0280	6,41	6,61	0,0414
6,4	2,56	2,66	0,0195	3,85	4,00	0,0282	6,43	6,64	0,0422
6,5	2,58	2,67	0,0193	3,87	4,01	0,0283	6,45	6,67	0,0430
6,6	2,59	2,69	0,0190	3,89	4,03	0,0284	6,48	6,70	0,0436
6,7	2,60	2,70	0,0188	3,90	4,05	0,0285	6,50	6,72	0,0442
6,8	2,61	2,71	0,0185	3,92	4,06	0,0285	6,53	6,75	0,0447
6,9	2,63	2,72	0,0184	3,94	4,08	0,0284	6,55	6,78	0,0451
7	2,64	2,73	0,0186	3,95	4,09	0,0283	6,58	6,80	0,0454
7,1	2,65	2,74	0,0188	3,97	4,11	0,0282	6,60	6,83	0,0457
7,2	2,65	2,75	0,0190	3,98	4,12	0,0280	6,63	6,85	0,0459
7,3	2,66	2,76	0,0191	4,00	4,14	0,0277	6,65	6,88	0,0460
7,4	2,67	2,77	0,0192	4,02	4,15	0,0275	6,67	6,90	0,0460
7,5	2,68	2,78	0,0193	4,03	4,17	0,0271	6,70	6,93	0,0460
7,6	2,69	2,79	0,0193	4,05	4,18	0,0268	6,72	6,95	0,0459
7,7	2,70	2,80	0,0194	4,06	4,20	0,0265	6,75	6,98	0,0457
7,8	2,71	2,81	0,0194	4,08	4,21	0,0266	6,77	7,00	0,0455
7,9	2,72	2,82	0,0194	4,09	4,23	0,0268	6,80	7,02	0,0452
8	2,73	2,83	0,0193	4,10	4,24	0,0270	6,82	7,05	0,0448
8,1	2,74	2,83	0,0193	4,12	4,25	0,0272	6,84	7,07	0,0444
8,2	2,75	2,84	0,0192	4,13	4,27	0,0273	6,87	7,09	0,0440
8,3	2,76	2,85	0,0191	4,14	4,28	0,0274	6,89	7,11	0,0439
8,4	2,77	2,86	0,0189	4,15	4,29	0,0275	6,91	7,13	0,0441
8,5	2,77	2,87	0,0188	4,17	4,30	0,0275	6,93	7,15	0,0444
8,6	2,78	2,88	0,0186	4,18	4,32	0,0275	6,95	7,18	0,0445
8,7	2,79	2,89	0,0184	4,19	4,33	0,0275	6,97	7,20	0,0446
8,8	2,80	2,89	0,0182	4,20	4,34	0,0274	6,99	7,22	0,0447
8,9	2,81	2,90	0,0180	4,22	4,35	0,0273	7,01	7,24	0,0447
9	2,82	2,91	0,0179	4,23	4,37	0,0272	7,03	7,26	0,0447
9,1	2,83	2,92	0,0178	4,24	4,38	0,0270	7,05	7,28	0,0446
9,2	2,84	2,93	0,0178	4,26	4,39	0,0268	7,07	7,30	0,0444
9,3	2,84	2,93	0,0177	4,27	4,40	0,0266	7,09	7,32	0,0442
9,4	2,85	2,94	0,0176	4,28	4,41	0,0264	7,11	7,34	0,0440
9,5	2,86	2,95	0,0175	4,29	4,42	0,0261	7,13	7,35	0,0438
9,6	2,87	2,96	0,0174	4,31	4,44	0,0258	7,15	7,37	0,0434
9,7	2,88	2,96	0,0173	4,32	4,45	0,0255	7,17	7,39	0,0431
9,8	2,88	2,97	0,0172	4,33	4,46	0,0253	7,19	7,41	0,0427
9,9	2,89	2,98	0,0171	4,34	4,47	0,0252	7,21	7,43	0,0422
10	2,90	2,98	0,0170	4,35	4,48	0,0250	7,23	7,44	0,0418
10,1	2,91	2,99	0,0169	4,36	4,49	0,0249	7,25	7,46	0,0413
10,2	2,91	3,00	0,0168	4,38	4,50	0,0248	7,27	7,48	0,0407
10,3	2,92	3,01	0,0167	4,39	4,51	0,0246	7,30	7,50	0,0404

10,4	2,93	3,01	0,0167	4,40	4,52	0,0244	7,31	7,51	0,0404
10,5	2,94	3,02	0,0166	4,41	4,53	0,0243	7,33	7,53	0,0404
10,6	2,94	3,03	0,0165	4,42	4,54	0,0241	7,35	7,55	0,0404
10,7	2,95	3,03	0,0164	4,43	4,55	0,0239	7,36	7,56	0,0403
10,8	2,96	3,04	0,0163	4,44	4,56	0,0238	7,38	7,58	0,0402
10,9	2,96	3,05	0,0162	4,45	4,57	0,0237	7,40	7,60	0,0401
11	2,97	3,05	0,0161	4,46	4,58	0,0235	7,41	7,61	0,0399
11,1	2,98	3,06	0,0160	4,47	4,59	0,0233	7,43	7,63	0,0397
11,2	2,98	3,06	0,0159	4,48	4,60	0,0232	7,45	7,64	0,0394
11,3	2,99	3,07	0,0158	4,49	4,61	0,0230	7,46	7,66	0,0392
11,4	3,00	3,08	0,0156	4,50	4,62	0,0228	7,48	7,67	0,0389
11,5	3,01	3,08	0,0154	4,51	4,63	0,0227	7,50	7,69	0,0385
11,6	3,01	3,09	0,0153	4,52	4,63	0,0225	7,51	7,70	0,0381
11,7	3,02	3,09	0,0152	4,53	4,64	0,0224	7,53	7,72	0,0378
11,8	3,02	3,10	0,0151	4,54	4,65	0,0222	7,55	7,73	0,0373
11,9	3,03	3,11	0,0149	4,55	4,66	0,0220	7,56	7,75	0,0369
12	3,04	3,11	0,0148	4,56	4,67	0,0218	7,58	7,76	0,0364
12,1	3,04	3,12	0,0146	4,57	4,68	0,0216	7,60	7,78	0,0359
12,2	3,05	3,12	0,0145	4,58	4,69	0,0214	7,61	7,79	0,0354
12,3	3,06	3,13	0,0143	4,59	4,70	0,0211	7,63	7,81	0,0349
12,4	3,06	3,13	0,0142	4,60	4,70	0,0209	7,65	7,82	0,0345
12,5	3,07	3,14	0,0141	4,61	4,71	0,0207	7,66	7,83	0,0341
12,6	3,08	3,15	0,0139	4,62	4,72	0,0205	7,68	7,85	0,0338
12,7	3,08	3,15	0,0138	4,63	4,73	0,0202	7,69	7,86	0,0334
12,8	3,09	3,16	0,0136	4,64	4,74	0,0200	7,71	7,87	0,0330
12,9	3,09	3,16	0,0135	4,64	4,74	0,0198	7,72	7,89	0,0326
13	3,10	3,17	0,0137	4,65	4,75	0,0196	7,74	7,90	0,0323
13,1	3,11	3,18	0,0141	4,66	4,76	0,0193	7,75	7,91	0,0319
13,2	3,11	3,18	0,0143	4,67	4,77	0,0191	7,77	7,93	0,0314
13,3	3,12	3,19	0,0142	4,68	4,78	0,0189	7,78	7,94	0,0310
13,4	3,12	3,19	0,0139	4,69	4,78	0,0187	7,80	7,95	0,0306
13,5	3,13	3,20	0,0136	4,70	4,79	0,0184	7,81	7,96	0,0302
13,6	3,14	3,20	0,0134	4,71	4,80	0,0182	7,83	7,98	0,0298
13,7	3,14	3,21	0,0131	4,72	4,81	0,0180	7,84	7,99	0,0294
13,8	3,15	3,21	0,0130	4,72	4,81	0,0177	7,86	8,00	0,0290
13,9	3,15	3,22	0,0128	4,73	4,82	0,0175	7,87	8,01	0,0286
14	3,16	3,22	0,0126	4,74	4,83	0,0172	7,88	8,03	0,0282
14,1	3,16	3,23	0,0125	4,75	4,83	0,0170	7,90	8,04	0,0278
14,2	3,17	3,23	0,0123	4,76	4,84	0,0167	7,91	8,05	0,0274
14,3	3,17	3,24	0,0121	4,77	4,85	0,0165	7,93	8,06	0,0269
14,4	3,18	3,24	0,0119	4,77	4,86	0,0162	7,94	8,07	0,0264
14,5	3,19	3,24	0,0118	4,78	4,86	0,0160	7,95	8,08	0,0260
14,6	3,19	3,25	0,0116	4,79	4,87	0,0157	7,97	8,10	0,0255
14,7	3,20	3,25	0,0114	4,80	4,88	0,0154	7,98	8,11	0,0251
14,8	3,20	3,26	0,0112	4,81	4,88	0,0152	7,99	8,12	0,0246

14,9	3,21	3,26	0,0111	4,81	4,89	0,0149	8,01	8,13	0,0242
15	3,21	3,27	0,0109	4,82	4,90	0,0146	8,02	8,14	0,0237
15,1	3,22	3,27	0,0107	4,83	4,90	0,0144	8,03	8,15	0,0232
15,2	3,22	3,28	0,0105	4,84	4,91	0,0141	8,05	8,16	0,0228
15,3	3,23	3,28	0,0103	4,85	4,92	0,0138	8,06	8,17	0,0223
15,4	3,23	3,28	0,0101	4,85	4,92	0,0136	8,07	8,18	0,0218
15,5	3,24	3,29	0,0099	4,86	4,93	0,0133	8,09	8,19	0,0214
15,6	3,24	3,29	0,0097	4,87	4,94	0,0131	8,10	8,21	0,0209
15,7	3,25	3,30	0,0095	4,88	4,94	0,0128	8,11	8,22	0,0204
15,8	3,25	3,30	0,0093	4,88	4,95	0,0126	8,13	8,23	0,0199
15,9	3,26	3,31	0,0091	4,89	4,95	0,0123	8,14	8,24	0,0194
16	3,26	3,31	0,0089	4,90	4,96	0,0120	8,15	8,25	0,0190
16,1	3,27	3,31	0,0088	4,91	4,97	0,0117	8,16	8,26	0,0185
16,2	3,27	3,32	0,0086	4,91	4,97	0,0114	8,18	8,27	0,0180
16,3	3,28	3,32	0,0084	4,92	4,98	0,0112	8,19	8,28	0,0175
16,4	3,28	3,33	0,0082	4,93	4,98	0,0109	8,20	8,29	0,0170
16,5	3,29	3,33	0,0080	4,94	4,99	0,0106	8,21	8,30	0,0166
16,6	3,29	3,33	0,0078	4,94	5,00	0,0103	8,22	8,31	0,0161
16,7	3,30	3,34	0,0076	4,95	5,00	0,0100	8,24	8,32	0,0156
16,8	3,30	3,34	0,0074	4,96	5,01	0,0097	8,25	8,33	0,0151
16,9	3,31	3,34	0,0072	4,97	5,01	0,0095	8,26	8,34	0,0146
17	3,31	3,35	0,0070	4,97	5,02	0,0092	8,27	8,34	0,0140
17,1	3,32	3,35	0,0068	4,98	5,02	0,0089	8,29	8,35	0,0135
17,2	3,32	3,36	0,0067	4,99	5,03	0,0086	8,30	8,36	0,0130
17,3	3,33	3,36	0,0064	4,99	5,04	0,0084	8,31	8,37	0,0126
17,4	3,33	3,36	0,0062	5,00	5,04	0,0081	8,32	8,38	0,0121
17,5	3,34	3,37	0,0060	5,01	5,05	0,0078	8,33	8,39	0,0116
17,6	3,34	3,37	0,0059	5,01	5,05	0,0075	8,34	8,40	0,0111
17,7	3,35	3,37	0,0057	5,02	5,06	0,0073	8,36	8,41	0,0106
17,8	3,35	3,38	0,0055	5,03	5,06	0,0070	8,37	8,42	0,0101
17,9	3,35	3,38	0,0053	5,03	5,07	0,0067	8,38	8,43	0,0096
18	3,36	3,38	0,0051	5,04	5,07	0,0064	8,39	8,44	0,0091
18,1	3,36	3,39	0,0048	5,05	5,08	0,0061	8,40	8,45	0,0086
18,2	3,37	3,39	0,0046	5,05	5,08	0,0058	8,41	8,45	0,0081
18,3	3,37	3,39	0,0044	5,06	5,09	0,0055	8,42	8,46	0,0076
18,4	3,38	3,40	0,0043	5,07	5,10	0,0052	8,43	8,47	0,0071
18,5	3,38	3,40	0,0041	5,07	5,10	0,0050	8,45	8,48	0,0066
18,6	3,39	3,41	0,0039	5,08	5,11	0,0047	8,46	8,49	0,0061
18,7	3,39	3,41	0,0037	5,09	5,11	0,0044	8,47	8,50	0,0056
18,8	3,39	3,41	0,0035	5,09	5,12	0,0041	8,48	8,51	0,0050
18,9	3,40	3,42	0,0033	5,10	5,12	0,0038	8,49	8,51	0,0045
19	3,40	3,42	0,0031	5,11	5,13	0,0035	8,50	8,52	0,0040
19,1	3,41	3,42	0,0029	5,11	5,13	0,0032	8,51	8,53	0,0035
19,2	3,41	3,43	0,0027	5,12	5,14	0,0029	8,52	8,54	0,0030
19,3	3,42	3,43	0,0025	5,13	5,14	0,0026	8,53	8,55	0,0025

19,4	3,42	3,43	0,0023	5,13	5,15	0,0023	8,54	8,55	0,0020
19,5	3,42	3,43	0,0021	5,14	5,15	0,0020	8,55	8,56	0,0015
19,6	3,43	3,44	0,0019	5,15	5,15	0,0018	8,56	8,57	0,0010
19,7	3,43	3,44	0,0016	5,15	5,16	0,0015	8,58	8,58	0,0005
19,8	3,44	3,44	0,0015	5,16	5,16	0,0012	8,59	8,59	0,0000
19,9	3,44	3,45	0,0013	5,16	5,17	0,0009	8,60	8,59	-0,0005
20	3,44	3,45		5,17	5,17		8,61	8,60	
Max			0,0232			0,0285			0,0460
Min			-0,0027			-0,0660			-0,1128

F. 3 Temperature increase Lexan Steel

[s]	Comsol 0,6 W	HotDisk 0,6 W	Curve fit	Comsol 0,8 W	HotDisk 0,8 W	Curve fit	Comsol 1 W	HotDisk 1 W	Curve fit
0,1	2,08	1,67	-0,0498	2,77	2,20	-0,0738	3,44	2,71	-0,0959
0,2	2,67	2,57	0,0027	3,56	3,39	-0,0074	4,42	4,19	-0,0188
0,3	3,12	3,24	0,0257	4,16	4,26	0,0209	5,23	5,28	0,0167
0,4	3,51	3,64	0,0220	4,69	4,80	0,0211	5,82	5,94	0,0153
0,5	3,87	3,95	0,0162	5,11	5,21	0,0125	6,42	6,46	-0,0034
0,6	4,14	4,22	0,0125	5,53	5,56	-0,0049	6,96	6,89	-0,0142
0,7	4,41	4,46	0,0059	5,96	5,88	-0,0138	7,37	7,29	-0,0171
0,8	4,68	4,69	-0,0030	6,26	6,19	-0,0120	7,77	7,68	-0,0238
0,9	4,96	4,92	-0,0092	6,54	6,49	-0,0119	8,18	8,04	-0,0343
1	5,18	5,13	-0,0082	6,83	6,76	-0,0148	8,59	8,39	-0,0486
1,1	5,35	5,32	-0,0050	7,11	7,03	-0,0207	9,00	8,72	-0,0570
1,2	5,53	5,51	-0,0037	7,40	7,28	-0,0291	9,31	9,03	-0,0536
1,3	5,71	5,69	-0,0042	7,68	7,51	-0,0400	9,57	9,32	-0,0476
1,4	5,88	5,86	-0,0064	7,97	7,74	-0,0441	9,83	9,60	-0,0443
1,5	6,06	6,02	-0,0101	8,17	7,95	-0,0387	10,08	9,87	-0,0434
1,6	6,24	6,18	-0,0151	8,34	8,16	-0,0329	10,34	10,12	-0,0448
1,7	6,41	6,33	-0,0214	8,51	8,36	-0,0288	10,60	10,37	-0,0482
1,8	6,59	6,47	-0,0284	8,68	8,55	-0,0262	10,86	10,61	-0,0537
1,9	6,76	6,60	-0,0288	8,85	8,73	-0,0251	11,12	10,83	-0,0609
2	6,86	6,73	-0,0230	9,03	8,90	-0,0254	11,37	11,05	-0,0699
2,1	6,96	6,86	-0,0182	9,20	9,07	-0,0270	11,63	11,26	-0,0805
2,2	7,06	6,98	-0,0143	9,37	9,23	-0,0299	11,89	11,46	-0,0896
2,3	7,16	7,10	-0,0113	9,54	9,38	-0,0338	12,12	11,65	-0,0889
2,4	7,26	7,21	-0,0091	9,72	9,53	-0,0389	12,26	11,84	-0,0814
2,5	7,36	7,32	-0,0076	9,89	9,68	-0,0449	12,41	12,02	-0,0750
2,6	7,46	7,42	-0,0070	10,06	9,82	-0,0520	12,55	12,19	-0,0698
2,7	7,56	7,53	-0,0070	10,23	9,95	-0,0599	12,70	12,36	-0,0659
2,8	7,66	7,62	-0,0076	10,40	10,08	-0,0644	12,84	12,52	-0,0629
2,9	7,76	7,72	-0,0088	10,53	10,21	-0,0625	12,99	12,68	-0,0610
3	7,86	7,81	-0,0107	10,63	10,33	-0,0584	13,13	12,83	-0,0601
3,1	7,96	7,90	-0,0131	10,73	10,45	-0,0550	13,28	12,98	-0,0601
3,2	8,06	7,99	-0,0161	10,83	10,56	-0,0523	13,42	13,12	-0,0609

3,3	8,16	8,07	-0,0195	10,93	10,68	-0,0503	13,57	13,26	-0,0626
3,4	8,26	8,15	-0,0234	11,03	10,78	-0,0489	13,71	13,39	-0,0651
3,5	8,36	8,23	-0,0278	11,13	10,89	-0,0482	13,86	13,52	-0,0684
3,6	8,46	8,31	-0,0326	11,23	10,99	-0,0480	14,00	13,65	-0,0723
3,7	8,56	8,38	-0,0373	11,33	11,09	-0,0483	14,15	13,78	-0,0770
3,8	8,65	8,45	-0,0384	11,43	11,19	-0,0492	14,29	13,90	-0,0822
3,9	8,71	8,52	-0,0363	11,53	11,28	-0,0506	14,44	14,01	-0,0882
4	8,77	8,59	-0,0346	11,63	11,37	-0,0525	14,58	14,13	-0,0947
4,1	8,83	8,66	-0,0332	11,73	11,46	-0,0548	14,73	14,24	-0,1018
4,2	8,89	8,72	-0,0322	11,83	11,55	-0,0575	14,87	14,35	-0,1079
4,3	8,95	8,79	-0,0316	11,93	11,63	-0,0607	15,00	14,45	-0,1089
4,4	9,01	8,85	-0,0312	12,03	11,71	-0,0643	15,09	14,55	-0,1061
4,5	9,06	8,91	-0,0311	12,13	11,79	-0,0683	15,18	14,66	-0,1039
4,6	9,12	8,97	-0,0312	12,22	11,87	-0,0727	15,27	14,75	-0,1020
4,7	9,18	9,03	-0,0317	12,32	11,95	-0,0774	15,36	14,85	-0,1007
4,8	9,24	9,08	-0,0324	12,42	12,02	-0,0802	15,44	14,94	-0,0997
4,9	9,30	9,14	-0,0334	12,50	12,10	-0,0795	15,53	15,03	-0,0992
5	9,36	9,19	-0,0346	12,56	12,17	-0,0776	15,62	15,12	-0,0990
5,1	9,42	9,24	-0,0360	12,62	12,24	-0,0761	15,71	15,21	-0,0993
5,2	9,48	9,30	-0,0377	12,69	12,31	-0,0748	15,79	15,30	-0,0999
5,3	9,54	9,35	-0,0395	12,75	12,38	-0,0738	15,88	15,38	-0,1009
5,4	9,60	9,40	-0,0416	12,81	12,44	-0,0730	15,97	15,46	-0,1022
5,5	9,66	9,44	-0,0439	12,87	12,51	-0,0725	16,06	15,54	-0,1038
5,6	9,72	9,49	-0,0463	12,93	12,57	-0,0723	16,15	15,62	-0,1058
5,7	9,78	9,54	-0,0487	12,99	12,63	-0,0723	16,23	15,70	-0,1081
5,8	9,83	9,58	-0,0491	13,05	12,69	-0,0726	16,32	15,78	-0,1106
5,9	9,87	9,63	-0,0477	13,12	12,75	-0,0731	16,41	15,85	-0,1135
6	9,91	9,67	-0,0466	13,18	12,81	-0,0739	16,50	15,92	-0,1166
6,1	9,95	9,72	-0,0456	13,24	12,87	-0,0748	16,59	15,99	-0,1200
6,2	9,98	9,76	-0,0448	13,30	12,92	-0,0760	16,67	16,07	-0,1229
6,3	10,02	9,80	-0,0441	13,36	12,98	-0,0773	16,75	16,13	-0,1228
6,4	10,06	9,84	-0,0436	13,42	13,03	-0,0789	16,81	16,20	-0,1208
6,5	10,10	9,88	-0,0432	13,48	13,09	-0,0806	16,87	16,27	-0,1189
6,6	10,13	9,92	-0,0429	13,55	13,14	-0,0825	16,92	16,33	-0,1173
6,7	10,17	9,96	-0,0428	13,61	13,19	-0,0846	16,98	16,40	-0,1159
6,8	10,21	10,00	-0,0429	13,67	13,24	-0,0857	17,04	16,46	-0,1148
6,9	10,25	10,03	-0,0430	13,72	13,29	-0,0848	17,09	16,52	-0,1139
7	10,28	10,07	-0,0433	13,76	13,34	-0,0832	17,15	16,58	-0,1131
7,1	10,32	10,11	-0,0437	13,80	13,39	-0,0817	17,21	16,64	-0,1125
7,2	10,36	10,14	-0,0442	13,84	13,43	-0,0804	17,26	16,70	-0,1122
7,3	10,40	10,18	-0,0448	13,88	13,48	-0,0793	17,32	16,76	-0,1120
7,4	10,44	10,21	-0,0456	13,92	13,53	-0,0783	17,38	16,82	-0,1120
7,5	10,47	10,24	-0,0464	13,96	13,57	-0,0774	17,43	16,87	-0,1123
7,6	10,51	10,28	-0,0473	14,00	13,62	-0,0767	17,49	16,93	-0,1126
7,7	10,55	10,31	-0,0482	14,04	13,66	-0,0761	17,55	16,98	-0,1132

7,8	10,59	10,34	-0,0480	14,08	13,70	-0,0757	17,60	17,04	-0,1139
7,9	10,61	10,37	-0,0468	14,12	13,74	-0,0754	17,66	17,09	-0,1148
8	10,64	10,41	-0,0456	14,16	13,79	-0,0752	17,72	17,14	-0,1158
8,1	10,66	10,44	-0,0446	14,20	13,83	-0,0751	17,78	17,19	-0,1169
8,2	10,69	10,47	-0,0436	14,24	13,87	-0,0752	17,83	17,24	-0,1178
8,3	10,71	10,50	-0,0428	14,28	13,91	-0,0753	17,88	17,29	-0,1170
8,4	10,74	10,53	-0,0420	14,32	13,95	-0,0756	17,92	17,34	-0,1150
8,5	10,76	10,55	-0,0413	14,36	13,99	-0,0760	17,96	17,39	-0,1131
8,6	10,79	10,58	-0,0407	14,40	14,02	-0,0765	18,00	17,44	-0,1114
8,7	10,81	10,61	-0,0402	14,45	14,06	-0,0772	18,04	17,49	-0,1099
8,8	10,84	10,64	-0,0397	14,49	14,10	-0,0771	18,08	17,53	-0,1084
8,9	10,86	10,67	-0,0393	14,52	14,13	-0,0760	18,12	17,58	-0,1071
9	10,89	10,69	-0,0391	14,55	14,17	-0,0744	18,16	17,62	-0,1059
9,1	10,92	10,72	-0,0388	14,57	14,21	-0,0729	18,19	17,67	-0,1048
9,2	10,94	10,75	-0,0387	14,60	14,24	-0,0715	18,23	17,71	-0,1038
9,3	10,97	10,77	-0,0386	14,63	14,28	-0,0703	18,27	17,75	-0,1030
9,4	10,99	10,80	-0,0386	14,66	14,31	-0,0691	18,31	17,80	-0,1023
9,5	11,02	10,82	-0,0386	14,69	14,34	-0,0679	18,35	17,84	-0,1017
9,6	11,04	10,85	-0,0387	14,71	14,38	-0,0669	18,39	17,88	-0,1012
9,7	11,07	10,87	-0,0388	14,74	14,41	-0,0660	18,43	17,92	-0,1007
9,8	11,09	10,90	-0,0383	14,77	14,44	-0,0652	18,46	17,96	-0,1004
9,9	11,11	10,92	-0,0372	14,80	14,47	-0,0644	18,50	18,00	-0,1002
10	11,13	10,95	-0,0363	14,83	14,51	-0,0637	18,54	18,04	-0,1001
10,1	11,15	10,97	-0,0353	14,85	14,54	-0,0631	18,58	18,08	-0,1002
10,2	11,17	10,99	-0,0345	14,88	14,57	-0,0626	18,62	18,12	-0,1000
10,3	11,19	11,01	-0,0336	14,91	14,60	-0,0621	18,65	18,16	-0,0987
10,4	11,20	11,04	-0,0329	14,94	14,63	-0,0617	18,68	18,19	-0,0968
10,5	11,22	11,06	-0,0322	14,97	14,66	-0,0614	18,71	18,23	-0,0950
10,6	11,24	11,08	-0,0315	14,99	14,69	-0,0612	18,74	18,27	-0,0933
10,7	11,26	11,10	-0,0309	15,02	14,72	-0,0610	18,77	18,30	-0,0916
10,8	11,28	11,12	-0,0304	15,05	14,74	-0,0605	18,79	18,34	-0,0901
10,9	11,30	11,15	-0,0299	15,07	14,77	-0,0594	18,82	18,37	-0,0886
11	11,32	11,17	-0,0295	15,09	14,80	-0,0580	18,85	18,41	-0,0872
11,1	11,33	11,19	-0,0291	15,11	14,83	-0,0567	18,88	18,44	-0,0859
11,2	11,35	11,21	-0,0287	15,14	14,86	-0,0555	18,90	18,48	-0,0846
11,3	11,37	11,23	-0,0284	15,16	14,88	-0,0543	18,93	18,51	-0,0835
11,4	11,39	11,25	-0,0282	15,18	14,91	-0,0532	18,96	18,54	-0,0824
11,5	11,41	11,27	-0,0280	15,20	14,94	-0,0522	18,99	18,58	-0,0814
11,6	11,43	11,29	-0,0278	15,22	14,96	-0,0512	19,01	18,61	-0,0805
11,7	11,45	11,31	-0,0276	15,24	14,99	-0,0502	19,04	18,64	-0,0796
11,8	11,46	11,33	-0,0269	15,26	15,01	-0,0493	19,07	18,67	-0,0788
11,9	11,48	11,35	-0,0259	15,28	15,04	-0,0485	19,10	18,71	-0,0781
12	11,49	11,36	-0,0249	15,30	15,06	-0,0478	19,13	18,74	-0,0774
12,1	11,50	11,38	-0,0239	15,32	15,09	-0,0471	19,15	18,77	-0,0769
12,2	11,52	11,40	-0,0230	15,35	15,11	-0,0464	19,18	18,80	-0,0762

12,3	11,53	11,42	-0,0221	15,37	15,14	-0,0458	19,21	18,83	-0,0750
12,4	11,54	11,44	-0,0212	15,39	15,16	-0,0453	19,23	18,86	-0,0735
12,5	11,56	11,45	-0,0204	15,41	15,18	-0,0448	19,25	18,89	-0,0717
12,6	11,57	11,47	-0,0197	15,43	15,21	-0,0443	19,27	18,92	-0,0700
12,7	11,59	11,49	-0,0189	15,45	15,23	-0,0440	19,29	18,94	-0,0686
12,8	11,60	11,51	-0,0182	15,47	15,25	-0,0433	19,31	18,97	-0,0673
12,9	11,61	11,52	-0,0175	15,49	15,27	-0,0421	19,33	19,00	-0,0661
13	11,63	11,54	-0,0169	15,50	15,30	-0,0407	19,36	19,03	-0,0646
13,1	11,64	11,56	-0,0163	15,52	15,32	-0,0395	19,38	19,06	-0,0632
13,2	11,65	11,57	-0,0157	15,54	15,34	-0,0382	19,40	19,08	-0,0621
13,3	11,67	11,59	-0,0152	15,55	15,36	-0,0370	19,42	19,11	-0,0611
13,4	11,68	11,61	-0,0147	15,57	15,38	-0,0359	19,44	19,14	-0,0602
13,5	11,69	11,62	-0,0142	15,58	15,41	-0,0348	19,46	19,16	-0,0593
13,6	11,71	11,64	-0,0138	15,60	15,43	-0,0337	19,48	19,19	-0,0581
13,7	11,72	11,65	-0,0134	15,61	15,45	-0,0327	19,50	19,22	-0,0570
13,8	11,73	11,67	-0,0128	15,63	15,47	-0,0318	19,53	19,24	-0,0563
13,9	11,75	11,68	-0,0122	15,64	15,49	-0,0308	19,55	19,27	-0,0556
14	11,76	11,70	-0,0115	15,66	15,51	-0,0299	19,57	19,29	-0,0549
14,1	11,77	11,71	-0,0108	15,68	15,53	-0,0290	19,59	19,32	-0,0540
14,2	11,78	11,73	-0,0101	15,69	15,55	-0,0282	19,61	19,34	-0,0532
14,3	11,79	11,74	-0,0094	15,71	15,57	-0,0274	19,63	19,37	-0,0521
14,4	11,80	11,76	-0,0087	15,72	15,59	-0,0267	19,65	19,39	-0,0503
14,5	11,81	11,77	-0,0081	15,74	15,61	-0,0259	19,66	19,42	-0,0487
14,6	11,83	11,79	-0,0074	15,75	15,63	-0,0253	19,68	19,44	-0,0474
14,7	11,84	11,80	-0,0067	15,77	15,64	-0,0246	19,70	19,46	-0,0461
14,8	11,85	11,82	-0,0060	15,78	15,66	-0,0240	19,71	19,49	-0,0446
14,9	11,86	11,83	-0,0053	15,80	15,68	-0,0231	19,73	19,51	-0,0431
15	11,87	11,84	-0,0046	15,81	15,70	-0,0222	19,74	19,53	-0,0420
15,1	11,88	11,86	-0,0039	15,83	15,72	-0,0213	19,76	19,55	-0,0409
15,2	11,89	11,87	-0,0032	15,84	15,74	-0,0204	19,78	19,58	-0,0396
15,3	11,90	11,88	-0,0025	15,85	15,75	-0,0195	19,79	19,60	-0,0383
15,4	11,91	11,90	-0,0018	15,87	15,77	-0,0186	19,81	19,62	-0,0373
15,5	11,92	11,91	-0,0010	15,88	15,79	-0,0176	19,83	19,64	-0,0364
15,6	11,93	11,92	-0,0003	15,89	15,81	-0,0167	19,84	19,66	-0,0352
15,7	11,94	11,94	0,0004	15,91	15,82	-0,0159	19,86	19,69	-0,0341
15,8	11,94	11,95	0,0012	15,92	15,84	-0,0150	19,88	19,71	-0,0329
15,9	11,95	11,96	0,0018	15,93	15,86	-0,0141	19,89	19,73	-0,0322
16	11,96	11,97	0,0025	15,94	15,87	-0,0132	19,91	19,75	-0,0314
16,1	11,97	11,99	0,0031	15,95	15,89	-0,0123	19,93	19,77	-0,0304
16,2	11,98	12,00	0,0038	15,97	15,91	-0,0113	19,94	19,79	-0,0295
16,3	11,99	12,01	0,0044	15,98	15,92	-0,0104	19,96	19,81	-0,0286
16,4	12,00	12,02	0,0051	15,99	15,94	-0,0095	19,97	19,83	-0,0277
16,5	12,01	12,04	0,0058	16,00	15,96	-0,0086	19,99	19,85	-0,0265
16,6	12,02	12,05	0,0064	16,01	15,97	-0,0077	20,00	19,87	-0,0254
16,7	12,03	12,06	0,0071	16,02	15,99	-0,0067	20,02	19,89	-0,0243

16,8	12,03	12,07	0,0078	16,03	16,00	-0,0058	20,03	19,91	-0,0232
16,9	12,04	12,08	0,0085	16,05	16,02	-0,0049	20,04	19,93	-0,0221
17	12,05	12,09	0,0092	16,06	16,03	-0,0041	20,06	19,95	-0,0208
17,1	12,06	12,11	0,0098	16,07	16,05	-0,0032	20,07	19,97	-0,0198
17,2	12,07	12,12	0,0105	16,08	16,06	-0,0024	20,08	19,99	-0,0189
17,3	12,07	12,13	0,0112	16,09	16,08	-0,0015	20,10	20,01	-0,0177
17,4	12,08	12,14	0,0119	16,10	16,09	-0,0007	20,11	20,02	-0,0165
17,5	12,09	12,15	0,0126	16,11	16,11	0,0002	20,12	20,04	-0,0156
17,6	12,10	12,16	0,0133	16,12	16,12	0,0011	20,14	20,06	-0,0148
17,7	12,10	12,17	0,0139	16,13	16,14	0,0019	20,15	20,08	-0,0137
17,8	12,11	12,18	0,0146	16,14	16,15	0,0027	20,16	20,10	-0,0126
17,9	12,12	12,19	0,0152	16,15	16,17	0,0036	20,18	20,11	-0,0116
18	12,13	12,20	0,0159	16,16	16,18	0,0045	20,19	20,13	-0,0106
18,1	12,13	12,21	0,0165	16,17	16,20	0,0053	20,20	20,15	-0,0093
18,2	12,14	12,23	0,0172	16,18	16,21	0,0062	20,21	20,17	-0,0080
18,3	12,15	12,24	0,0178	16,19	16,22	0,0070	20,22	20,18	-0,0071
18,4	12,16	12,25	0,0185	16,20	16,24	0,0079	20,23	20,20	-0,0062
18,5	12,16	12,26	0,0191	16,21	16,25	0,0088	20,25	20,22	-0,0053
18,6	12,17	12,27	0,0197	16,22	16,26	0,0096	20,26	20,24	-0,0041
18,7	12,18	12,28	0,0204	16,23	16,28	0,0105	20,27	20,25	-0,0030
18,8	12,18	12,29	0,0210	16,24	16,29	0,0113	20,28	20,27	-0,0022
18,9	12,19	12,30	0,0217	16,24	16,30	0,0122	20,29	20,28	-0,0011
19	12,20	12,31	0,0223	16,25	16,32	0,0130	20,30	20,30	0,0000
19,1	12,20	12,32	0,0229	16,26	16,33	0,0138	20,32	20,32	0,0007
19,2	12,21	12,33	0,0236	16,27	16,34	0,0146	20,33	20,33	0,0017
19,3	12,22	12,34	0,0242	16,28	16,36	0,0154	20,34	20,35	0,0027
19,4	12,22	12,34	0,0249	16,29	16,37	0,0162	20,35	20,37	0,0037
19,5	12,23	12,35	0,0255	16,30	16,38	0,0170	20,36	20,38	0,0046
19,6	12,23	12,36	0,0262	16,31	16,39	0,0178	20,37	20,40	0,0056
19,7	12,24	12,37	0,0269	16,31	16,41	0,0186	20,38	20,41	0,0068
19,8	12,25	12,38	0,0275	16,32	16,42	0,0194	20,39	20,43	0,0076
19,9	12,25	12,39	0,0281	16,33	16,43	0,0202	20,40	20,44	0,0085
20	12,26	12,40		16,34	16,44		20,41	20,46	
Max			0,0281			0,0211			0,0167
Min			-0,0498			-0,0857			-0,1229

F.4 Temperature increase Steel Lexan

t [s]	Comsol 0,6 W	HotDisk 0,6 W	Curve fit	Comsol 0,8 W	HotDisk 0,8 W	Curve fit	Comsol 1 W	HotDisk 1 W	Curve fit
0,1	0,71	1,09	0,0187	0,98	1,44	0,0187	1,23	1,78	0,0192
0,2	1,62	1,43	-0,0236	2,17	1,90	-0,0327	2,71	2,35	-0,0449
0,3	1,72	1,68	-0,0078	2,30	2,24	-0,0113	2,87	2,78	-0,0186
0,4	1,81	1,78	-0,0081	2,42	2,37	-0,0120	3,03	2,94	-0,0192
0,5	1,90	1,86	-0,0110	2,54	2,47	-0,0152	3,17	3,07	-0,0232
0,6	1,99	1,92	-0,0132	2,64	2,56	-0,0182	3,31	3,18	-0,0283

0,7	2,06	1,99	-0,0137	2,75	2,65	-0,0203	3,45	3,29	-0,0300
0,8	2,14	2,07	-0,0141	2,85	2,75	-0,0214	3,56	3,41	-0,0293
0,9	2,21	2,14	-0,0146	2,95	2,84	-0,0206	3,68	3,53	-0,0288
1	2,28	2,21	-0,0153	3,04	2,94	-0,0193	3,79	3,65	-0,0291
1,1	2,35	2,28	-0,0146	3,12	3,03	-0,0187	3,91	3,76	-0,0302
1,2	2,41	2,34	-0,0129	3,21	3,11	-0,0187	4,02	3,87	-0,0320
1,3	2,46	2,40	-0,0116	3,29	3,20	-0,0193	4,14	3,97	-0,0314
1,4	2,52	2,46	-0,0107	3,38	3,28	-0,0204	4,22	4,08	-0,0283
1,5	2,58	2,52	-0,0102	3,46	3,36	-0,0220	4,31	4,17	-0,0257
1,6	2,63	2,58	-0,0100	3,55	3,43	-0,0215	4,39	4,27	-0,0237
1,7	2,69	2,64	-0,0102	3,61	3,51	-0,0187	4,47	4,36	-0,0221
1,8	2,74	2,69	-0,0106	3,67	3,58	-0,0163	4,56	4,45	-0,0212
1,9	2,80	2,74	-0,0113	3,73	3,65	-0,0142	4,64	4,54	-0,0206
2	2,85	2,79	-0,0117	3,78	3,72	-0,0126	4,73	4,62	-0,0206
2,1	2,90	2,84	-0,0105	3,84	3,78	-0,0113	4,81	4,71	-0,0209
2,2	2,94	2,89	-0,0084	3,90	3,85	-0,0103	4,89	4,79	-0,0217
2,3	2,98	2,94	-0,0065	3,96	3,91	-0,0096	4,98	4,86	-0,0229
2,4	3,01	2,99	-0,0049	4,02	3,97	-0,0092	5,06	4,94	-0,0245
2,5	3,05	3,03	-0,0035	4,08	4,03	-0,0092	5,14	5,02	-0,0239
2,6	3,09	3,08	-0,0023	4,14	4,09	-0,0094	5,20	5,09	-0,0210
2,7	3,13	3,12	-0,0013	4,20	4,15	-0,0099	5,26	5,16	-0,0183
2,8	3,16	3,16	-0,0005	4,25	4,20	-0,0106	5,31	5,23	-0,0159
2,9	3,20	3,20	0,0001	4,31	4,26	-0,0116	5,37	5,30	-0,0138
3	3,24	3,24	0,0005	4,37	4,31	-0,0128	5,43	5,36	-0,0121
3,1	3,28	3,28	0,0008	4,43	4,36	-0,0126	5,49	5,43	-0,0106
3,2	3,31	3,32	0,0009	4,47	4,41	-0,0108	5,54	5,49	-0,0094
3,3	3,35	3,36	0,0008	4,51	4,46	-0,0091	5,60	5,55	-0,0084
3,4	3,39	3,39	0,0006	4,55	4,51	-0,0076	5,66	5,62	-0,0078
3,5	3,43	3,43	0,0002	4,60	4,56	-0,0063	5,71	5,68	-0,0073
3,6	3,46	3,46	-0,0003	4,64	4,61	-0,0052	5,77	5,73	-0,0072
3,7	3,50	3,50	-0,0010	4,68	4,65	-0,0043	5,83	5,79	-0,0072
3,8	3,54	3,53	-0,0018	4,72	4,70	-0,0035	5,88	5,85	-0,0075
3,9	3,58	3,56	-0,0027	4,76	4,74	-0,0030	5,94	5,90	-0,0080
4	3,61	3,60	-0,0030	4,80	4,79	-0,0026	6,00	5,96	-0,0087
4,1	3,64	3,63	-0,0023	4,84	4,83	-0,0024	6,05	6,01	-0,0096
4,2	3,67	3,66	-0,0014	4,88	4,87	-0,0023	6,11	6,06	-0,0108
4,3	3,70	3,69	-0,0007	4,92	4,91	-0,0024	6,17	6,11	-0,0121
4,4	3,72	3,72	0,0000	4,96	4,95	-0,0027	6,22	6,16	-0,0136
4,5	3,75	3,75	0,0005	5,00	4,99	-0,0031	6,28	6,21	-0,0138
4,6	3,77	3,78	0,0009	5,04	5,03	-0,0036	6,32	6,26	-0,0125
4,7	3,80	3,81	0,0012	5,08	5,06	-0,0043	6,36	6,30	-0,0114
4,8	3,83	3,83	0,0014	5,13	5,10	-0,0051	6,40	6,35	-0,0104
4,9	3,85	3,86	0,0016	5,17	5,14	-0,0060	6,45	6,40	-0,0095
5	3,88	3,89	0,0016	5,21	5,17	-0,0071	6,49	6,44	-0,0088
5,1	3,91	3,92	0,0015	5,25	5,21	-0,0073	6,53	6,48	-0,0083

5,2	3,93	3,94	0,0013	5,28	5,24	-0,0064	6,57	6,53	-0,0079
5,3	3,96	3,97	0,0011	5,31	5,28	-0,0056	6,61	6,57	-0,0077
5,4	3,99	3,99	0,0008	5,34	5,31	-0,0050	6,65	6,61	-0,0076
5,5	4,01	4,02	0,0004	5,37	5,34	-0,0045	6,69	6,65	-0,0077
5,6	4,04	4,04	-0,0001	5,40	5,38	-0,0040	6,73	6,69	-0,0078
5,7	4,07	4,06	-0,0007	5,43	5,41	-0,0037	6,77	6,73	-0,0082
5,8	4,09	4,09	-0,0013	5,46	5,44	-0,0035	6,81	6,77	-0,0086
5,9	4,12	4,11	-0,0020	5,49	5,47	-0,0033	6,85	6,81	-0,0092
6	4,15	4,13	-0,0024	5,52	5,50	-0,0033	6,89	6,85	-0,0099
6,1	4,17	4,16	-0,0022	5,55	5,53	-0,0033	6,93	6,88	-0,0107
6,2	4,19	4,18	-0,0019	5,58	5,56	-0,0035	6,98	6,92	-0,0116
6,3	4,21	4,20	-0,0017	5,61	5,59	-0,0038	7,02	6,96	-0,0126
6,4	4,23	4,22	-0,0015	5,63	5,62	-0,0041	7,06	6,99	-0,0138
6,5	4,25	4,24	-0,0014	5,66	5,64	-0,0045	7,10	7,03	-0,0141
6,6	4,27	4,26	-0,0014	5,69	5,67	-0,0050	7,13	7,06	-0,0135
6,7	4,29	4,28	-0,0014	5,72	5,70	-0,0056	7,16	7,09	-0,0129
6,8	4,31	4,30	-0,0015	5,75	5,72	-0,0062	7,19	7,13	-0,0125
6,9	4,33	4,32	-0,0017	5,78	5,75	-0,0069	7,22	7,16	-0,0121
7	4,35	4,34	-0,0019	5,81	5,78	-0,0077	7,25	7,19	-0,0119
7,1	4,37	4,36	-0,0021	5,84	5,80	-0,0080	7,28	7,22	-0,0117
7,2	4,39	4,38	-0,0024	5,87	5,83	-0,0077	7,31	7,26	-0,0116
7,3	4,41	4,40	-0,0028	5,89	5,85	-0,0075	7,34	7,29	-0,0116
7,4	4,43	4,42	-0,0032	5,91	5,88	-0,0074	7,38	7,32	-0,0117
7,5	4,45	4,44	-0,0037	5,94	5,90	-0,0073	7,41	7,35	-0,0119
7,6	4,47	4,45	-0,0042	5,96	5,92	-0,0072	7,44	7,38	-0,0121
7,7	4,49	4,47	-0,0048	5,98	5,95	-0,0072	7,47	7,41	-0,0125
7,8	4,51	4,49	-0,0054	6,01	5,97	-0,0073	7,50	7,43	-0,0129
7,9	4,53	4,50	-0,0061	6,03	5,99	-0,0074	7,53	7,46	-0,0134
8	4,55	4,52	-0,0064	6,05	6,02	-0,0077	7,56	7,49	-0,0140
8,1	4,57	4,54	-0,0064	6,08	6,04	-0,0079	7,59	7,52	-0,0146
8,2	4,59	4,56	-0,0062	6,10	6,06	-0,0083	7,62	7,55	-0,0154
8,3	4,60	4,57	-0,0061	6,12	6,08	-0,0086	7,65	7,57	-0,0161
8,4	4,62	4,59	-0,0060	6,15	6,10	-0,0090	7,68	7,60	-0,0170
8,5	4,63	4,60	-0,0060	6,17	6,12	-0,0096	7,71	7,63	-0,0174
8,6	4,65	4,62	-0,0061	6,19	6,14	-0,0101	7,74	7,65	-0,0172
8,7	4,66	4,63	-0,0061	6,22	6,17	-0,0107	7,76	7,68	-0,0171
8,8	4,68	4,65	-0,0062	6,24	6,19	-0,0114	7,79	7,70	-0,0170
8,9	4,70	4,66	-0,0063	6,26	6,21	-0,0121	7,81	7,73	-0,0170
9	4,71	4,68	-0,0065	6,29	6,23	-0,0128	7,84	7,75	-0,0170
9,1	4,73	4,69	-0,0067	6,31	6,25	-0,0131	7,86	7,78	-0,0172
9,2	4,74	4,71	-0,0070	6,33	6,26	-0,0130	7,89	7,80	-0,0173
9,3	4,76	4,72	-0,0072	6,35	6,28	-0,0129	7,91	7,82	-0,0176
9,4	4,77	4,74	-0,0075	6,37	6,30	-0,0128	7,94	7,85	-0,0179
9,5	4,79	4,75	-0,0079	6,38	6,32	-0,0128	7,96	7,87	-0,0182
9,6	4,81	4,76	-0,0083	6,40	6,34	-0,0128	7,99	7,89	-0,0186

9,7	4,82	4,78	-0,0087	6,42	6,36	-0,0129	8,01	7,92	-0,0190
9,8	4,84	4,79	-0,0091	6,44	6,38	-0,0130	8,04	7,94	-0,0195
9,9	4,85	4,81	-0,0096	6,46	6,39	-0,0132	8,06	7,96	-0,0201
10	4,87	4,82	-0,0100	6,48	6,41	-0,0133	8,09	7,98	-0,0207
10,1	4,88	4,83	-0,0102	6,50	6,43	-0,0136	8,11	8,01	-0,0213
10,2	4,90	4,84	-0,0105	6,51	6,45	-0,0138	8,14	8,03	-0,0220
10,3	4,91	4,86	-0,0107	6,53	6,46	-0,0141	8,16	8,05	-0,0228
10,4	4,92	4,87	-0,0109	6,55	6,48	-0,0145	8,18	8,07	-0,0236
10,5	4,94	4,88	-0,0111	6,57	6,50	-0,0149	8,21	8,09	-0,0240
10,6	4,95	4,89	-0,0114	6,59	6,51	-0,0153	8,23	8,11	-0,0239
10,7	4,96	4,91	-0,0116	6,61	6,53	-0,0157	8,25	8,13	-0,0239
10,8	4,98	4,92	-0,0118	6,62	6,54	-0,0162	8,27	8,15	-0,0239
10,9	4,99	4,93	-0,0120	6,64	6,56	-0,0167	8,29	8,17	-0,0240
11	5,00	4,94	-0,0123	6,66	6,58	-0,0173	8,31	8,19	-0,0241
11,1	5,02	4,95	-0,0125	6,68	6,59	-0,0177	8,33	8,21	-0,0242
11,2	5,03	4,97	-0,0127	6,70	6,61	-0,0180	8,35	8,23	-0,0244
11,3	5,04	4,98	-0,0129	6,71	6,62	-0,0183	8,37	8,25	-0,0246
11,4	5,05	4,99	-0,0130	6,73	6,64	-0,0186	8,39	8,27	-0,0249
11,5	5,07	5,00	-0,0133	6,75	6,65	-0,0189	8,41	8,28	-0,0252
11,6	5,08	5,01	-0,0134	6,76	6,67	-0,0192	8,43	8,30	-0,0256
11,7	5,09	5,02	-0,0136	6,78	6,68	-0,0195	8,45	8,32	-0,0259
11,8	5,10	5,03	-0,0138	6,79	6,70	-0,0198	8,47	8,34	-0,0263
11,9	5,11	5,04	-0,0140	6,81	6,71	-0,0200	8,49	8,36	-0,0268
12	5,12	5,05	-0,0141	6,82	6,72	-0,0203	8,51	8,37	-0,0273
12,1	5,14	5,06	-0,0143	6,84	6,74	-0,0206	8,53	8,39	-0,0278
12,2	5,15	5,07	-0,0146	6,86	6,75	-0,0209	8,55	8,41	-0,0283
12,3	5,16	5,09	-0,0148	6,87	6,77	-0,0212	8,57	8,43	-0,0289
12,4	5,17	5,10	-0,0151	6,89	6,78	-0,0214	8,59	8,44	-0,0295
12,5	5,18	5,11	-0,0153	6,90	6,79	-0,0217	8,61	8,46	-0,0300
12,6	5,19	5,12	-0,0155	6,91	6,81	-0,0219	8,63	8,48	-0,0304
12,7	5,20	5,13	-0,0157	6,93	6,82	-0,0222	8,65	8,49	-0,0308
12,8	5,21	5,14	-0,0159	6,94	6,83	-0,0225	8,66	8,51	-0,0311
12,9	5,23	5,15	-0,0161	6,96	6,85	-0,0227	8,68	8,53	-0,0315
13	5,24	5,15	-0,0163	6,97	6,86	-0,0229	8,70	8,54	-0,0318
13,1	5,25	5,16	-0,0165	6,99	6,87	-0,0232	8,72	8,56	-0,0322
13,2	5,26	5,17	-0,0167	7,00	6,88	-0,0235	8,74	8,57	-0,0326
13,3	5,27	5,18	-0,0169	7,01	6,90	-0,0238	8,75	8,59	-0,0329
13,4	5,28	5,19	-0,0171	7,03	6,91	-0,0241	8,77	8,60	-0,0333
13,5	5,29	5,20	-0,0173	7,04	6,92	-0,0244	8,79	8,62	-0,0337
13,6	5,30	5,21	-0,0175	7,06	6,93	-0,0247	8,80	8,63	-0,0340
13,7	5,31	5,22	-0,0177	7,07	6,94	-0,0250	8,82	8,65	-0,0344
13,8	5,32	5,23	-0,0178	7,08	6,96	-0,0252	8,84	8,66	-0,0348
13,9	5,33	5,24	-0,0180	7,10	6,97	-0,0255	8,85	8,68	-0,0351
14	5,34	5,25	-0,0182	7,11	6,98	-0,0258	8,87	8,69	-0,0354
14,1	5,35	5,26	-0,0184	7,12	6,99	-0,0261	8,89	8,71	-0,0358

14,2	5,36	5,26	-0,0186	7,13	7,00	-0,0264	8,90	8,72	-0,0361
14,3	5,37	5,27	-0,0188	7,15	7,01	-0,0267	8,92	8,74	-0,0364
14,4	5,38	5,28	-0,0190	7,16	7,03	-0,0269	8,93	8,75	-0,0368
14,5	5,39	5,29	-0,0192	7,17	7,04	-0,0272	8,95	8,77	-0,0371
14,6	5,39	5,30	-0,0194	7,19	7,05	-0,0274	8,97	8,78	-0,0375
14,7	5,40	5,31	-0,0196	7,20	7,06	-0,0277	8,98	8,79	-0,0379
14,8	5,41	5,31	-0,0198	7,21	7,07	-0,0279	9,00	8,81	-0,0382
14,9	5,42	5,32	-0,0200	7,22	7,08	-0,0282	9,01	8,82	-0,0386
15	5,43	5,33	-0,0202	7,23	7,09	-0,0284	9,03	8,83	-0,0390
15,1	5,44	5,34	-0,0203	7,25	7,10	-0,0287	9,04	8,85	-0,0394
15,2	5,45	5,35	-0,0205	7,26	7,11	-0,0290	9,06	8,86	-0,0397
15,3	5,46	5,35	-0,0207	7,27	7,12	-0,0292	9,07	8,87	-0,0401
15,4	5,47	5,36	-0,0209	7,28	7,13	-0,0295	9,09	8,89	-0,0405
15,5	5,48	5,37	-0,0211	7,29	7,14	-0,0298	9,10	8,90	-0,0408
15,6	5,48	5,38	-0,0212	7,30	7,16	-0,0301	9,12	8,91	-0,0412
15,7	5,49	5,39	-0,0214	7,32	7,17	-0,0303	9,13	8,93	-0,0416
15,8	5,50	5,39	-0,0215	7,33	7,18	-0,0306	9,15	8,94	-0,0419
15,9	5,51	5,40	-0,0217	7,34	7,19	-0,0309	9,16	8,95	-0,0422
16	5,52	5,41	-0,0218	7,35	7,20	-0,0311	9,17	8,96	-0,0426
16,1	5,53	5,42	-0,0220	7,36	7,21	-0,0314	9,19	8,97	-0,0429
16,2	5,53	5,42	-0,0222	7,37	7,21	-0,0316	9,20	8,99	-0,0433
16,3	5,54	5,43	-0,0224	7,38	7,22	-0,0319	9,22	9,00	-0,0436
16,4	5,55	5,44	-0,0226	7,39	7,23	-0,0322	9,23	9,01	-0,0439
16,5	5,56	5,44	-0,0228	7,41	7,24	-0,0324	9,24	9,02	-0,0443
16,6	5,57	5,45	-0,0229	7,42	7,25	-0,0326	9,26	9,04	-0,0446
16,7	5,57	5,46	-0,0231	7,43	7,26	-0,0328	9,27	9,05	-0,0450
16,8	5,58	5,47	-0,0233	7,44	7,27	-0,0331	9,28	9,06	-0,0453
16,9	5,59	5,47	-0,0234	7,45	7,28	-0,0333	9,30	9,07	-0,0457
17	5,60	5,48	-0,0236	7,46	7,29	-0,0336	9,31	9,08	-0,0461
17,1	5,61	5,49	-0,0238	7,47	7,30	-0,0338	9,32	9,09	-0,0464
17,2	5,61	5,49	-0,0240	7,48	7,31	-0,0340	9,34	9,10	-0,0468
17,3	5,62	5,50	-0,0241	7,49	7,32	-0,0343	9,35	9,12	-0,0471
17,4	5,63	5,51	-0,0243	7,50	7,33	-0,0346	9,36	9,13	-0,0475
17,5	5,64	5,51	-0,0245	7,51	7,34	-0,0348	9,38	9,14	-0,0478
17,6	5,64	5,52	-0,0247	7,52	7,34	-0,0351	9,39	9,15	-0,0482
17,7	5,65	5,53	-0,0248	7,53	7,35	-0,0354	9,40	9,16	-0,0485
17,8	5,66	5,53	-0,0249	7,54	7,36	-0,0356	9,41	9,17	-0,0488
17,9	5,67	5,54	-0,0251	7,55	7,37	-0,0358	9,43	9,18	-0,0491
18	5,67	5,55	-0,0253	7,56	7,38	-0,0361	9,44	9,19	-0,0495
18,1	5,68	5,55	-0,0255	7,57	7,39	-0,0363	9,45	9,20	-0,0498
18,2	5,69	5,56	-0,0256	7,58	7,40	-0,0366	9,46	9,21	-0,0501
18,3	5,69	5,57	-0,0258	7,59	7,40	-0,0368	9,48	9,22	-0,0504
18,4	5,70	5,57	-0,0260	7,60	7,41	-0,0371	9,49	9,23	-0,0507
18,5	5,71	5,58	-0,0261	7,61	7,42	-0,0373	9,50	9,24	-0,0511
18,6	5,72	5,58	-0,0263	7,62	7,43	-0,0376	9,51	9,25	-0,0514

18,7	5,72	5,59	-0,0265	7,63	7,44	-0,0378	9,52	9,26	-0,0518
18,8	5,73	5,60	-0,0267	7,63	7,45	-0,0380	9,53	9,27	-0,0521
18,9	5,74	5,60	-0,0268	7,64	7,45	-0,0382	9,55	9,28	-0,0524
19	5,74	5,61	-0,0270	7,65	7,46	-0,0385	9,56	9,29	-0,0528
19,1	5,75	5,61	-0,0272	7,66	7,47	-0,0387	9,57	9,30	-0,0531
19,2	5,76	5,62	-0,0274	7,67	7,48	-0,0389	9,58	9,31	-0,0535
19,3	5,76	5,63	-0,0276	7,68	7,49	-0,0392	9,59	9,32	-0,0538
19,4	5,77	5,63	-0,0277	7,69	7,49	-0,0394	9,60	9,33	-0,0541
19,5	5,78	5,64	-0,0279	7,70	7,50	-0,0397	9,62	9,34	-0,0545
19,6	5,78	5,64	-0,0280	7,71	7,51	-0,0400	9,63	9,35	-0,0548
19,7	5,79	5,65	-0,0282	7,72	7,52	-0,0402	9,64	9,36	-0,0551
19,8	5,80	5,66	-0,0284	7,73	7,52	-0,0404	9,65	9,37	-0,0555
19,9	5,80	5,66	-0,0285	7,73	7,53	-0,0407	9,66	9,38	-0,0558
20	5,81	5,67		7,74	7,54		9,67	9,39	
Max			0,0187			0,0187			0,0192
Min			-0,0285			-0,0407			-0,0558

Appendix G: Uncertainty analysis

G.1 Teflon

Uncertainty from balance		0,1	mg	0,0000001	kg
Uncertainty from sliding caliber		0,025	millim	0,000025	m
Uncertainty Volume					
	dl/l	dh/h	dw/w		
	0,060195/0,06022	4,75*10^-4/0,0005	0,060125/0,06015		
Nom	0,06022	0,0005	0,06015		
Change l	0,060195	0,0005	0,06015		
Change h	0,06022	0,000475	0,06015		
Change w	0,06022	0,0005	0,060125		
V	1,81112E-06				
dV/dl	1,81036E-06	1,72345E-07			
dV/dh	1,72056E-06	0,0025			
dV/dw	1,81036E-06	1,72746E-07			
		0,002500345	Sum of all uncertainties		
		0,050003451	Root of this		
		5,00 %			
Uncertainty Density					
	dm/m	dV/V			
	3,9853*10^-3/0,0039854	9,055*10^-8/1,81*10^-6			
Nom	0,0039854	0,00000181			
Change m	0,0039853	0,00000181			
Change V	0,0039854	1,71945E-06			
Density	2201,88				
drho/dm	2201,82	6,29588E-10			
drho/dV	2317,8	0,002773306			
		0,002773307			
		0,052662194			
		5,27 %			
Uncertainty thermal conductivity					
	drho/rho	dCp/Cp	dalpha/alpha		
	116,04/2200	69,35/990,7	0,006/0,12		
Nom	2200	990,7	0,00000012		
Change rho	2083,96	990,7	0,00000012		

Change Cp	2200	921,35	0,00000012		
Change a	2200	990,7	0,000000114		
Th.cond	0,2615448				
drho/rho	0,247749501	0,002782083			
dCp/Cp	0,2432364	0,004900141			
dalpha/alpha	0,24846756	0,0025			
		0,010182224			
		0,100907008			
		10,09 %			

G.2 Lexan

Uncertainty Volume			
	dl/l	dh/h	dw/w
	0,060195/0,06022	7,75*10^-4/0,0008	0,060195/0,06002
Nom	0,06022	0,0008	0,06002
Change l	0,060195	0,0008	0,06002
Change h	0,06022	0,000775	0,06002
Change w	0,06022	0,0008	0,060195
V	2,89152E-06		
dV/dl	2,89032E-06	1,72345E-07	
dV/dh	2,80116E-06	0,000976562	
dV/dw	2,89995E-06	8,50128E-06	
		0,000985236	Sum of all uncertainties
		0,031388471	Root of this
		3,139 %	
Uncertainty Density			
	dm/m	dV/V	
	3,2344*10^-3/3,2345*10^-3	9,07171*10^-8/2,89*10^-6	
Nom	0,0032345	0,00000289	
Change m	0,0032344	0,00000289	
Change V	0,0032345	2,79928E-06	
Density	1119,20		
drho/dm	1119,17	9,55841E-10	
drho/dV	1155,5	0,001050231	
		0,001050232	
		0,032407279	
		3,241 %	

Uncertainty thermal conductivity			
	drho/rho	dCp/Cp	dalpha/alpha
	36,26/1119,2	88,2/1260	0,0075/0,15
Nom	1119,2	1260	0,00000015
Change rho	1082,94	1260	0,00000015
Change Cp	1119,2	1171,8	0,00000015
Change alpha	1119,2	1260	1,425E-07
Th.cond	0,2115288		
drho/rho	0,20467566	0,00104964	
dCp/Cp	0,196721784	0,0049	
dalpha/alpha	0,20095236	0,0025	
		0,00844964	
		0,091921921	
		9,19 %	

G. 3 Stainless steel

Uncertainty Volume			
	dl/l	dh/h	dw/w
	0,059385/0,05941	4,75*10^-4/0,0005	0,059655/0,05968
Nom	0,05941	0,0005	0,05968
Change l	0,059385	0,0005	0,05968
Change h	0,05941	0,000475	0,05968
Change w	0,05941	0,0005	0,059655
V	1,77279E-06		
dV/dl	1,77205E-06	1,77076E-07	
dV/dh	1,68415E-06	0,0025	
dV/dw	1,77205E-06	1,75478E-07	
		0,002500353	Sum of all uncertainties
		0,050003525	Root of this
		5,000 %	
Uncertainty Density			
	dm/m	dV/V	
	0,0137754/0,0137755	8,85*10^-8/1,77*10^-6	
Nom	0,0137755	0,00000177	
Change m	0,0137754	0,00000177	
Change V	0,0137755	1,6815E-06	
Density	7782,77		
drho/dm	7782,71	5,26969E-11	
drho/dV	8192,4	0,002770083	

		0,002770083	
		0,052631579	
		5,263 %	
Uncertainty thermal conductivity			
	drho/rho	dCp/Cp	dalpha/alpha
	409,6/7782,77	34,77/496,7	0,189/3,78
Nom	7782,77	496,7	0,00000378
Change rho	7373,17	496,7	0,00000378
Change Cp	7782,77	461,93	0,00000378
Change alpha	7782,77	496,7	0,000003591
Th.cond	14,61235303		
drho/rho	13,84331838	0,00276982	
dCp/Cp	13,5894589	0,004900282	
dalpha/alpha	13,88173538	0,0025	
		0,010170102	
		0,100846922	
		10,08 %	

Appendix H: Risk assessment

Risk Assessment Report

Termisk konduktivitetsrigg: måling av termisk konduktivitet i porøse medier.

[Thermal conductivity rig: measurements of thermal conductivity in porous media]

Prosjekttittel	**Conductivity rig: thermal conductivity measurements in porous media**
Prosjektleder	Erling Næss/Christian Schlemminger
Enhet	NTNU
HMS-koordinator	Erik Langørgen
Linjeleder	Olav Bolland
Plassering	VATlab
Romnummer	Finlab
Riggansvarlig	Ane Ringseth/Christian Schlemminger
Risikovurdering utført av	Erik Langørgen/Christian Schlemminger/Jan Georg Henriksen

TABLE OF CONTENTS

1 INTRODUCTION

The experiment is about measuring the thermal conductivity in a packed bed of porous and non porous media, in order to calculate the respective conductivity's of the sample media.

The rig is located in the FinLab in floor 1B, inside the VATlab.

2 ORGANISATION

Rolle	NTNU	Sintef
Lab Ansvarlig:	Morten Grønli	Harald Mæhlum
Linjeleder:	Olav Bolland	Mona Mølnvik
HMS ansvarlig: HMS koordinator HMS koordinator	Olav Bolland Erik Langørgen Bård Brandåstrø	Mona Mølnvik Harald Mæhlum
Romansvarlig:	Jan Georg Henriksen	
Prosjektleder:	Erling Næss/Christian Schlemminger	
Ansvarlig riggoperatører:	Jan Georg Henriksen	

3 RISK MANAGEMENT IN THE PROJECT

Hovedaktiviteter risikostyring	Nødvendige tiltak, dokumentasjon	DATE
Prosjekt initiering	Prosjekt initiering mal	15.01.2013
Veiledningsmøte Guidance Meeting	Skjema for Veiledningsmøte med pre-risikovurdering	n.a
Innledende risikovurdering Initial Assessment	Fareidentifikasjon – HAZID Skjema grovanalyse	20.02.2013
Vurdering av teknisk sikkerhet Evaluation of technical security	Prosess-HAZOP Tekniske dokumentasjoner	15.05.2013
Vurdering av operasjonell sikkerhet Evaluation of operational safety	Prosedyre-HAZOP Opplæringsplan for operatører	15.05.2013
Sluttvurdering, kvalitetssikring Final assessment, quality assurance	Uavhengig kontroll Utstedelse av apparaturkort Utstedelse av forsøk pågår kort	15.05.2013

4 DRAWINGS, PHOTOS, DESCRIPTIONS OF TEST SETUP

Test setup description/location of equipment

The thermal conductivity measurement rig is located in the FinLab in the VATLab. The HotDisk TPS 2500S is supplied by the Swedish company Hot Disc AB. It utilizes a small electrical power (<2W) to heat up a special shaped resistance, which is used as a temperature sensor simultaneously. The transient temperature rise of the sensor is recorded and analyzed by the TPS2500S. As result the material thermal diffusivity, specific heat capacity and thermal conductivity are determined. Different material

types e.g. solid materials or powders can be measured. In the particular case different sorts of powders are used for the measurements.

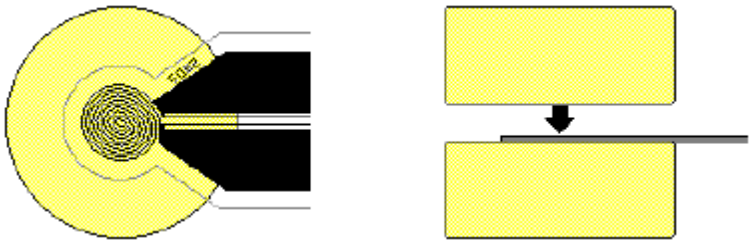

Figure 1 Sensor position between sample pieces

. Porous media is poured in to a sample holder, and a HotDisk sensor is placed in between the samples, as shown in Figure. 1.

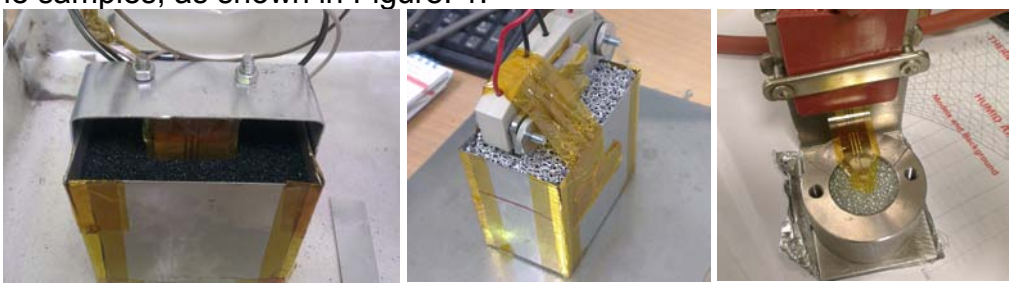

Figure 2 Sample holders

Different sample holders are used for different types of porous media. Graphic examples are given in Fig. 2. If room-temperature measurements with air are conducted, measurements can start as soon as the wires are connected to the sensor.

Figure 3 Vacuum cell

Most measurements however, are conducted at a range of -30 °C<T<150 °C with pressurized gas (He/N2, at 0.1 ...0.4 bar relative). In order to do this, the sample holder, or sometimes the porous media itself, is lowered into the vacuum / pressure cell. This pressure cell is provided by HotDisk AB as well and can withstand pressures of 1 bar relative and 200°C, see attachment B. Wires are then connected to the vacuum / pressure cell itself (from inside and outside), as shown in Figure 3. The lid is then sealed with a silicone gasket and if necessary with silicon vacuum grease and lowered into a thermal bath. The oil bath can stabilize at any given temperature between -35 and +200 degrees Celsius. After connecting the vacuum suction line with pressure sensors and the gas supply (Figure 4 or 5, next page) a

final leakage test is necessary to guaranty safe and reliable measurements. Once thermal bath has stabilized, measurements can start.

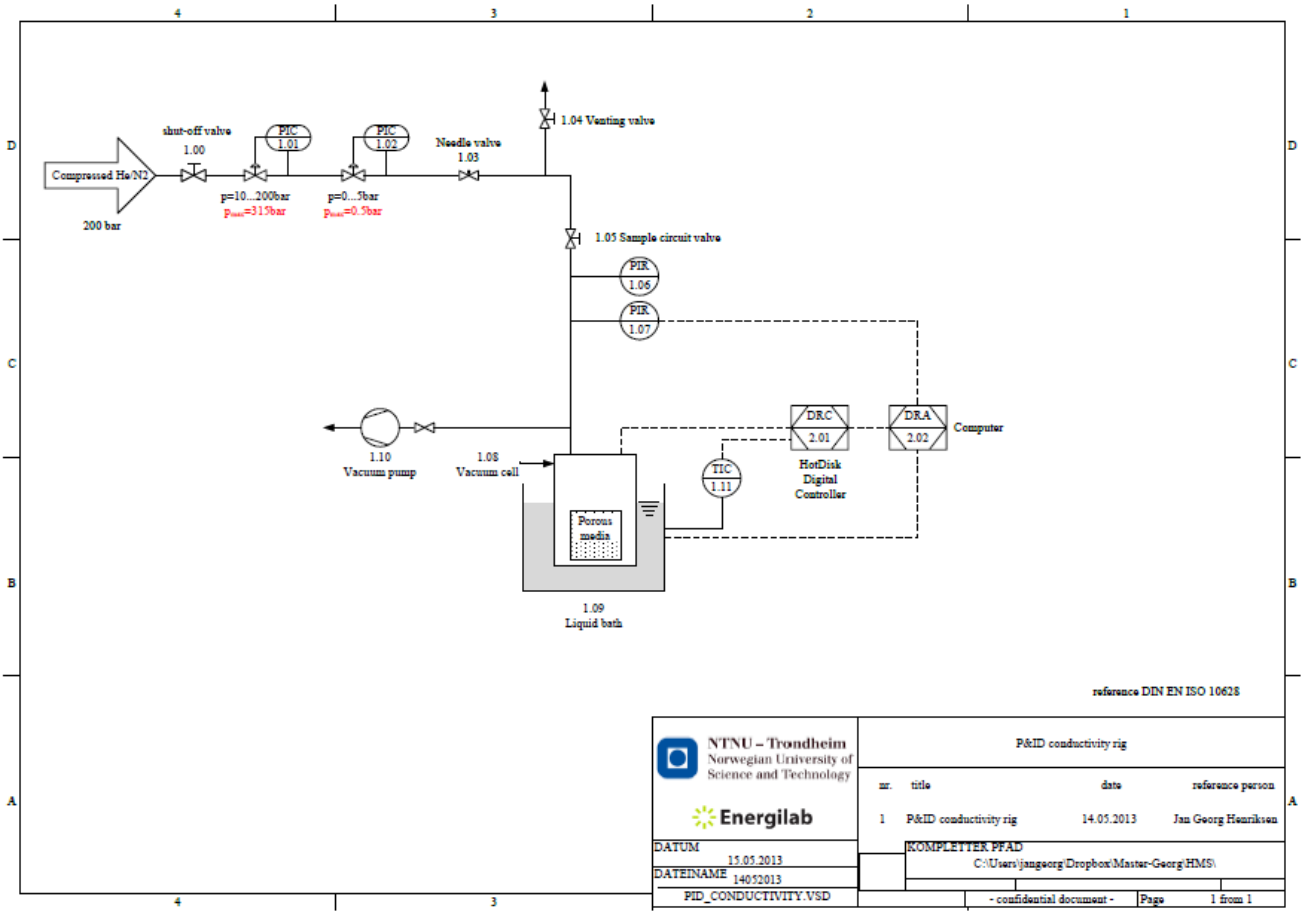

Figure 4 flow schematic conductivity rig (larger version attached at the very end of the report)

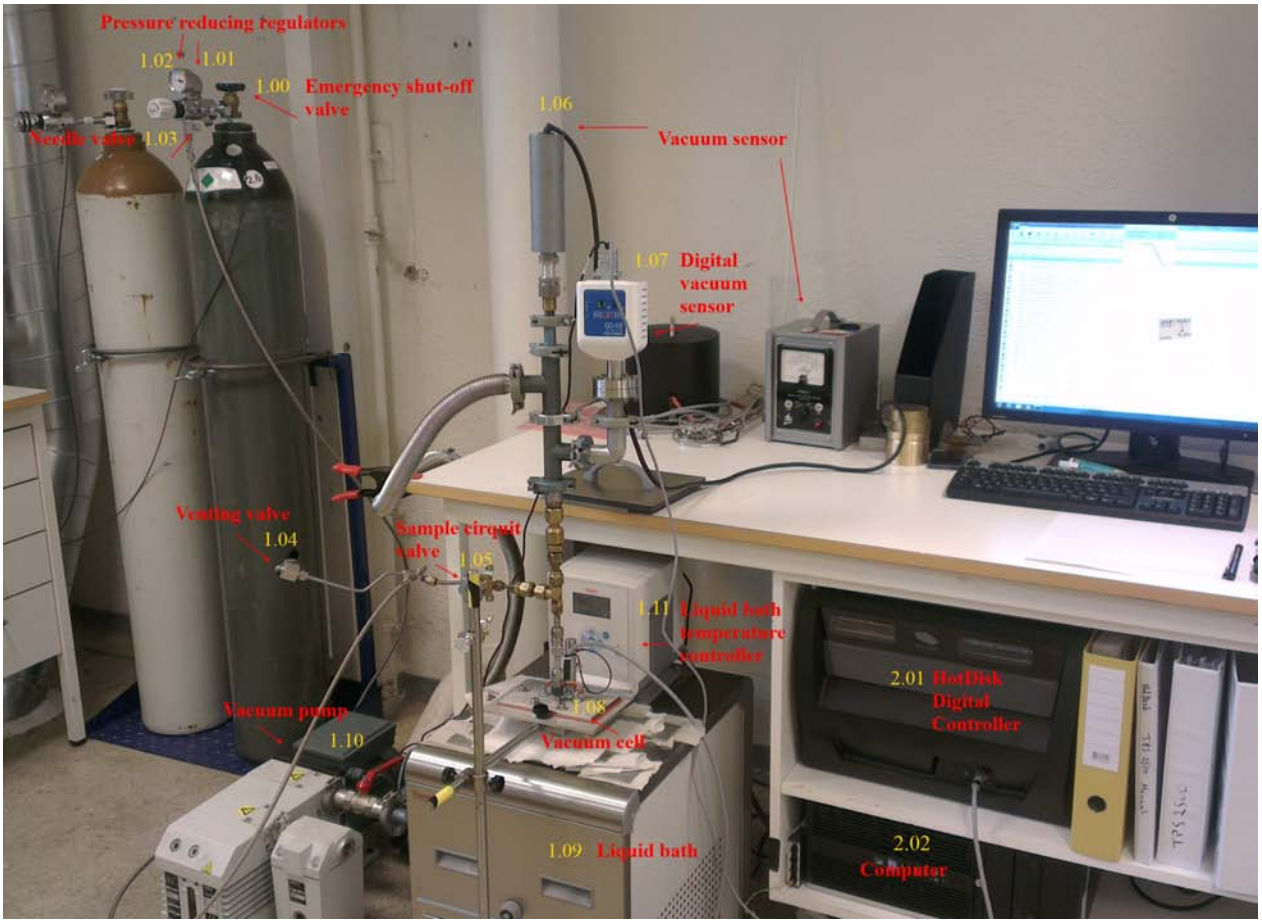

Figure 5- Thermal conductivity setup with gas supply, vacuum sensors and computer analyser. Location: Finlab.

As shown in Figure 4 and Figure 5, compressed gas (N2 or He at approximately 200 bar) from a gas bottle is supplied after opening the shut-off valve (1.00). A maximal allowed pressure is set with the pressure regulators (max 1.4 bar (absolute)) (1.01) and (1.02). Experiments are preformed usually at 1.2...1.4 bar (absolute). Next follows a needle valve (1.03) for extra security, and a venting valve (1.04). The venting valve is there in order to ensure that pressure can be released if it is too high, or for venting before gas change. By turning the pressure regulator (1.02) up, or turning it down and venting through (1.04) one can regulate the pressure. By opening up the sample circuit valve (1.05) the system is supplied with gas.

The porous medium is located inside the pressure cell (1.08), which again is lowered in the liquid bath (1.09). Before one starts any measurements the porous medium must be evacuated. This is because the porous powder contains humid air which can interfere with the measurement. Evacuation is monitored through the vacuum pressure indicators (1.06) and (1.07). In order to evacuate, the sample circuit valve (1.05) is closed, the vacuum pump (1.10) is started and its valve is opened. When vacuum reaches 10^{-2} torr (0.13 bar), the valve on the vacuum pump (1.10) is closed and the sample circuit valve (1.05) is opened. Gas is then purged into the system.

To ensure that all humidity is gone, the porous medium must also be activated. In order to heat it, the liquid bath controller (1.11) is then set to 150 degrees Celsius. The evacuation process is then repeated five times over.

The HotDisk Digital Controller TPS2500S (2.01) governs the measurements together with a timetable set up in the software on the computer (2.02).

The filling and emptying procedure is explained short further down. An additional "Procedure for running experiments" summarizes all important steps for carrying out safe measurements and is added in Appendix G.

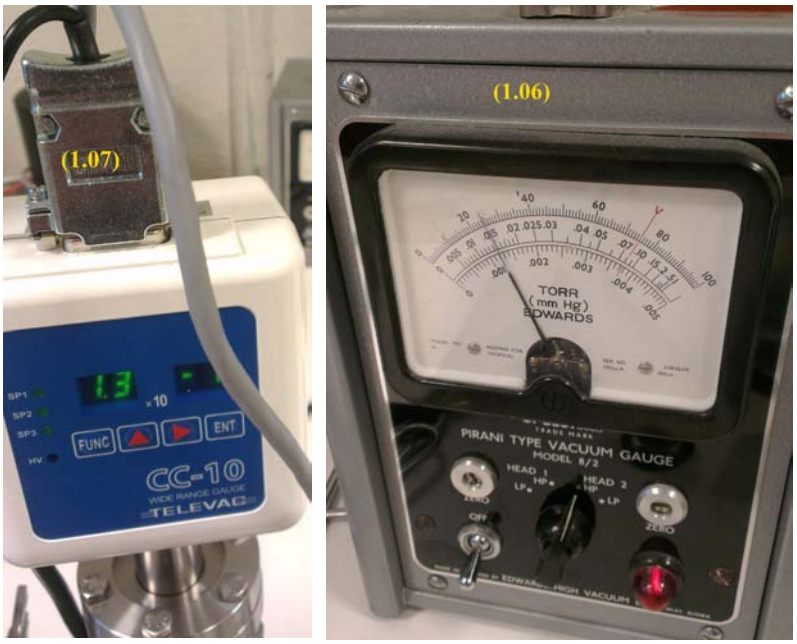

Figure 6 Vacuum pressure indicators

The components installed at the conductivity rig are listed in Table 1 below. The list can be used to identify the main instrument parameters.

Table 1 Sensor actor list conductivity rig

Sensoric und Actoric Permeability Rig

NTNU – Trondheim Norwegian University of Science and Technology

Energilab

Lfd.	P&ID	measurement position		measure-/actuating variable			device specification			signal	comments
Nr.	Nr.	medium	position	sensor / device	S/A	EMSR	device typ	measure-/ control value	U / I / P	range	
							(z.B. producer, name (typ).)		[V, A,W]		
1	**1.00**	compressed N2/He	gas bottle	shut-off valve	A		Yara Praxair	200bar	bar		
2	**1.01**	compressed N2/He	gas bottle	Pressure reducing regulator	A/S	PIC	Yara Praxair	200bar	bar	p_max=315 bar	
3	**1.02**	compressed N2/He	gas bottle	Pressure reducing regulator	A/S	PIC	Yara Praxair	operating @ < 0.5 bar	bar	p_max=5 bar	
4	**1.03**	compressed N2/He	gas bottle	Needle valve	A		Yara Praxair	operating @ 0.2/0.4 bar	bar	p_max= 60 bar	
5	**1.04**	compressed N2/He	between gas bottle/sample circuit	Venting valve	A		Swagelok SS 43GS 6mm	operating @ 0.2/0.4 bar	bar	0.5bar	
6	**1.05**	compressed or evacuated N2/He	between venting valve/sample holder	Sample circuit valve	A		Danfoss	operating @ 0.2/0.4 bar	bar	0.5bar	
7	**1.06**	compressed or evacuated N2/He	above sample holder	Vacuum pressure indicator	S	PIR	SPEEDIVAC	0.005…1 torr	torr	0.005…1 torr	1 torr =0.013 bar
8	**1.07**	compressed or evacuated N2/He	above sample holder	Vacuum pressure indicator	S	PIR	TELEVAC CC-10	10^{-9}…10^{-3} torr 10^{-3}…10^{-1} torr 10^{-1}…10^{1} torr 10^{1}…10^{3} torr	torr	10^{-9}…10^{3} torr	can log to pc
9	**1.08**	compressed or evacuated N2/He	in liquid bath	Vacuum pressure cell (sample inside)	-		HotDisk Vacuum cell 11502	operating @ 0.2/0.4 bar	bar	Tmax =200°C p_max=2.5 bar	
10	**1.09**	Oil	floor	Liquid bath	-		AC200				
11	**1.10**	compressed or evacuated N2/He	floor next to liquid bath	Vacuum pump	A		Oerlikon AF-16-25	p=10^{3}…$5\cdot10^{-3}$	torr	p=10^{3}…$5\cdot10^{-3}$ torr	<=10^{-4} mbar (given from producer)
12	**1.11**		on top of liquid bath	liquid bath temperature controller	A/S	TIC	Thermo Scientific AC 200	T=243…423	K	T=238…473K	
13	**2.01**		in desk next to liquid bath	Hotdisk digital measurement controller	A/S	DRC	HotDisk Th. Const. Analyser TPS 2500S				Bridge: Keithley 2400, Off balance: Keithley 2700 (6.5 digits resolution)
14	**2.02**		in desk next to liquid bath	Computer	A/S	DRA	HotDisk Th. Const. Ana. Version 7.0.16	Thermal conductivity k	W/mK	0.005-500 W/mK	Repeatability +-0.5%, Thermal conductivity uncertainty=+-5%

Filling of new powder

1. If rig is running, set liquid bath to 22 degrees and close shut-off and needle valve. Open the sample circuit valve and vent the system to ambient pressure.
2. When liquid bath has been at 22 degrees for 10 minutes, shut of the bath.
3. Remove wires from pressure cell.
4. Then remove the pressure cell from the bath.
5. Remove the pressure cell lid and disconnect the inner wires.
6. Control possible leakages and damages at the gasket
7. Wear glasses, hand gloves and dusk mask for protection.
8. Remove silicone gasket and take out the sample/sample holder.
9. Weigh the sample holder and measure sample height.
10. Empty sample holder and remove sensor.
11. Clean vacuum pressure cell, sensor, rubber sealing, and sample holder.
12. Weigh the sample holder without any powder in it. One can now tell how much mass the powder has lost during evacuation.
13. Pour in a new powder sample using a funnel.
14. Weigh new powder and measure filling height.
15. If the powder consists of small light grains, tape aluminum foil over the sample in order to prevent powder loss during evacuation.
16. Put sample holder back into the pressure cell.
17. Lubricate the sample holder and its lid with vacuum grease if necessary.
18. Connect wires and close the lid.
19. Mount the pressure cell into the liquid bath.
20. Cover the gap between pressure cell and bath to prevent oil vaporization.
21. Then start new experiment (described below)

The dismantling, empting and filling of the cylinder, which contains the powder sample is shown more in detail in figure 7.

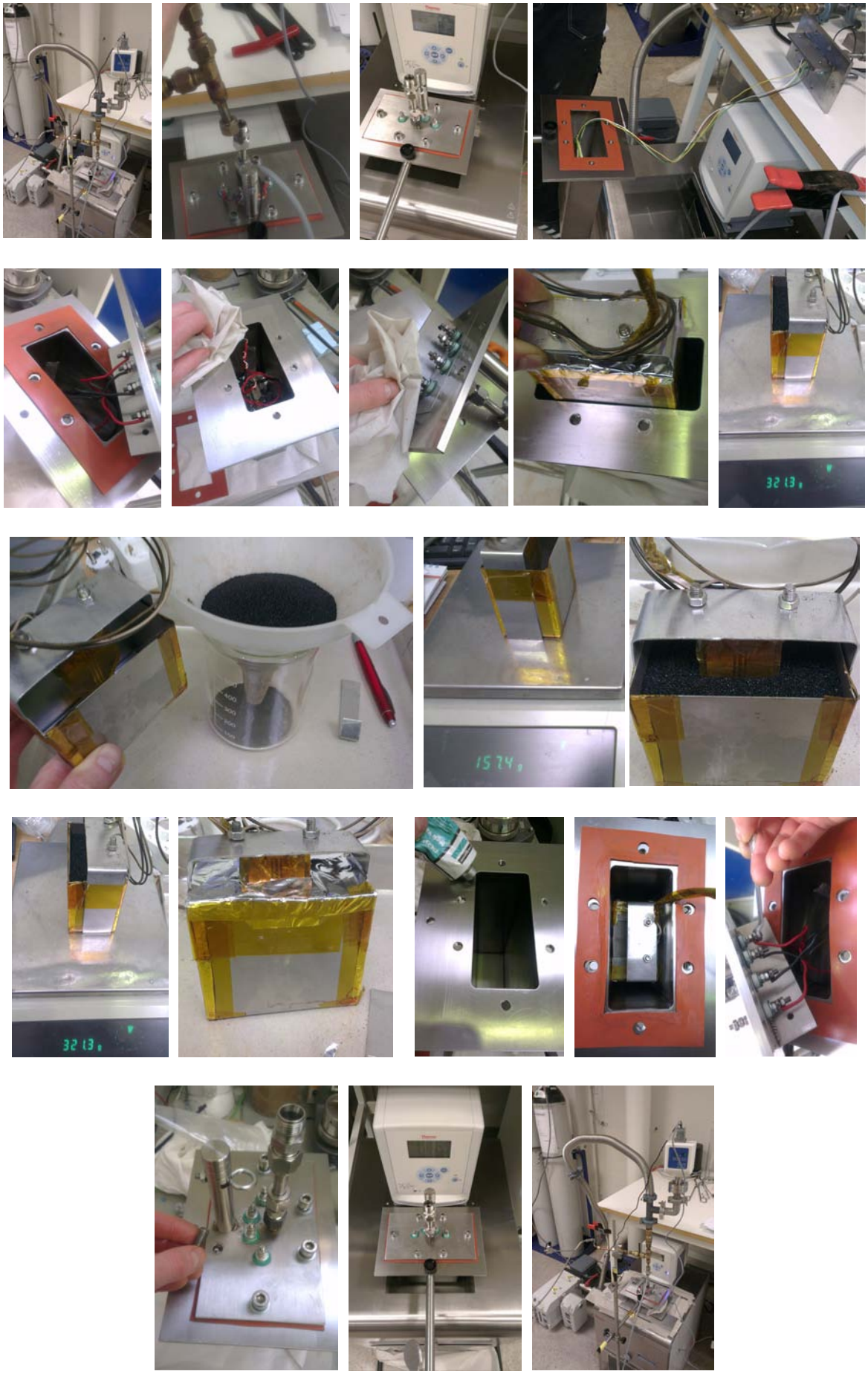

Figure 7 Dismantling, emptying filling and mantling.

Experimental procedure

1. Restart liquid bath and computer.
2. Use glasses and gloves.
3. All valves are closed.
4. Set liquid bath (1.09) to 150 degrees and start vacuum pump (1.10).
5. Open the shut-off valve.
6. Adjust pressure with the pressure regulator (1.02). Pressure must be <0.5bar.
7. Open needle valve (1.03).
8. Open venting valve (1.04) and regulate (1.02) to desired pressure (0.4 or 0.2 bar). Then close the venting valve (1.04).
9. Open sample circuit valve (1.05). Gas now flows into the pressure cell (1.08).
10. Wait 10 seconds and close sample circuit valve (1.05)
11. Open valve on the vacuum pump (1.10).
12. When vacuum is below 10^{-2}torr (0.13 bar), close vacuum pump valve (1.10).
13. Repeat point 9-12 six times.
14. Open sample circuit valve (1.05) and turn off vacuum pump (1.10).
15. Close needle valve (1.03) and wait one hour before starting the experiment.

5 EVACUATION FROM THE EXPERIMENT AREA

Evacuate at signal from the alarm system or local gas alarms with its own local alert with sound and light outside the room in question, see 6.2
Evacuation from the rigging area takes place through the marked emergency exits to the assembly point, (corner of Old Chemistry Kjelhuset or parking 1a-b.)
Action on rig before evacuation:

1. Shut off the gas (N2 or He) supply (1.00) marked with sign “Emergency shut-off valve”
2. Power off the electrical supply.

6 WARNING

6.1 Before experiments

E-mail with information about the planned experiment to: iept-experiments@ivt.ntnu.no
The e-mail should contain the following items:

- Name of responsible person:
- Experimental setup/rig:
- Start Experiments: (date and time)
- Stop Experiments: (date and time)

You should get the approval back from the laboratory management before start up. All running experiments are notified in the activity calendar for the lab to be sure they are coordinated with other activity.

6.2 Nonconformance

FIRE
For fires which you are not able to put out with locally available fire extinguishers, activate the nearest fire alarm and evacuate area. Be then available for fire brigade

and building caretaker to detect fire place.
If possible, notify:

NTNU	SINTEF
Labsjef Morten Grønli, tlf: 918 97 515	Labsjef Harald Mæhlum tlf 930 149 86
HMS: Erik Langørgen, tlf: 91897160 HMS: Bård Brandåstrø, tlf918 97 257	Forskningssjef Mona Mølnvik 93008868
Instituttleder: Olav Bolland: 91897209	
NTNU Sintef Beredskapstelefon	800 80 388

GASALARM

At a gas alarm, close gas bottles immediately and ventilated the area. If the level of gas concentration does not decrease within a reasonable time, activate the fire alarm and evacuate the lab. Designated personnel or fire department checks the leak to determine whether it is possible to seal the leak and ventilate the area in a responsible manner.
Alert Order in the above paragraph.

PERSONAL INJURY

- First aid kit in the fire / first aid stations
- Shout for help
- Start life-saving first aid•

CALL 113 if there is any doubt whether there is a serious injury

Other Nonconformance (AVVIK)

NTNU:

Reporting nonconformance, Innsida, avviksmelding:
https://innsida.ntnu.no/lenkesamling_vis.php?katid=1398

SINTEF:

Synergi

7 ASSESSMENT OF TECHNICAL SAFETY

7.1 HAZOP

The experiment set up is divided into the following nodes:

Node 1	Sections filled with pressurized N2/He.

Attachments: skjema: Hazop_mal
Conclusion: Safety taken care of

7.2 Flammable, reactive and pressurized substances and gas

Contains the experiments Flammable, reactive and pressurized substances and gas

N0	YES. Explosion document have to be made and or documented pressure test, (See 7.3)

Attachments: n.a.
Conclusion: n.a.

7.3 Pressurized equipment

Contain the set up pressurized equipment?

NO	YES, but working at a total pressure of max 1.5 bar

Attachments: NO.

Pressure in rig never exceeds 1,5 $bar_{absolute}$ respective 0,5 $bar_{relative}$, and will therefore cause no risk, since the working medium is only N2 or He @ -30…150 °C.
Conclusion*: all devices downstream from valve (1.02) are working around ambient pressure*

7.4 Effects on the environment (emissions, noise, temperature, vibration, smell)

NEI	YES

Conclusion: n.a.

7.5 Radiation

NEI	JA, Radiation source need to have an own risk assessment

Attachments: n.a.
Conclusion: n.a.

7.6 Usage and handling of chemicals.

NEI	JA, Do a risk assessment of the use

Attachments: MSDS

7.7 El safety (need to deviate from the current regulations and standards.)

NEI	JA, El safety have to be evaluated

Attachments: none
Conclusion: only regular devices with 220V are used

8 ASSESSMENT OF OPERATIONAL SAFETY

For ensuring that established procedures cover all identified risk factors that must be taken care of through procedures and ensure that the operators and technical performance have sufficient expertise.

8.1 Prosedure HAZOP

The method is a procedure to identify causes and sources of danger to operational problems.
Attachments: HAZOP_MAL_Prosedyre
Conclusion: procedure is uncomplicated and easy to understand → Safety taken care of

8.2 Operation and emergency shutdown procedure

The operating procedure is a checklist that must be filled out for each experiment.
Emergency procedure should attempt to set the experiment set up in a harmless state by unforeseen events.

Attachments: Procedure for running experiments
Emergency shutdown procedure:

1. Shut off the gas (He or N2) supply by closing valve (1.00) marked with sign “Emergency shut-off valve”.
2. Power off the liquid bath.

8.3 Training of operators

A Document showing training plan for operators

What are the requirements for the training of operators?

- *What it takes to be an independent operator*
- *Job Description for operators*

Attachments*:* Training program for operators

8.4 Technical modifications

- Technical modifications made by the Operator
  - Yes

- What technical modifications give a need for a new risk assessment; (by changing the risk picture)?
  - If more pressure is needed (>1,5 bar), or other types of samples with higher safety requirements than already described is used.

Conclusion: All modifications can be made by the operator

8.5 Personal protective equipment

- It is mandatory use of eye protection when handling fine powder.
- Use gloves when handling fine powder.
- Use of respiratory protection apparatus when handling fine powder.

Conclusion: always glasses, dust mask and gloves nearby during powder handling.

8.6 General Safety

- Monitoring: operator must start the experiment. After start: experiment can execute itself without operator presence.

Conclusion: The operator is allowed to leave during the experiment.

8.7 Safety equipment

- Warning signs, see the Regulations on Safety signs and signaling in the workplace

8.8 Special actions.

none

9 QUANTIFYING OF RISK - RISK MATRIX

See Chapter 13 "Guide to the report template".

The risk matrix will provide visualization and an overview of activity risks so that management and users get the most complete picture of risk factors.

IDnr	Aktivitet-hendelse	Frekv-Sans	Kons	RV
Xx	*Pipes are torn; N2 or He@<0,5 bar stream out*	1	B2	B2
	Liquid bath not covered; water is spilled into it	1	B1	B1

Conclusion : *Participants will make a comprehensive assessment to determine whether the remaining risks of the activity / process is acceptable. Barriers and driving outside working hours e.g.*

10 CONCLUSJON

The rig is built in good laboratory practice (GLP).

Experiment unit card get a period of **24 months**
Experiment in progress card get a period of **24 months**

11 REGULATIONS AND GUIDELINES

Se http://www.arbeidstilsynet.no/regelverk/index.html

- Lov om tilsyn med elektriske anlegg og elektrisk utstyr (1929)
- Arbeidsmiljøloven
- Forskrift om systematisk helse-, miljø- og sikkerhetsarbeid (HMS Internkontrollforskrift)
- Forskrift om sikkerhet ved arbeid og drift av elektriske anlegg (FSE 2006)
- Forskrift om elektriske forsyningsanlegg (FEF 2006)
- Forskrift om utstyr og sikkerhetssystem til bruk i eksplosjonsfarlig område NEK 420
- Forskrift om håndtering av brannfarlig, reaksjonsfarlig og trykksatt stoff samt utstyr og anlegg som benyttes ved håndteringen
- Forskrift om Håndtering av eksplosjonsfarlig stoff
- Forskrift om bruk av arbeidsutstyr.
- Forskrift om Arbeidsplasser og arbeidslokaler
- Forskrift om Bruk av personlig verneutstyr på arbeidsplassen
- Forskrift om Helse og sikkerhet i eksplosjonsfarlige atmosfærer
- Forskrift om Høytrykksspyling
- Forskrift om Maskiner
- Forskrift om Sikkerhetsskilting og signalgivning på arbeidsplassen
- Forskrift om Stillaser, stiger og arbeid på tak m.m.
- Forskrift om Sveising, termisk skjæring, termisk sprøyting, kullbuemeisling, lodding og sliping (varmt arbeid)
- Forskrift om Tekniske innretninger
- Forskrift om Tungt og ensformig arbeid
- Forskrift om Vern mot eksponering for kjemikalier på arbeidsplassen (Kjemikalieforskriften)
- Forskrift om Vern mot kunstig optisk stråling på arbeidsplassen
- Forskrift om Vern mot mekaniske vibrasjoner
- Forskrift om Vern mot støy på arbeidsplassen

Veiledninger fra arbeidstilsynet
se: http://www.arbeidstilsynet.no/regelverk/veiledninger.html

12 DOCUMENTATION

- Tegninger, foto, beskrivelser av forsøksoppsetningen
- Hazop_mal
- Sertifikat for trykkpåkjent utstyr
- Håndtering avfall i NTNU
- Sikker bruk av LASERE, retningslinje
- HAZOP_MAL_Prosedyre
- Forsøksprosedyre
- Opplæringsplan for operatører
- Skjema for sikker jobb analyse, (SJA)
- Apparaturkortet
- Forsøk pågår kort

13 GUIDANCE TO RISK ASSESSMENT TEMPLATE

Kap 7 Assessment of technical safety.

Ensure that the design of the experiment set up is optimized in terms of technical safety. Identifying risk factors related to the selected design, and possibly to initiate re-design to ensure that risk is eliminated as much as possible through technical security.

This should describe what the experimental setup actually are able to manage and acceptance for emission.

7.1 HAZOP

The experimental set up is divided into nodes (eg motor unit, pump unit, cooling unit.). By using guidewords to identify causes, consequences and safeguards, recommendations and conclusions are made according to if necessary safety is obtained. When actions are performed the HAZOP is completed.

(e.g. "No flow", cause: the pipe is deformed, consequence: pump runs hot, precaution: measurement of flow with a link to the emergency or if the consequence is not critical used manual monitoring and are written into the operational procedure.)

7.2 Flammable, reactive and pressurized substances and gas.

According to the Regulations for handling of flammable, reactive and pressurized substances and equipment and facilities used for this:

Flammable material: Solid, liquid or gaseous substance, preparation, and substance with occurrence or combination of these conditions, by its flash point, contact with other substances, pressure, temperature or other chemical properties represent a danger of fire.
Reactive substances: Solid, liquid, or gaseous substances, preparations and substances that occur in combinations of these conditions, which on contact with water, by its pressure, temperature or chemical conditions, represents a potentially dangerous reaction, explosion or release of hazardous gas, steam, dust or fog.
Pressurized : Other solid, liquid or gaseous substance or mixes havinig fire or hazardous material response, when under pressure, and thus may represent a risk of uncontrolled emissions

Further criteria for the classification of flammable, reactive and pressurized substances are set out in Annex 1 of the Guide to the Regulations "Flammable, reactive and pressurized substances"
http://www.dsb.no/Global/Publikasjoner/2009/Veiledning/Generell%20veiledning.pdf
http://www.dsb.no/Global/Publikasjoner/2010/Tema/Temaveiledning_bruk_av_farlig_stoff_Del_1.pdf

Experiment setup area should be reviewed with respect to the assessment of Ex zone

• Zone 0: Always explosive atmosphere, such as inside the tank with gas, flammable liquid.
• Zone 1: Primary zone, sometimes explosive atmosphere such as a complete drain point
• Zone 2: secondary discharge could cause an explosive atmosphere by accident, such as flanges, valves and connection points

7.4 Effects on the environment

With pollution means: bringing solids, liquid or gas to air, water or ground, noise and vibrations, influence of temperature that may cause damage or inconvenience effect to the environment.
Regulations: http://www.lovdata.no/all/hl-19810313-006.html#6
NTNU guidance to handling of waste:http://www.ntnu.no/hms/retningslinjer/HMSR18B.pdf

7.5 Radiation

Definition of radiation

Ionizing radiation: Electromagnetic radiation (in radiation issues with wawelength <100 nm) or rapid atomic particles (e.g. alpha and beta particles) with the ability to stream ionized atoms or molecules.
Non ionizing radiation: Electromagnetic radiation (wavelength >100 nm), og ultrasound$_1$ with small or no capability to ionize.
Radiation sources: All ionizing and powerful non-ionizing radiation sources.
Ionizing radiation sources: Sources giving ionizing radiation e.g. all types of radiation sources, x-ray, and electron microscopes.
Powerful non ionizing radiation sources: Sources giving powerful non ionizing radiation which can harm health and/or environment, e.g. class 3B and 4. MR$_2$ systems, UVC$_3$ sources, powerful IR sources$_4$.
$_1$Ultrasound is an acoustic radiation ("sound") over the audible frequency range (> 20 kHz). In radiation protection regulations are referred to ultrasound with electromagnetic non-ionizing radiation. $_2$MR (e.g. NMR) - nuclear magnetic resonance method that is used to "depict" inner structures of different materials. $_3$UVC is electromagnetic radiation in the wavelength range 100-280 nm. $_4$IR is electromagnetic radiation in the wavelength range 700 nm - 1 mm.

For each laser there should be an information binder (HMSRV3404B) which shall include:

• General information
• Name of the instrument manager, deputy, and local radiation protection coordinator
• Key data on the apparatus
• Instrument-specific documentation
• References to (or copies of) data sheets, radiation protection regulations, etc.
• Assessments of risk factors
• Instructions for users

• Instructions for practical use, startup, operation, shutdown, safety precautions, logging, locking, or use of radiation sensor, etc.
• Emergency procedures

See NTNU for laser: http://www.ntnu.no/hms/retningslinjer/HMSR34B.pdf

7.6 Usage and handling of chemicals.

In the meaning chemicals, a element that can pose a danger to employee safety and health
See: http://www.lovdata.no/cgi-wift/ldles?doc=/sf/sf/sf-20010430-0443.html
Safety datasheet is to be kept in the HSE binder for the experiment set up and registered in the database for chemicals.

Kap 8 Assessment of operational procedures.

Ensures that established procedures meet all identified risk factors that must be taken care of through operational barriers and that the operators and technical performance have sufficient expertise.

8.1 Prosedure Hazop

Procedural HAZOP is a systematic review of the current procedure, using the fixed HAZOP methodology and defined guidewords. The procedure is broken into individual operations (nodes) and analyzed using guidewords to identify possible nonconformity, confusion or sources of inadequate performance and failure.

8.2 Procedure for running experiments and emergency shutdown.

Have to be prepared for all experiment setups.

The operating procedure has to describe stepwise preparation, startup, during and ending conditions of an experiment. The procedure should describe the assumptions and conditions for starting, operating parameters with the deviation allowed before aborting the experiment and the condition of the rig to be abandoned.

Emergency procedure describes how an emergency shutdown have to be done, (conducted by the uninitiated),

what happens when emergency shutdown, is activated. (electricity / gas supply) and

which events will activate the emergency shutdown (fire, leakage).

Kap 9 Quantifying of RISK

Quantifying of the residue hazards, Risk matrix

To illustrate the overall risk, compared to the risk assessment, each activity is plotted with values for the probability and consequence into the matrix. Use task IDnr.

Example: If activity IDnr. 1 has been given a probability 3 and D for consequence the risk value become D3, red. This is done for all activities giving them risk values.

In the matrix are different degrees of risk highlighted in red, yellow or green. When an activity ends up on a red risk (= unacceptable risk), risk reducing action has to be taken

CONSEQUENSES						
	Svært alvorlig	E1	E2	E3	E4	E5
	Alvorlig	D1	D2	D3	D4	D5
	Moderat	C1	C2	C3	C4	C5
	Liten	B1	B2	B3	B4	B5
	Svært liten	A1	A2	A3	A4	A5
		Svært liten	Liten	Middels	Stor	Svært Stor
		PROBABILITY				

The principle of the acceptance criterion. Explanation of the colors used in the matrix

Farge		Beskrivelse
Rød		Unacceptable risk Action has to be taken to reduce risk
Gul		Assessment area. Actions has to be concidered
Grønn		Acceptable risk. Action can be taken based on other criteria

Attachment to Risk Assessment report

[Conductivity rig: thermal conductivity measurements of porous media in a packed bed]

Project name	**Conductivity rig: conductivity measurements in porous media**
Project leader	Erling Næss/Christian Schlemminger
Organization	NTNU
HSE-koordinator	Erik Langørgen
Head of Department	Olav Bolland
Rig name	Conductivity rig
Plassering	VATlab
Room number	FinLab
Rig responsible	Ane Ringseth/Christian Schlemminger

TABLE OF CONTENTS

• ATTACHMENT A HAZOP MAL

Project: **Node: 1** Sections filled with pressurized N2 or He, vacuum, and liquid bath containing hot/cold oil.						**Page**	
Ref	**Guideword**	**Causes**	**Consequences**	**Safeguards**	**Recommendations**	**Action**	**Date/ Sign**
1	No flow	valves closed /Pipes blocked etc. Gas bottle is empty.	Can't conduct experiment/wrong measurement values No safety hazards	Always conduct experiment according to procedure		Check all valves. If not ok; dismantle & check for blockage	
2	Reverse flow	n.a.					
3	More flow	High pressure <5bar	Torn pipes (most likely not)	Always check pressure before starting experiment. Keep sample circuit valve closed. Close Needle Valve (1.03)	Check if instruments states zero before exp. Open venting valve.	Close (if not already) sample circuit valve). Adjust pressure regulator and vent out pressure	
4	Less flow	Blockage in pipes or leakage.	Pressure chamber not flushed→Air and moist may still be inside. No safety hazards.	Clean pipes regularly. Make sure everything is tight and sealed.	Set pressure to the system and spray sealing's with soap water	Check for leaks. If not ok-> Dismantle and check for blockage.	
5	More level	Amount of filled powder is too much	Powder floats out of sample holder→ could be evacuated/ plug the pipes.	Make sure to fill the proper height. Have filter inside piping system.		Dismantle setup and refill powder	
6	Less level	Amount of filled powder is too less	Wrong measurements	Make sure to measure probing depth.	Put in the correct probing depth in	Dismantle setup and refill powder	

Project: **Node: 1** Sections filled with pressurized N2 or He, vacuum, and liquid bath containing hot/cold oil.					**Page**		
Ref	**Guideword**	**Causes**	**Consequences**	**Safeguards**	**Recommendations**	**Action**	**Date/ Sign**
					Analyser software.		
7	No vacuum when evacuating.	Vacuum pump valve not open/Sample circuit valve not closed/leakage.	Wrong measurement values (moist still inside powder) No safety hazards	Conducti experiment according to procedure. Always close the sample circuit valve during evacuation.	Always check pressure before and after valves are turned on	Check valves. Check for leaks with soap water. If not ok→dismantle and clean setup and start over.	
8	Some vacuum (but not enough	leakage	Wrong measurement values (moist still inside powder) No safety hazards	Screw the pressure cell lid on firm (but not too firm). Use vacuum grease.	Always check pressure before and after valves are turned on	Stop the leakage. Clean setup and screw sealing's tighter together.	
9	More temperature	Oil in liquid bath increases in volume→high-level warning.	Measurement stops. Slippery floor. Evaporated oil.	Make sure no warning comes during evacuation. If also no oil is evaporated it is a good sign. Cover bath.	Test @ 150 degrees: if high level warning not sho within an hour it is ok.	Raise the pressure cell.	
10	Less temperature	Oil in liquid bath decreases in volume→/low-level warning.	Measurement stops	Have enough oil in the bath/lower the pressure cell far enough.	Test @ 150 degrees: if high level warning not sho within an hour it is ok.	Lower pressure cell.	
11	More viscosity	n.a.					
12	Less viscosity	n.a.					
13	Composition	Spilling water into	Boiling water, oil	Cover bath. Keep bath at		Put lid on.	

Project: **Node: 1** Sections filled with pressurized N2 or He, vacuum, and liquid bath containing hot/cold oil.					**Page**		
Ref	**Guideword**	**Causes**	**Consequences**	**Safeguards**	**Recommendations**	**Action**	**Date/ Sign**
	Change	the oil.	bursts out.	room temperature between experiments.			
14	Contamination	n.a.					
15	Relief	n.a.					
16	Instrumentation	Damage or failure zeroing	See 1;3;4;5;6;7;8;9;10	See 1;3;4;5;6;7;8;9;10	See 1;3;4;5;6;7;8;9;10	See 1;3;4;5;6;7;8;9;10	
17	Sampling	See 5 and 6	See 5 and 6	See 5 and 6	See 5 and 6	See 5 and 6	
18	Corrosion/erosion	n.a.					
19	Service failure	n.a.					
20	Abnormal Operation	See 1;3;4;5;6;7;8	Can't use values	Always conduct according to same procedure – no shortcuts	Take your time	Turn off and recalibrate instruments. Go through checklist	
21	Maintenance	Rig not run properly	maintenance	Always follow same procedure		Change whatever needs to be changed	
22	Ignition	Non-flammable oil/gas.	-	-	-	-	
23	Spare equipment	Not used				Store in C165	
24	Safety						

- **ATTACHMENT B – MSDS USED MATERIALS**

- **ATTACHMENT F - HAZOP MAL PROSEDURE**

Project: **Node: 1**						**Page**	
Ref#	**Guideword**	**Causes**	**Consequences**	**Safeguards**	**Recommendations**	**Action**	**Date/Sign**
	Not clear procedure	Procedure is to ambitious, or confusingly	Fail in measurement point	Simple procedure **Note: already applied**			
	Step in the wrong place	The procedure can lead to actions done in the wrong pattern or sequence	Pressurized N2 or He <5 bar can leak out.	no parts can be connected in wrong direction and fail positions **Note: already applied**			
	Wrong actions	Procedure improperly specified	Fail in measurement point; Pressurized N2 or He <5 bar can leak out.	Marks at setup sign clearly the actions, linked to the procedure steps, **Note: already applied**			
	Incorrect information	Information provided in advance of the specified action is wrong	Fail in measurement point; Pressurized N2 or He <5 bar can leak out.	Procedure is written clearly and prevents misunderstanding. Contact to project leaders is accessible. **Note: already**			

Project: Node: 1						Page	
Ref#	**Guideword**	**Causes**	**Consequences**	**Safeguards**	**Recommendations**	**Action**	**Date/Sign**
				applied			
	Step missing	Missing step, or step requires too much of operator	Fail in measurement point; Pressurized N2 or He <5 bar can leak out.	Proven procedure is applied and Operator training in necessary **Note: already applied**			
	Step unsucessful	Step has a high probability of failure	Fail in measurement point; Pressurized N2 or He <5 bar can leak out.	Operator training **Note: already applied**			
	Influence and effects from other	Procedure's performance can be affected by other sources	Fail in measurement point;	Notification of measurements to responsible person **Note: clear mention in procedure**			

• ATTACHMENT G PROCEDURE FOR RUNNING EXPERIMENTS

Experiment, name, number: **Conductivity rig: measuring conductivity in porous media**	**Date/ Sign**
Project Leader: **Erling Næss/Christian Schlemminger**	
Experiment Leader: **Jan Georg Henriksen/Christian Schlemminger**	
Operator, Duties: **Jan Georg Henriksen/Christian Schlemminger**	

	Conditions for the experiment:	**Completed**
1	Experiments should be run in normal working hours, 08:00-16:00 during winter time and 08.00-15.00 during summer time. Experiments outside normal working hours shall be approved.	
2	The operator must start the experiment. After start operator may leave and experiment will run itself.	
3	An early warning is given according to the lab rules, and accepted by authorized personnel.	
4	Be sure that everyone taking part of the experiment is wearing the necessary protecting equipment and is aware of the shut down procedure and escape routes.	
		Carried out
	Filling of new powder	
5	If rig is running, set liquid bath to 22 degrees and close shut-off and needle valve. Open the sample circuit valve and vent the system to ambient pressure.	
6	When liquid bath has been at 22 degrees for 10 minutes, shut of the bath.	
7	Remove wires from pressure cell.	
8	Then remove the pressure cell from the bath.	
9	Remove the pressure cell lid and disconnect the inner wires.	
10	Remove rubber sealing and take out the sample/sample holder.	
11	Use glasses eye protection, gloves and dusk mask	
12	Weigh the sample holder and measure sample height.	
13	Empty sample holder and remove sensor.	
14	Clean vacuum pressure cell, sensor, rubber sealing, and sample holder.	
15	Weigh the sample holder without any powder in it. One can now tell how much mass the powder has lost during evacuation.	
16	Pour in a new powder sample using a funnel.	
17	Weigh new powder and measure filling height.	
18	If the powder consists of small light grains, tape aluminum foil over the sample in order to prevent powder loss during evacuation.	
19	Put sample holder back into the pressure cell.	
20	Lubricate the sample holder and its lid with vacuum grease.	
21	Connect wires and close the lid. Connect to computer.	

22	Mount the pressure cell into the liquid bath.	
23	Cover the gap between pressure cell and bath to prevent oil vaporization.	
24	Then start new experiment (described below)	

	Experimental procedure	
25	Restart liquid bath and computer.	
26	Use glasses and gloves.	
27	All valves are closed.	
28	Set liquid bath (1.09) to 150 degrees and start vacuum pump (1.10).	
29	Open the shut-off valve.	
30	Adjust pressure with the pressure regulator (1.02). Pressure must be <0.5bar.	
31	Open needle valve (1.03).	
32	Open venting valve (1.04) and regulate (1.02) to desired pressure (0.4 or 0.2 bar). Then close the venting valve (1.04).	
33	Open sample circuit valve (1.05). Gas now flows into the pressure cell (1.08).	
34	Wait 10 seconds and close sample circuit valve (1.05)	
35	Open valve on the vacuum pump (1.10).	
36	When vacuum is below 10^{-2}torr (0.13 bar), close vacuum pump valve (1.10).	
37	Repeat point 37-40 six times.	
38	Open sample circuit valve (1.05) and turn off vacuum pump (1.10).	
39	Close the needle valve (1.03) and wait 1 hour before starting the experiment.	
	End of experiment	
40	Close all valves starting with the shut-off valve (1.00)	
41	Open venting valve (1.04) and sample circuit valve (1.05) and vent the system to ambient pressure.	
42	Turn of liquid bath (1.09)	
43	Empty sample holder (if not used afterwards) and cover liquid bath.	
	Also:	
44	Remove all obstructions/barriers/signs around the experiment.	
45	Tide up and return all tools and equipment.	
46	Tidy and clean work areas.	
47	Return equipment and systems back to their normal operation settings	
48	**To reflect on before the next experiment and experience useful for others**	
49	Was the experiment completed as planned and on scheduled in professional terms?	
50	Was the competence which was needed for security and completion of the experiment available to you?	
51	Do you have any information/ knowledge from the experiment that you should document and share with fellow colleagues?	

• ATTACHMENT H TRAINING OF OPERATORS

Experiment, name, number: **Thermal conductivity measurements of reference materials**		
Project Leader: **Christian Schlemminger / Erling Næss**	**01.10.2013**	**Date/Sign**
Operator **Ane Ringseth**		

	Knowledge to EPT LAB in general	
	Lab - Access - Routines and rules - Working hour	
	Knowledge about the evacuation procedures.	
	Activity calendar for the Lab	
	Early warning, iept-experiments@ivt.ntnu.no	
	Knowledge to the experiments	
	MSDS	
	Use of personal safety equipment	
	Procedures for the experiments	
	Emergency shutdown	
	Nearest fire and first aid station	
	Practical training with project leader	

I hereby declare by my signing, that I have reviewed and understood the HSE regulations, have been given appropriate training for running this experiment and am aware of my personal responsibility by working in EPT laboratories.

Operatør

Dato 01.10.2013

Signert Ane Ringseth

- **ATTACHMENT I FORM FOR SAFE JOB ANALYSIS**

SJA name:	
Date:	Location:
Mark for completed checklist:	

Participators:		
SJA-responsible:		

Specification of work (What and how?):
Risks associated with the work:
Safeguards: (plan for actions, see next page):
Conclusions/comments:

Recommended/approved	**Date/Signature:**	**Recommended/approved**	**Date/Signature:**
SJA-responsible:		HSE responsible:	
Responsible for work:		Other, (position):	

HSE aspect	Yes	No	NA	Comments / actions	Resp.
Documentation, experience, qualifications					
Known operation or work?					
Knowledge of experiences / incidents from similar operations?					
Necessary personnel?					
Communication and coordinating					
Potential conflicts with other operations?					
Handling of an eventually incident (alarm, evacuation)?					
Need for extra assistance / watch?					
Working area					
Unusual working position					
Work in tanks, manhole?					
Work in ditch, shaft or pit?					
Clean and tidy?					
Protective equipment beyond the personal?					
Weather, wind, visibility, lighting, ventilation?					
Usage of scaffolding/lifts/belts/ straps, anti-falling device?					
Work at hights?					
Ionizing radiation?					
Influence of escape routes?					
Chemical hazards					
Usage of hazardous/toxic/corrosive chemicals?					
Usage of flammable or explosive chemicals?					
Risk assessment of usage?					
Biological materials/substances?					
Dust/asbestos/dust from insulation?					
Mechanical hazards					
Stability/strength/tension?					
Crush/clamp/cut/hit?					
Dust/pressure/temperature?					
Handling of waste disposal?					
Need of special tools?					
Electrical hazards					
Current/Voltage/over 1000V?					
Current surge, short circuit?					
Loss of current supply?					
Area					
Need for inspection?					
Marking/system of signs/rope off?					
Environmental consequences?					
Key physical security systems					
Work on or demounting of safety systems?					
Other					

• ATTACHMENT J APPARATURKORT UNITCARD

Apparatur/unit

Dette kortet SKAL henges godt synlig på apparaturen!*This card MUST be posted on a visible place on the unit!*

Faglig Ansvarlig (Scientific Responsible) **Christian Schlemminger** / Erling Næss	**Telefon mobil/privat** (Phone no. mobile/private) **41063418** / 91897970
Apparaturansvarlig (Unit Responsible) Christian Schlemminger/ **Ane Ringseth**	**Telefon mobil/privat** (Phone no. mobile/private) 41063418
NTNU – Sintef Beredskapstelefon	800 80 388

Sikkerhetsrisikoer (Safety hazards)

- **Pressurized He/N2**
- **Hot/cold liquid bath**

Sikkerhetsregler (Safety rules)

Use eye protection glasses.

Do not touch liquid bath and/or nearby components.

Nødstopp prosedyre
(Emergency shutdown)
Close gas shut-off valve signed as "Emergency shut-off valve"

Disable power supply to liquid bath

Her finner du (Here you will find):

Prosedyrer (Procedures)	**above computer screen**, in FinLab.
Bruksanvisning (User's manual)	**in computer desk** in the FinLab.

Nærmeste (nearest)

Brannslukningsapparat (fire extinguisher)	**beside elevator**
Førstehjelpsskap (first aid cabinet)	**beside elevator**

NTNU
Institutt for energi og prosessteknikk

Dato

Signert

SINTEF Energi
Avdeling energiprosesser

Dato

Signert

FORSØK PÅGÅR

Enhet (unit) og bygg/romnr. (building/room no.):

NTNU-E 302	C165C	1. etg
Laboratorium		Finlab 1

Dette kortet SKAL henges opp før forsøk kan starte!

This card MUST be posted on the unit before the experiment startup!

Apparatur (Unit)	**Dato godkjent (Date Approved)**
Thermal conductivity rig	31. mai 2013
Prosjektleder (Project Leader)	**Telefon mobil/privat (Phone no. mobile/private)**
Erling Næss	918 97 970
Apparaturansvarlig (Unit Responsible)	**Telefon mobil/privat (Phone no. mobile/private)**
Erling Næss	918 97 970

Godkjente operatører (Approved Operators)

Navn/Name	Telefon/Phone	Mobil
Schlemminger, Christian		410 63 418
Henriksen, Jan Georg		99432522
Ane, Ringseth		90759199

Prosjekt (Project)

Thermal conductivity measurements in porous media

Forsøkstid / Experimental time (start - stop))

31.05.2013 - 31.05.2014

Kort beskrivelse av forsøket og relaterte farer (Short description of the experiment and related hazards)

- Hot/cold liquid bath and nearby componets do not touch!
- Liquid bath may evaporate il, be aware of slippery floor!
- Vacuum pump causes noise.
- Pressurized Helium or Nitrogen can cause noise
- Pressurized Helium or Nitrogen may cause tubes to crack
- Don't eat and drink in the area

NTNU

Institutt for energi og prosessteknikk

Dato 4/6 – 2013

Signert

NTNU SINTEF